Residence Time Distribution Studies on Continuous Flow Pulping Digester Using Radiotracer

Thesis
Submitted in partial fulfillment for the award of the Degree
of

Doctor of Philosophy

By

MEENAKSHI
(Registration No. - 901401016)

Under the guidance of

Dr. Avinash Chandra
Associate Professor
Department of Chemical Engineering,
Thapar Institute of Engineering &
Technology, (Deemed to be University), Patiala

Dr. Haripada Bhunia
Professor
Department of Chemical Engineering,
Thapar Institute of Engineering &
Technology, (Deemed to be University), Patiala

Department of Chemical Engineering
Thapar Institute of Engineering & Technology (Deemed to be University)
Patiala-147004, Punjab (India)
www.thapar.edu

April 2019

Dedicated

to

My husband

Mr. Sunil Nandal

and

My in-laws

Mrs. Sheela Devi and Mr. Pale Ram

CERTIFICATE

This is to be certify that the thesis entitled "**Residence time distribution studies on continuous flow pulping digester using radiotracer**" being submitted by **Ms. Meenakshi** to the Department of Chemical Engineering, Thapar Institute of Engineering & Technology, Patiala, for the award of degree of **Doctor of Philosophy** is a record of bonafide research work carried out by her. **Ms. Meenakshi** has worked under our guidance and supervision. She has fulfilled the requisite standard for the submission of the thesis.

To the best of our knowledge, the matter embodied in this thesis has not been submitted to any other university/institute for the award of any degree or diploma.

Dr. Avinash Chandra
Associate Professor
Department of Chemical Engineering,
Thapar Institute of Engineering &
Technology, Patiala

Dr. Haripada Bhunia
Professor
Department of Chemical Engineering,
Thapar Institute of Engineering &
Technology, Patiala

ACKNOWLEDGEMENTS

Words are often less to reveals one's deep gratitude. With an understanding that work like this can never be the outcome of a single person. Through this acknowledgement I would like to express my special thanks, gratitude and regards to all those who supported, helped and guided me in completing this work.

At first, my heartfelt thanks to the **ALMIGHTY** for his abundant blessing showered on me throughout this endeavor to complete this successful work of mine.

I express my deep and sincere gratitude as well as profound regards to **Dr. Avinash Chandra** and **Dr. Haripada Bhunia** for providing me an opportunity to work under their guidance. Their wide knowledge, expertise, valuable suggestions, encouragement and freedom of independent work provided a platform for learning and performing research. Their enthusiasm and optimism made this experience both rewarding and enjoyable. Their feedback and editorial comments were also valuable for the writing of this thesis.

I would like to thank my doctoral committee members **Dr. Sanjeev K. Ahuja** for his terrific guidance and support through the duration of this work. I would also thank to the other committee members **Dr. S. K. Singh and Dr. Bonamali Pal**.

I would like to thank **all the faculty members** of the Department of Chemical Engineering for encouraging me to write the thesis report. I would like to thank **all the employees** of the Department of Chemical Engineering for their everlasting support.

I would express my sincere gratitude to **Dr. P. K. Bajpai**, Ex-Distinguished Professor, for providing guidance and support for successfully conducting this work.

I am extremely thankful to **Dr. H. J. Pant** and his team members Dr. V. K. Sharma, Dr. Jaishree Biswal and Mr. Sunil Goswami for providing radiotracer and support during industrial experiments.

I sincerely thank the **DAE-BRNS** and **Thapar Institute of Engineering and Technology** for providing financial support and conducive environment to undertake the research work.

I express my deep sense of gratitude to my family. I am thankful to my parents for their great support throughout my life. Words cannot express how grateful I am to my parents **Mrs.**

Jaiwanti and **Mr. Vijender Singh**, my mother-in-law **Mrs. Sheela Devi**, my father-in-law **Mr. Pale Ram** and my sister-in-law **Mrs. Sumitra Nandal** for all of the sacrifices that they have made on my behalf. Their prayers for me were what sustained me thus far. I would cherish every moment where my parents were so keen and curious to know about the details and progress of my work, which boosted my confidence. I would like to express appreciation to my beloved husband **Mr. Sunil Nandal**, who has always been my support in the moments when there was no one to answer my queries.

I would like to thank all my colleagues and friends **(Ms. Metali Sarkar, Ms. Sehaspreet Kaur, Ms. Bandhana Sharma, Ms. Steffi Talwar, Ms. Ravneet Kaur, Ms. Parminder Kaur, Dr. Deepak Tiwari, Dr. Dev Kumar Mandal, and Mr. Kamaljeet Singh)** for their support and encouragement in carrying out my research smoothly.

Meenakshi

ABSTRACT

Radiotracer technique has been used to measure the residence time distribution (RTD) of the industrial scale three-tube continuous pulping digester used for pulp production from wheat straw. RTD experiments were performed to observe the mean residence time (MRT), flow behavior and to optimize the operating conditions of the digester in M/s SATIA Industries Ltd. Muktsar, Punjab (India). The experiments were performed with different operating conditions using ^{82}Br and ^{198}Au radio-isotopes as radiotracers. The radiotracer was injected instantaneously in the form of impulse input in the liquid phase at the inlet of the first tube. Sodium iodide scintillation detectors were mounted at inlet and outlet of each tube to measure the concentration of radiotracer. Each experiment was repeated three times to check the repeatability of the results. The data recorded by detectors were plotted as a function of time. The obtained concentration data were treated for zero shifting, background subtraction, decay correction and data extrapolation. Mean residence time was calculated for each experiment and RTD curves were obtained. Analysis of the RTD curves showed the flow channeling or occurrence of parallel flow paths in the first and second tube of the digester. Axial dispersion model and tank-in-series with back-mixing model with a plug flow component in series were found suitable to describe the flow behavior of the liquid phase in the pulping digester. The results of the model fitting indicated plug flow behavior of the liquid phase in the digester. The degree of delignification and value of residual alkali were found optimum for a screw speed of 65 rpm (wheat straw feed rate of 6.3 m^3/min) and white liquor (8.28 w/w % of NaOH) flow rate of 355 l/min. For second and third tubes, convolution procedure was used for simulating the experimental data due to non-ideal impulse input in tube two and three. Highly dispersed flow was observed in the first tube and the dispersion decreased as the material passed through the first tube to the third tube of the digester.

In another radiotracer experiment, at M/s Trident Industries Ltd. Barnala (India), ^{99m}Tc in the form of sodium pertechnetate was used to carry the RTD experiment in two identical two-tube continuous pulping digesters which have the same operating conditions. The data obtained after RTD experiments were pretreated and modeled using the same models that were used for the previous set of experiments. Flow behavior was analyzed using the obtained model parameters in terms of dispersion or mixing. It was observed that the old digester had very low

MRT as compared to the theoretical MRT. The output parameters of the old digester in terms of Kappa number and residual alkali were found to be poor even at same operating parameters. In old digester, low MRT was probably due to the channeling and scaling. Operation of the new digester was found normal.

Figure 1 shows the schematic of the overall thesis work.

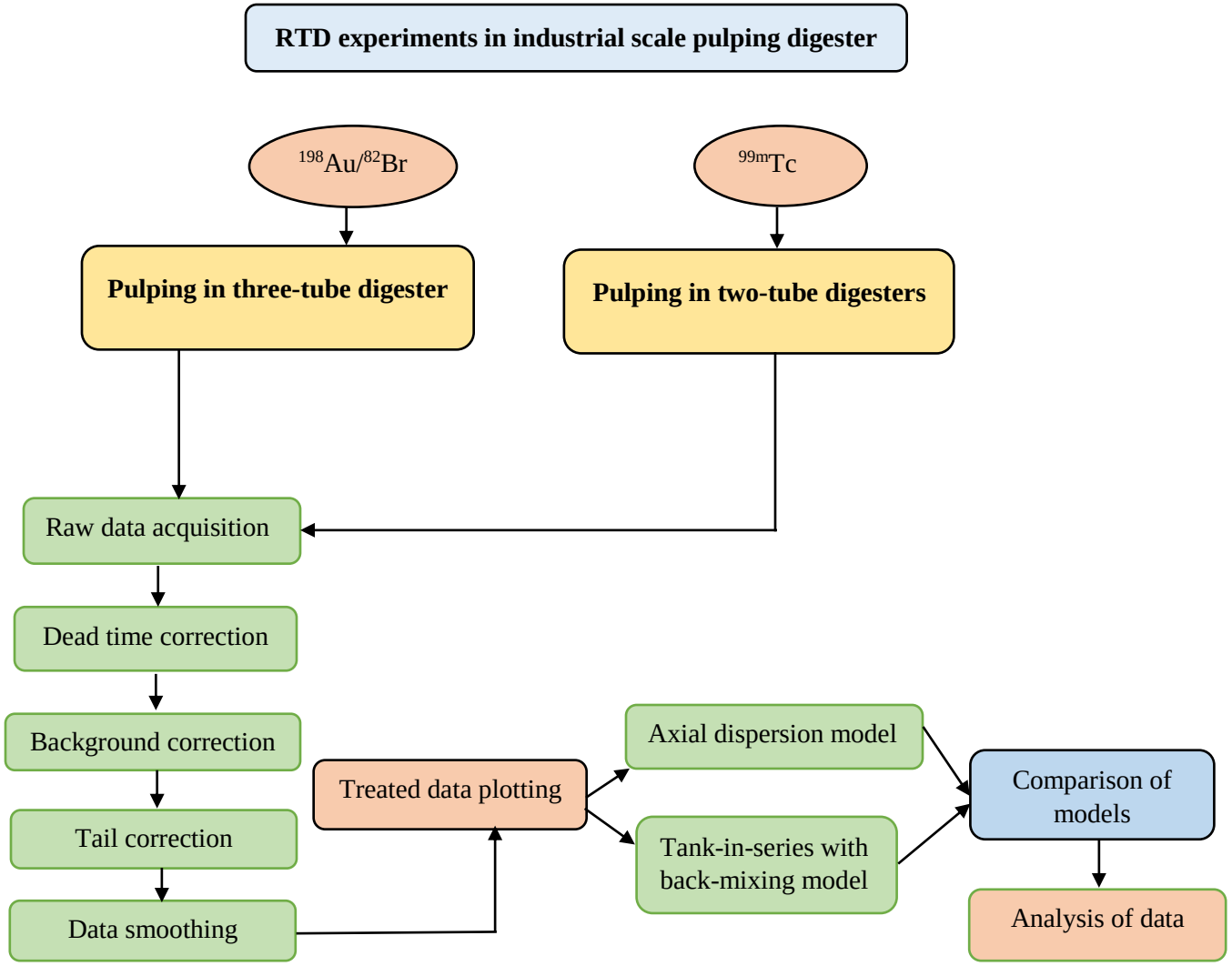

Figure 1. Schematic of overall thesis work

TABLE OF CONTENTS

List of Figures

List of Tables

List of symbols

C	Concentration of the tracer (counts/s)
D	Dispersion coefficient (m^2/s)
D_i	Detectors
Di	Digesters
E	Exit age distribution of the models (s^{-1})
E_{ad}	Exit age distribution for axial dispersion model
E_{sd}	Exit age distribution for axial dispersion model for small extent of dispersion
I	Normalized tracer input signal
i	1, 2, 3…
K	Ratio of the volume of exchange stream to the volume of the mainstream
L	Length between two detectors (m)
N	Number of tanks
N_i	Number of tanks for different tubes
$N_{1\text{-}3}$	Number of tanks for three-tube digester
Pe	Peclet number
Q	Volumetric flow rate (m^3/s)
Q_r	Flow rate of recycling stream (m^3/s)
t	Time (s)
t_i	Sampling time instant (s)
t_j	Difference between the sampling time and the time instant of the input

	considered (s)
u	Velocity of the liquid phase inside the digester (m/s)
V	Volume

Greek letters

α	Back-mixing ratio
α_i	Back-mixing ratio for whole digester
τ	Mean residence time
τ_i	Mean residence time (min) for different tubes
τ_m	Mean residence time for the volume fraction that exchange between stagnant zone and main flow stream
τ_{pf}	Mean residence time for plug flow component (min)
τ_{ADM}	Mean residence time for axial dispersion component (min)
τ_{TIBM}	Mean residence time for tank-in-series with back-mixing component (min)
$\tau_{1\text{-}3}$	Mean residence time of three-tube digester (min)
$\tau_{1\text{-}2}$	Mean residence time of two-tube digester (min)

List of abbreviations

ADM	Axial dispersion model
CFD	Computational fluid dynamics
CSTR	Continuous stirrer tank reactor

DAS	Data acquisition system
MRT	Mean residence time (min)
MRT_a	Mean residence time for axial dispersion model
MRT_b	Mean residence time for tank-in-series with back-mixing model
PF	Plug flow component
PFR	Plug flow reactor
RA	Residual alkali (g/l)
RTD	Residence time distribution
RMS	Root mean square
TIBM	Tank-in-series with back-mixing model
TIS	Tank-in-series model

Chapter-1 Introduction

Paper is used in our daily life extensively such as for writing, printing, cleaning, packaging, etc. As per the history of the paper, the first paper was invented by Chinese around 150 AD and with time its popularity spread in the world [1]. Even in the present age of digitization, the paper has a better impact on recording the data, understanding, retaining and use of information than the digital medium [2]. In India, the overall demand of paper increases continuously with an average rate of 6.6 % per annum. The paper consumption in India is about 13 kg per capita in FY17-18 which is much below the global average of 57 kg per capita [3]. The consumption status shows that paper is being extensively used around the world. There are approximately 750 units for paper, newsprint and cardboard production in India with a turnover of INR 50,000 crore per annum. The total installed capacity for paper production is 24 million tons (maximum) with a total operating capacity of 20 million tons. The 750 units for pulp production are using wood, recycled paper, and agro-residue as raw material with an individual production share of 30-35 %, 50-55 % and 15-20 %, respectively [4].

1.1 Raw material for Pulping

Wood (softwood or hardwood) is the most abundant raw material for pulp production due to the fact that it provides uniform quality pulp [5]. Continuous increase in the demand of paper leads to the worldwide shortage of woody plants [6, 7]. Due to the decreasing forest area, pulp and paper producing industries are using non-woody plant fibers which are obtained largely from grasses, bast fibers, cereal straw, canes, etc. and out of these, straws are the most abundant agricultural by-product obtained worldwide [8]. Straws included wheat straw, rice straw, barley, etc. [7, 9]. Recycled paper products are also used for pulp production [10, 11].

Wheat is one of the main crop that is cultivated all over the world. In India, wheat production area covers 25% of the total crop area [12]. India is the subsequent largest producer of the wheat after China [12]. The large and inexpensive availability of the wheat straw promotes its use as a raw material for paper production. The low lignin content of wheat straw as compared to other agro-residues is the added advantages for pulp manufacturers [11]. Moreover, the paper produced from wheat straw has good mechanical

strength properties in comparison to other non-woody raw materials like cotton stalks pulps and sunflower stalk pulp [13].

1.2 Pulping processes

Pulping is a process of the extraction of cellulose from wood or non-wood raw material by removing lignin, which acts as a natural binder material for cellulose fibers [14]. The process of removing the lignin is termed as delignification process. The delignification is carried out by mechanical separation or by using different chemical treatments. The pulping process is classified into three categories i.e. mechanical pulping, chemical pulping and semi-chemical pulping (combination of chemical pulping and mechanical pulping) [1, 9].

1.2.1 Mechanical pulping

Mechanical pulping is the oldest technique for pulping. In the mechanical pulping, the cellulose fibers are separated using mechanical energy by breaking the bonds between fiber bundles. The yield is very high in this process as compared to the chemical pulping. Lignin is a polymeric material with a high molecular weight that binds the cellulose fiber together in cellulose rich biomass. The mechanical pulping provides pulp with higher lignin content as compared to other pulping processes. The mechanically produced paper turns yellowish with time [15]. In 1960, virtually all the mechanical pulps were produced by basic stone ground-wood (SGW) process [9]. The traditional mechanical pulping involves forcing of logs into grinders. Presently, the rotating discs are used instead of a grinder, which converts the logs into pulp with the help of mechanical energy [16]. Water is added into grinders to prevent the damage to the fibers due to heat or friction. The paper produced from the mechanical pulp is of low brightness, due to high lignin content. The pulp has to be bleached for further improvements in the quality [9]. The main advantage of mechanical pulping is a high yield of production than chemical pulping but the energy required for mechanical pulping is more than the chemical pulping. Low whiteness of the paper product produced through mechanical pulping makes it less favorable [17]. Further mechanical pulping is of four types (a) Thermo-mechanical process, (b) Chemi-thermomechanical process, (c) Stone ground-wood mechanical process, (d) Refiner mechanical process and (e) Chemi-mechanical pulping.

1.2.2 Chemical pulping

The chemical pulping process is the most favorable commercial pulping process used all over the world. In chemical pulping, wood or other raw material is cooked in the presence of chemicals at high temperature and pressure [17]. At these conditions, some of the cellulose and hemicellulose are also degraded and results in lower yield as compared to mechanical pulping. The pulp obtained by chemical pulping is of high quality with lower lignin content. A high-quality pulp with high brightness and low energy requirement makes it more favorable as compared to the mechanical pulping in industries. Chemical pulping processes include the kraft process, sulfite process and soda pulping process [9]. These processes are described in the following section.

1.2.2.1 Sulphate or kraft process

The kraft pulping process is the most popular and dominant chemical pulping process due to high strength paper and chemical recovery [18]. The chemicals used in the kraft process are sodium hydroxide and sodium sulfide. It is a modification of the soda process which involved only sodium hydroxide for pulping [19]. The aqueous solution of these chemicals is known as white liquor. The cooking of wood is carried out for 1-2 h at 70 °C to 170 °C. After the digestion process, the black liquor, pulp and other undigested material with residual alkali are discharged in a blow tank at lower pressure and temperature [15]. The main drawback of the kraft process is the production of the malodorous sulfur-containing compound and the incomplete delignification. The relatively high temperature is required in the kraft process to achieve a sufficient rate of delignification [18].

1.2.2.2 Sulfite process

Sulfite pulping is the second most popular pulping process. In sulfite pulping process sulphurous salts are used to extract the cellulose fibers by removing lignin. Sulfite pulping is carried out at a pH range of 1.5-5 depending on base to sulphurous acid ratio and counter ion (magnesium ions and calcium ions) to sulfite. The wood remains in the contact of pulping chemicals from 4 to 14 hours and between the temperature ranges of 130 ^{0}C – 160 ^{0}C. The main drawback of the sulfite process is that the pulp fibers produced from the sulfite process are not as strong as that of kraft process due to acidic conditions [1]. It hydrolyzes some of the cellulose fibers. Although, the pulp yield is higher than the kraft

process and easy to bleach. This process is used to make pulp to produce fine papers and tissue papers.

1.2.2.3 Soda process

This process is a first successful chemical cooking process which does not involve the use of sulfur compounds [20]. The sulfur compounds used in kraft or sulfite process are the main concern for the environment. In the soda process, only caustic soda is used as a main chemical agent for pulping, hence, reduced burden on the environment [21]. The soda process pulp has a lower tear strength than other chemical pulping processes. Nowadays, anthraquinone soda pulping has become an important pulping method to reduce silica scaling caused due to the presence of silicates in raw materials and to enhance the delignification process [21].

1.2.3 Semi-chemical pulping

In semi-chemical pulping, wood chips are converted into pulp by using the chemical as well as mechanical pulping method. In this process, firstly, chips are cooked with chemicals such as sodium sulfite, sodium carbonate, sodium hydroxide, etc. and remaining pulping action is done mechanically. Pulp yield of semi-mechanical pulping is between 60%-80%. There are three types of semi-chemical pulping process (a) neutral sulfite semi-chemical pulping (b) green liquor (c) no-sulfur process. Neutral sulfite semi-chemical pulping process is the main process to produce approximately 150,000 tonnes of pulp annually. [22].

1.3 Pulping digester

The pulping digester is the heart of any pulp and paper industry which is used for cooking of biomass for pulping [23]. In the pulping process, digester operates in two ways, continuous and batch basis. In continuous digester, a large tube-shaped reactor is used which contains pre-steaming, liquor impregnation, heating, cooking, and washing all these in a continuous manner [24]. It is easy to operate and less labor is required to run this digester. On the other hand, in batch digester, there are 5 to 6 digesters in a plant. The vessel is filled with chips and white liquor to cover chips and heated by steam injection until the maximum cooking temperature is achieved. It takes approximately 90 minutes to achieve the required temperature and pressure. Heat and other non-condensable gases are released through pressure valve which is on the top of the digester. In continuous digester,

a lower amount of energy is required, but this digester is unsuccessful to give high yield, high strength and better quality paper [9].

1.4 Basics of Residence time distribution (RTD) study

Most of the industrial scale processes are based upon the working principle of continuous flow reactors which includes plug flow reactor (PFR) and continuous stirred tank reactor (CSTR). But in real practice, no chemical reactor behaves ideally and shows some deviation from the ideal conditions [25]. Hence, the industrial reactors behave in between these ideal reactors PFR and CSTR. There may be various causes of this deviation from the ideal conditions which include unstable operating conditions, inadequate design, different sources of raw material, scale-up effects, non-uniform heating/cooling during operation, etc. The deviations from the ideal conditions may cause malfunctioning in reactors or failure of the plant process and may result in non-uniform or inferior quality product [26].

The inadequate performance of the reactor may also lead to different types of abnormalities in flow behavior. These flow abnormalities and hydrodynamics of any chemical reactor can be predicted with the help of fluid mechanics theory by conducting the residence time distribution (RTD) study. The RTD principle is the most useful tool to predict the flow abnormalities of a non-ideal reactor and this irregular behavior can be explained in the form of the probability distribution function of the process material flowing inside the reactor or process equipment [27]. Moreover, RTD study provides the provision to estimate the efficiency of the reactor, its mixing time, back-mixing, bypassing, dead zone, channeling, etc. inside the reactor [28]. The inadequate design of the process vessel/reactor can be evaluated using the RTD analysis by predicting the hydrodynamic behavior for different operating conditions even at the designing stage. Though the RTD analysis of any reactor restricted to provide global facts only about the flow behavior and it is not possible to gather the information regarding the local distribution inside the reactor using RTD study. To determine the localized or spatial flow responses, advanced computational tools (computational fluid dynamics (CFD)) can be used [29, 30]. In literature, some CFD results are used to verify the RTD results [31].

1.4.1 Types of available tracers

There are various studies presented in the literature, in which different types of flow reactors are investigated using RTD analysis using different types of tracers. These

tracers are used to tracer the different phases of the different types of continuous or batch flow reactors (solid, liquid and gas).

Generally, a unique property of any tracer is used for RTD analysis to identify the behavior of the process vessel. These process may be of different types such as chemical, physical or biological with different length of residence time. The characteristic of the tracer which is used for RTD analysis may be chemical, physical, nuclear or biological. A very small quantity of the tracer is used to conducting the RTD test. The tracer is injected as impulse or step input with one of the phase (solid, liquid or gas) of the reaction vessel and travels along with the tracing phase [32]. Various types of conventional tracers are used according to the process of reactor conditions. These conventional tracers include ions, dyes, electrolytes, salts of different compound, etc. but these tracers have some common problems associated with them which are as follows:

- The conventional tracers cannot be used for industrial systems which have very high temperature and pressure. At these conditions, it is not possible to take samples manually.
- RTD analysis of the reactor having very complex geometry is not possible using conventional tracers. Using conventional tracer, the sample can be taken only at the outlet of the process vessel which does not provide the information of all sections of the reactor.

The tracer specific problems are as follows:

a) **Dyes:** The coloring properties of dyes are used to obtain the RTD of a system by observing the color or using a spectrophotometer. At low concentrations of dyes, the results obtained will not be accurate. Most of the chemicals used in industries may not be traced using dyes because of their color and probability to react with other compounds [33].

Sometimes a fluorescent dye is used for better visualization, but the fluorescent dyes can be toxic if used in high concentrations. The behavior of these chemical compounds is also influenced by their ionic and molecular structure. In the case of fluorescent dyes, the chemical properties can be destroyed or changed by the attack of process chemicals. Also, when the pH of the solution is changed, it affects the molecular structure of the dye and it may result in different behaviors of the dye in the tracing

system. Some of these dyes are carcinogenic when used in concentrated form under extended exposure [32, 33].

b) **Ions:** The ions can be used as tracers to measure the RTD of the system but they have low detectability and have retardation characteristics in a specific medium such as porous media, etc. Some ions have very low chemical stability in the polluted environment (water), e.g., ions of nitrates have very high background concentration and may pose problems in detection and they are not stable in ground or surface water [33].
c) **Electrolytes:** Lithium chloride and sodium chloride are commonly used electrolytes for RTD measurements due to their non-hazardous nature and of low-cost. Electrolytes have the capability to be detected in small amount but they can be absorbed by the surface or may react with other ions present in the system. Some of the electrolytes commonly present in the system exhibiting high background concentration, reduce detectability leading to low-resolution RTD curve [33].
d) **Acids or bases**: Acids or bases are also used as tracers in systems where the change in pH is having no effect on the system.

Besides these conventional tracers, radiotracers are also available to study the RTD in chemical sectors in the industry.

1.4.2 Radiotracer

Radioactive properties of radiotracers are used to follow the process fluid for online RTD diagnosis [34]. A number of radiotracers are available depending on their half-life, activity, activation energy, cost, availability, physical or chemical properties, etc. Radiotracers may be intrinsic or extrinsic. Intrinsic tracers should be chemically identical with the process material [35]. Also, the sample of the process material can be activated and can be used as an intrinsic tracer [32]. The intrinsic tracers can be used where the process is dominated by atomic or molecular diffusion like reaction kinetics or solubility which has to be studied. For example, sodium (^{24}Na) is used as an intrinsic tracer to trace the NaOH phase. Tritium is also an intrinsic radiotracer [36, 37]. In the case of extrinsic tracer, the detectable constituents are outside the molecular structure and have identical dynamic properties that of the tracing material to be traced [32, 38]. The chemically identical radiotracer is not required in case of extrinsic tracer, e.g. to follow the water,

$Na^{131}I$ can be used as an extrinsic radiotracer. The only requirement in the case of extrinsic radiotracer is that they should behave like that of flowing phase.

Radioisotopes can be of following types:

a) Naturally occurring radioisotopes
b) Artificially produced radioisotopes

Artificial radiotracers are either produced in a nuclear reactor or by particle acceleration [39]. These artificially produced radiotracers can be classified as follows according to the type of radiation emitted:

1.4.2.1 β ray radiotracer

The β ray radioisotopes are generally used to measure the thickness of aluminum or plastic sheets, hydrological investigation, etc. All of these β emitting radioisotopes are measured by liquid scintillation counting technique in which a liquid sample is mixed with a solution. Generally, Geiger Muller counters are used for this process. The β rays when passed through the solution, cause emission of light, which is measured by a photomultiplier tube [40]. The β sources include the tritium (^{3}H), which has a half-life of 12.6 years with low energy radiations [38, 41] and Carbon-14 (^{14}C) which is also used as a radiotracer for organic fluids but has low energy radiation. Phosphorous-32 (^{32}P) also is a β emitter with high energy radiation [40].

1.4.2.2 γ ray radiotracer

The γ ray emitting radiotracers are used in health science, agriculture as well as in industries. The applications of γ ray emitting radiotracers are discussed in detail in the previous study [32]. Semiconductor detectors and solid scintillation detectors are used to measure the rays emitted by γ-emitting radiotracers. In scintillation detectors, a crystal of sodium iodide is doped with thallium and connected to a photo-multiplier. The crystal emits the light when it interacts with gamma rays and the light photons are detected by a photomultiplier. The photo-multiplier records the results in a multi-channel analyzer. The γ radiotracer includes ^{24}Na, ^{82}Br, ^{140}La, ^{198}Au, ^{131}I, ^{46}Sc, ^{85}Kr ^{192}Ir, etc. [42].

1.4.3 Advantages and selection criteria of radiotracer

The radiotracers are having numerous advantages over conventional tracers [43]. Some of the advantages are:

- Radiotracers are advantageous in opaque systems.
- Radiotracers are detected in very low concentration.
- Continuous sensing of the radiotracers is possible using the data acquisition system.
- Radiotracers are available in wide range and provide physical/chemical compatibility with the process material [44].

The radiotracer disappears from the tagged system with time and the contamination caused by radiation is removed automatically due to their radioactive decay property. It is not possible to examine the industrial system with conventional tracers due to very high temperature and pressure conditions. Also, the sample collection procedure is difficult at intermediate positions for long pipe reactors and reactors have bends, so, the only way to carry out the investigation using radiotracers.

Radiotracer based technology plays a growing role in different industries. This technology has various applications like wear measurement, monitoring of scale deposition, flow rate measurement in different industries like petroleum, mineral processing, petrochemicals, waste water treatment, etc. [45-49]. The selection criteria of the radiotracer include half-life, specific activity, availability, cost, the energy of radiation emitted. The tracer should be detectable even in very low concentration inside the system and completely miscible with the process fluid. That is the motive we select the tracer having similar physical properties (density, viscosity, etc.) with the fluid under investigation. The availability and cost of the tracer are also a major concern. The tracer should be injected in a trace amount so that it does not affect the flow parameters of the process and minimize the contamination. Using a large amount of tracer has the risk of sticking on the wall of the process vessel and may cause a detrimental effect on the process. To get the high quality of the RTD signal, the activity of the radiotracer should be high enough as compared to the background signal.

1.4.4 Safety aspects with radiotracer

Safety concern is very important while handling the radioactive material. According to Pedro Vaz [50], most of the radiological accidents occur due to the lack of awareness, no safety programs, failure of equipment, orphan source (lost, stolen and abandoned). Another main issue is related to waste disposal. The waste produced from radiological activities should be minimized by using the guidelines of radiological safety

provided by IAEA [51]. Radiological and environmental aspects of the radiotracers are based on ALARA (as low as reasonably achievable) principle. All safety measures should be considered to avoid the unnecessary exposure of radiation to human beings. The exposure to the radiation can be minimized by decreasing the exposure time around the radioisotope and increasing the distance from the radiation source. One should use the optimum thickness of shielding against radiation exposure. Concrete or lead shielding is preferred for gamma radiation. The annual dose limit of the exposure is 1 mSv for public and 20 mSv for a person working in a radiation environment [36, 51, 52]. All radioactive sites have to be routinely checked and monitored for detection of any radiological accident [53]. The radiation survey meters are used to monitor the radiation nearby the working place and dosimeters are used for personal safety. The rules and regulations for safety are continuously reviewed and revised from time to time [52].

1.4.5 Radiotracer injection and detection system

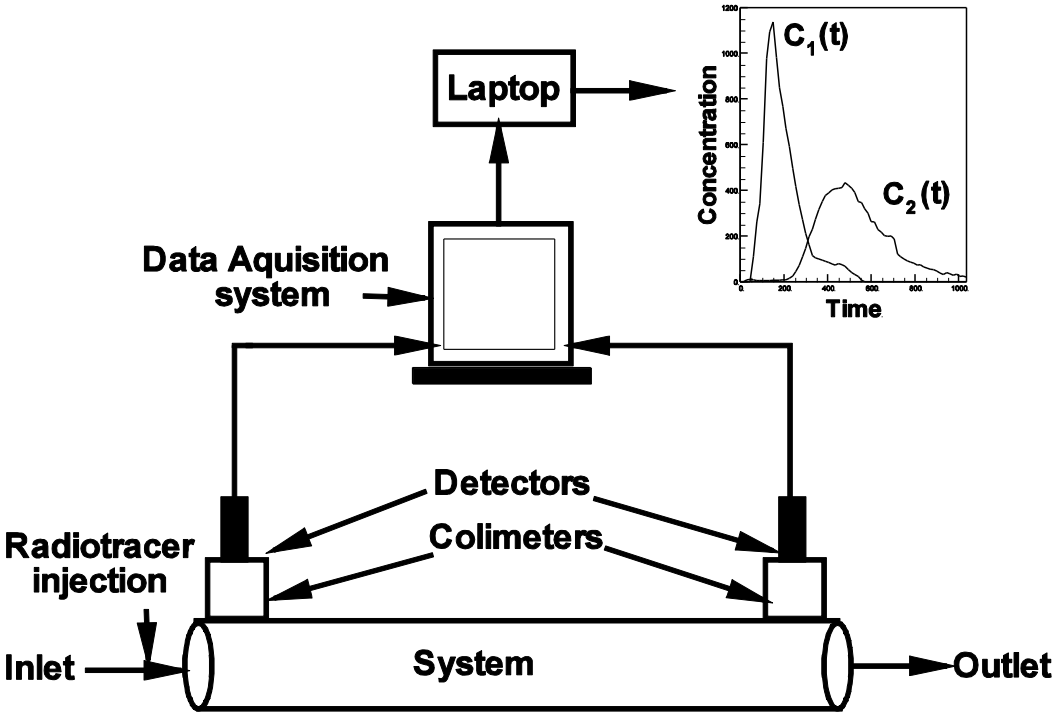

Figure 1.1. General procedure of the radiotracer experiment

The general procedure of the radiotracer technique is shown in Figure 1.1. There are various methods to inject the radiotracer which includes step response, random, sinusoidal, impulse, etc. but commonly impulse response method is used to measure the

RTD of any system [27, 32]. In this method, the radiotracer is injected at the inlet section of the system spontaneously and measured at the inlet and outlet by locating or mounting the detectors at the outlet as shown in Figure 1.1. The mixing length can be reduced by injecting the tracer in the center of the pipe using a high-speed injection system. Ideality of injection can be improved by decreasing or keeping the injection time as short as possible. The impulse injection system is very common for commercial processes as compared to step injection due to rather longer disturbance time than impulse method. The injection and detection of the radiotracer give the data in concentration versus time that can be easily analyzed to obtain the RTD of the system [54].

Sodium iodide doped with TI scintillation detectors are commonly used detectors for γ ray source in industrial applications [55]. Two scintillation detectors are shown in Figure 1.1. During detection or measurement of the concentration of the tracer signal, detectors are mounted externally on the system and connected to the data acquisition system (DAS) through the wired network. The DAS further sends the data to the laptop/computer. The detail description of detection systems is given in the literature [27].

After conducting a radiotracer test, the data are obtained in the form of counts of gamma energy against time. The raw data cannot be directly used to extract information about the system and thus needs to be treated before further analysis [27, 56].

1.5 Thesis motivation and objectives

There is a number of process equipment used in the industry and every equipment needs to operate at optimum conditions to maximize the economic gain and product quality. RTD analysis is the simplest and economic way to find out the flow behavior inside the process equipment. Further, the pulping digester has never been investigated for its RTD and hydrodynamic behavior. The optimization of the pulping process may help to meet the ever ending demand for paper globally. The review of the available body of literature is suggesting the following gaps in literature to the best of our knowledge:

- RTD study on continuous horizontal pulping digester (three-tube and two-tube) based on agro residue is not available.
- No hydrodynamic study is available (experimental as well as numerical) on continuous/batch pulping digester.

The overall objective of the present work is to conduct RTD studies on continuous flow pulping digester. To achieve these objectives, these sub-objectives are proposed:

- To conduct RTD studies on continuous flow pulping digester (tube digester):
    - Identification of suitable radiotracer(s)
    - RTD experiments on digester
    - Analysis of obtained RTD data
        - RTD modelling and determination of model parameters
        - Identification of suitable model based on optimum process conditions

1.6 Thesis overview

The presented thesis is divided into 8 chapters. In the presents work residence time distribution study is carried out using different radiotracer on three-tube and two identical two-tubes pulping digesters in different paper industries in India.

CHAPTER 1 covers the background of the paper industry, pulping processes, RTD technique using radiotracer. Benefits of radiotracer, selection criteria, advantages, and safety procedure are discussed. It also included the general procedure used for conducting RTD experiments using radiotracers. The pretreatment of the radiotracer RTD data for dead time correction, back-ground correction, decay correction, tail correction and data smoothing is also explained.

CHAPTER 2 covers the literature review related to the present work. The RTD studies using radiotracers at industrial, pilot and lab scales are presented separately. Residence time distribution studies using axial dispersion model, tank-in-series model, and other compartment models are also explained.

CHAPTER 3 focused on the materials and methods used in this study. It also covers the methods used for the RTD experiments carried out at industrial scale using radiotracer. The procedure of pulping at industrial scale is explained. The procedures for the analysis of black liquor and pulp are also discussed.

CHAPTER 4 included the details of the models (axial dispersion model and tank-in-series with back-mixing model) used for fitting of the experimental data. Convolution procedure

is explained in detail which is used for the modeling of the data having non-ideal input. Theoretical and experimental mean residence times with the procedure of parameters' estimation have also been discussed.

CHAPTER 5 presented the data obtained after industrial experiments conducted on three-tube horizontal continuous pulping digester at M/s Satia Industries Ltd., Muktsar Sahib, Punjab (India), using ^{198}Au and ^{82}Br radiotracer at different operating conditions. The RTD modeling for each tube and the whole digester have been explained in detail. The mean residence times and flow patterns of liquid phase in different sections as well as in entire digester were estimated at different operating conditions. To predict the flow behavior, model fitting is done using axial dispersion model (ADM) and tank-in-series with back mixing model (TIBM) with a plug flow component connected in series. The dispersion is decreasing as the material passes through the first to the third tube of the digester. The optimum conditions for the operation and pulp quality have also been obtained. The industry has started operating the digester at the optimum conditions as per recommendations based on this study.

CHAPTER 6 covers the RTD modeling of the data obtained after experiments conducted on two identical two-tube pulping digesters (old and new) at M/s Trident Industries Ltd. Barnala, Punjab (India) using ^{99m}Tc radioisotopes. Axial dispersion model and tank-in-series with back-mixing models were used for fitting the data. In the case of the two-tube digester, at a low wheat straw feed rate, the recycling of white liquor was observed and it affected the delignification, which resulted in high residual alkali in black liquor and Kappa number of the pulp (low delignification). Inside the second digester (old one), a 23% reduction in MRT was observed as compared to the first digester probably due to the channeling of white liquor and/or scaling inside the digester. The lower values of MRTs for the second digester than the theoretical MRTs show the lower effective volume which further affected the delignification. The industry has started taking action to repair the old digester for optimum performance. They identified the scaling inside old digester which was the reason behind low MRT and started different measures to remove the scaling.

CHAPTER 7 provides the conclusions for present work and the future scope of the work.

In the end, recommendations for future work has been given which presents an idea to extent the work.

References have been listed and publications list has been also included in the end of thesis.

Chapter-2 Literature Review

In any industry, optimum product quality and economic gain is the main objective of the process plants. Chemical reactors are the heart of any industry/plant. The efficiency and performance of these reactors depend upon various factors. RTD of any reactor is one of the most informative tool which provides the knowledge about flow behavior and other dynamics of the reactor [57]. RTD study using radiotracer is one of the methods to investigate the performance of any reactor. In the next section, various RTD studies using radiotracer on industrial, pilot and lab scale are summarized.

2.1 RTD study using radiotracer

A number of RTD studies have been conducted on various industrial, laboratory and pilot scale systems using radiotracers. A review of various radiotracer studies has been published by Pant et al. in 2001 [58]. The review shows that the troubleshooting and analysis using radiotracer technique provides huge economic benefits to the chemical process industry. Measurement of residence time distribution in various industries is discussed with some other applications of the radiotracer. These applications of radiotracer technique include blockage detection, leak detection, flow rate measurement, residence time distribution measurement, material or volume measurement, separation efficiency, groundwater direction and velocity measurement, effluent dispersion and other miscellaneous applications are extensively discussed with their methods. Slow growth of the radiotracer technique was observed in earlier decades as explained by Pant et al. [58]. The reason behind the slow growth was the lack of awareness of tracer technologies and the interaction between this technology and industries. Very little literature availability on radiotracer application also a reason for slow growth at that time [58]. Here, RTD studies using radiotracer technique on industrial, laboratory scale and pilot scale systems after 2001 have been explained. Some of the selected industrial experiments using radiotracer in different industries are discussed here.

2.1.1 RTD studies on industrial scale

At the industrial scale, radiotracer studies are classified according to their production area. The classification includes oil and gas industry, pharmaceutical and bioprocessing industry, polymer, plastic and fiber industry, fertilizer and pesticide industry, mineral processing, organic and inorganic chemical industries.

2.1.1.1 Oil and gas industry

Oil and gas industry is among the core industries which largely influences the economy of the country. In this industry, various equipments are used to carry out the process and out of these, the fluidized bed is the equipment which is widely used for different processes. The selected RTD experiments using radiotracer technique are listed in Table 2.1.

The main problem associated with the fluidized bed is how to control the circulation rate of the solid particle. A study was carried out by Abellon et al. [59] to measure the circulation rate of solid particles using MRT in cold four-cell, interconnected fluidized bed reactor. Glass beads containing ^{24}Na radionuclide were used to follow the process. ^{192}Ir radiotracer was used on the melted glass in such a manner that the density of the glass bead does not change. It was ensured that the mean residence time was not influenced by the size of the radiotracer. The fluidized bed was considered as fully mixed and the presence of static electricity influenced the residence time distribution inside the bed [59].

Similar fluid catalytic cracking (FCC) units of two different refineries were tested in 2009 for constituents present in a catalyst which can be activated [60]. The catalyst samples were activated via instrumental neutron activation analysis (INAA). Eleven components of the catalyst were activated but the radioactivity of the lanthanum and sodium was observed highest as compared to the other components of the catalyst. These irradiated samples were used as an intrinsic radiotracer to find out the MRT and axial mixing in the FCCU. It was also observed that lanthanum and sodium were present in higher concentration than other elements [60].

Pant et al. also studied the flow behavior in a fluidized bed of coal gasifier (Table 2.1) [37]. The ^{140}La and ^{198}Au radiotracers adsorbed on the surface of coal particles were used as independent tracers. 70-80% activity of radiotracer was adsorbed on the coal particles. The same process of adsorption of ^{198}Au radiotracer on the surface of coal particles was used to estimate the circulation rate of coal particles in a circulating fluidized bed system [28]. Circulation rate was measured by using mean residence time.

The radiotracer technique was also used in the sieve plate extraction column to estimate the axial mixing, liquid holdup and slip velocity in the dispersed phase of the system [61].

Table 2.1 Some RTD studies in oil and gas industry

System	Tracer used	Model used for simulation	Parameters analyzed	References
Interconnected fluidized beds	^{24}Na and ^{192}Ir adsorbed on glass	---	Solid circulation rate, MRT, comparison of RTD and models, flow patterns	[59]
Fluid catalytic cracking unit	^{140}La, ^{24}Na as intrinsic radiotracer	Axial dispersion model	Degree of mixing, MRT	[60]
Fluidized bed gasifier	^{140}La and ^{198}Au	The tanks-in-series model	Degree of axial mixing, flow behavior, and MRT	[37]
Circulating fluidized bed system	^{198}Au	Plug flow model	Circulation rate and MRT	[28]
Liquid-liquid sieve plate extraction column	^{99m}Tc (Sodium pertechnetate)	Axial dispersion model	Axial mixing, slip velocity, holdup, MRT	[61]
Hydrocarbon transmission pipeline	^{131}I (Sodium iodide and iodobenzene)	Tanks-in-series model	Flow rate of water and crude oil, flow pattern	[62]
Trickle bed reactor	^{82}Br	Axial dispersion with exchange model	Liquid holdup, axial mixing, and MRT	[63]

^{99m}Tc was used as a radiotracer in water as the dispersed phase (Table 2.1). At the same time, ^{131}I as ^{131}INa and $^{131}IC_6H_5$ radiotracers were used to determine the flow rate of the multiphase flow system in a pipeline containing water, crude oil, and gas [62]. ^{131}INa was injected in the water phase and $^{131}IC_6H_5$ in the oil phase. From the obtained curve, it was observed that the flow rate of water was faster than crude oil due to the friction

between the layers of two fluids. Also, the density of the water is greater than crude oil and the system is water dominated.

The liquid holdup and dispersion of trickle bed reactor which was packed with the hydrophobic and hydrophilic material were estimated using ^{82}Br as radiotracer [63]. It was observed that the dispersion changed when bed packing material was changed.

2.1.1.2 Pharmaceutical and bioprocessing industry

In pharmaceuticals and bioprocessing industry, RTD technique is applied to determine the influence of the parameters or process variables on the efficiency of the system and/or to study the behavior of fluid particle inside the reactors (Table 2.2).

A water disinfection photoreactor has been studied to analyze the different inlet conditions in which 1st inlet located at central bottom position causes dead zones but these dead zones can be reduced by using lateral inlet conditions. The high efficiency of the system can be obtained by using the three lateral configurations which limit the axial dispersion [64]. A plug flow component with ADM is used to describe the lateral inlet conditions.

Table 2.2 RTD study in pharmaceutical industry

System	Tracer used	Model used for simulation	Remarks	References
Photocatalytic reactor for water disinfection	^{113m}In	Plug flow with perfect mixer and plug flow with axial dispersion model	Flow behavior inside reactor	[64]

2.1.1.3 Polymer, plastic and fiber industry

The RTD studies related to polymer, plastic and fiber industries are listed in Table 2.3. A bubble column reactor used to produce dimethyl terephthalate is investigated using ^{82}Br [65]. Dimethyl terephthalate is commonly used in the production of plastic, fibers, film, etc. To analyze the degree of mixing and MRT of the reactor, it was needed to carry out an RTD test (Table 2.3). To set up another reactor for production enhancement, it is necessary to identify any flow abnormalities in the present reactor. There was no flow meter installed in the recycling loop, the flow rate of the recycling stream (liquid phase)

was measured by the radiotracer test. A tank in a series model with a plug flow component in the recirculation loop was used to characterize the experimental data and recirculation rate was measured. The results obtained through this study were also used to validate the theoretical calculation and to design a new oxidizer [65].

Table 2.3 RTD study in polymer, plastic and fiber industry

System	Tracer used	Model used for simulation	Remarks	References
Oxidizer (bubble column reactor)	^{82}Br (p-dibromo-biphenyl)	Single tank with a plug flow component in recirculation	Degree of axial mixing, MRT, recirculation rate	[65]

2.1.1.4 Fertilizer and pesticide industry

The phosphoric acid is used in the production of phosphate fertilizer (Table 2.4). The investigation of phosphoric acid production plant has been done using ^{99m}Tc radiotracer by Abdelouahed and Reguigui [66]. The radiotracer ^{99m}Tc and ^{131}I were used to trace the process material. Also, the safety aspect related to the radioactive material, injection protocol, detection system and radiotracer advantages are described in this paper. The main aim of the study was to obtain the maximum information which was not possible by using conventional tracer [67].

Table 2.4 RTD study in fertilizer and pesticide industry

System	Tracer used	Model used for simulation	Remarks	References
Phosphate reactor	^{99m}Tc and ^{131}I	Perfect mixers with recycle	Reason for operation below specification, flow rate, degree of mixing and MRT	[67]

2.1.1.5 Mineral processing, organic and inorganic chemical industry

Radiotracer study was carried out to determine the RTD of two identical aniline production reactors by Pant in 2002 [68]. The RTD of the normal reactor was used as a

signature RTD for the abnormally operating reactor (Table 2.5). An industrial-scale analysis has been carried out to determine the inadequate heat transfer from the shell side of the aniline production reactor (Table 2.5).

In the case of the second reactor, theoretical MRT is almost equal to the experimentally obtained MRT which indicates the normally functioned reactor. For the first reactor, theoretical MRT is greater than the experimentally measured MRT which indicates the decrease in the geometric volume of the reactor which is caused by scaling or fouling.

$$\% \, Scaling \; or \; Fouling = \left(1 - \frac{\bar{t}}{\tau}\right) 100 \tag{2.1}$$

Table 2.5 RTD studies in mineral processing, organic and inorganic chemical industry

System	Tracer used	Model used for simulation	Remarks	References
Aniline production reactor	^{82}Br as para dibromo-benzene	Tanks-in-series with two parallel flow streams	Abnormal operation with low efficiency, 60% fouling	[68]
Gold leaching tank	^{131}I	Tanks-in-series model with exchange	Validity of design, operational efficiency, malfunctioning, dead volume	[69]
Copper (thickening, filtration, drying) process	^{64}Cu	Tanks in series with different combinations	MRT, Separation efficiency, mixing, flow rate	[70]

From this study, it was observed that the reason behind the inadequate heat transfer was the reduction in the effective volume of the reactor due to the fouling/scaling [68].

To determine the effective volume and to validate the design of the gold leaching tanks (Table 2.5) connected in series, ^{131}I was used as a radiotracer [69]. During the investigation, both online detections and manual sampling were used to measure the

concentration curve. The online data measurement process was found to be more convenient than sampling, though the data obtained by both processes were identical.

RTD study was used to analyze the Dorr thickener, filter and drier of the copper ore concentrate and dewatering process [70]. Flow parameters like separation coefficient and flow rate were determined for process simulation and to control the process. It was observed that the radiotracer technique is best to determine the RTD in the opaque system. Simulation results obtained have provided the details of the system.

2.1.2 RTD study on pilot scale

The selected pilot scale RTD studies using radiotracer technique are given Table 2.6. Radiotracer ^{131}I as sodium iodide was used to investigate the hydrodynamic characteristics of the liquid phase in a pilot scale hydrogenation process (Table 2.6). Very random behavior was observed in the hydrogenation process. The drops of liquid were formed at different locations in the packing and these drops when fell down, a peak of tracer concentration was observed using NaI scintillation detector [71].

The flow pattern in a riser of cold fluid catalytic cracking was determined using radiotracer ^{60}Co and ^{82}Br to trace the gas phase [72]. The flow follower technique was used to find out the flow behavior in the riser (Table 2.6). The RTD measurement using radiotracer technique provides the best results for the system. Further, the fluidized catalytic cracking unit in refinery was studied to monitor the different parameters at pilot scale. Radiotracer gas was used to measure the holdup of syngas in a bubble column reactor which was being used for methanol synthesis [73]. In the chemical industry, it is desirable that the bubble column reactor should have high superficial gas phase velocity with high pressure. The ADM with interface mass transfer is the basis for the design of a bubble column reactor, however, this type of correlation does not provide a reliable estimate for scale up. So, the liquid phase mixing is predicted by using two-compartment mechanistic models. These models also provide the tools for reactor scale-up and to determine the efficiency of the reactor.

RTD test was performed on a pilot scale poison tank using ^{82}Br as a radiotracer [74]. Liquid pumped with time was determined by filling the tank with a radiotracer and measuring the concentration at the outlet (Table 2.6). MRT and stagnant regions were determined using the radiotracer test. ADM and tank-in-series with back-mixing model were used for simulation. The tank-in-series with the back-mixing model gave the better

fit with experimental data. Results obtained from simulations were used for scale-up of the system. ^{82}Br was also used to test the hydrodynamic behavior of the pilot scale continuous leaching reactor [75]. RTD test was carried out to validate the design of pilot scale reactor. Tank-in-series model is used for RTD modeling and to measure the degree of mixing.

Table 2.6 RTD studies on pilot scale reactors

System	Tracer used	Model used for simulation	Remarks	References
Hydrogenation column	^{131}I	---	Random residence time behavior	[71]
Riser tube of catalytic cracking unit	^{60}Co and ^{82}Br (gaseous phase)	---	Transit time, MRT and flow pattern	[72]
Methanol synthesis bubble column reactor	^{41}Ar	Single bubble class model, two bubble class model	Slip velocity of gas phase, gas holdup, efficiency	[73]
Boron poison tank	^{82}Br	Axial dispersion model, tank-in-series with back-mixing model	Mixing properties, flow rate, flow pattern, MRT, (Pe=2, N=2-4, back-mixing ratio=10-53)	[74]
Uranium continuous leaching reactor	^{82}Br	Tanks-in-series model	Dead zone, MRT, (N=1-2)	[75]
Soaker visbreaking unit	^{82}Br	Tanks in series with back-mixing model	Effect of perforated plates on back-mixing, MRT, (N=2-7, back-mixing ratio=3-6)	[46]
Circulating fluidized bed system	^{198}Au	Axial dispersion model	Circulation rate and MRT	[28]

To measure the RTD of the heavy residue of the petroleum, a radiotracer test was carried out in a soaker or vis-breaker unit of the refinery using ^{82}Br [46]. The study was carried out at very high temperature (430 °C) and pressure (≈11 kg/cm^2) which was not possible using conventional tracers. The system consists of three parts as feed section,

furnace section and the product recovery section. The feed is preheated in a heating device at the feed section and sent to the furnace. The pilot plant is designed for a flow rate of 20 l/min. The outlet of the furnace was connected to the soaker where cracking was taking place and hydrocarbons were evolved. Ten radiotracer experiments were carried out successfully using short residue and vacuum gas oil at different operating conditions.

As the liquid phase was converting in the gaseous phase, the general equation used for MRT was not provided the system RTD. Tank-in-series with the back-mixing model was used to simulate the experimental data and to obtain the MRT of the system.

The process of adsorption of ^{198}Au radiotracer on the surface of coal particles was used to estimate the circulation rate of coal particles in a circulating fluidized bed system [28]. Circulation rate was measured by using mean residence time. The system was described by the ADM. The particle circulation rate was affected by the bed height and fluidization velocity.

2.1.3 RTD study on laboratory scale

The selected RTD studies using radiotracer performed at laboratory scale are tabulated in Table 2.7. It is easier to carry out the RTD study on laboratory scale rather than directly carrying out on the plant site. Hence, a preliminary study was carried out by Oriol et al. in a horizontal tube with two-phase flow using radiotracer technique [76]. The gas phase radiotracer (^{81m}Kr) was used to measure the velocities of gas phases and the volumetric void fraction which is possible only using the radiotracer technique. The response for the gas phase allows determination of the gas-liquid regimes [76].

Kasban et al. [56] performed the RTD experiment to measure the mixing time, flow rate and RTD of the mixing process (Table 2.7). The laboratory set up consisted of a tank with a height of 80 cm and diameter 30 cm. The four mixing paddles were mounted inside the tank.

The obtained simulation results showed that as the speed of the motor increased, mixing time decreased. The readings of both the detectors at input and output were used to measure the flow rate of the liquid phase which was not possible without the radiotracer test.

Recently, nanoparticles of the gold radiotracer (^{198}Au-NPs) have been synthesized and used to trace the laboratory scale bubble column reactor. Results were compared with

an experiment conducted using another radiotracer (^{82}Br) [77]. The obtained results with both radiotracers were found identical. It was also noticed that the hydrodynamics of the bubble column reactor was influenced by a change in the liquid flow rates. The dynamics are identified using the tank-in-series with the back-mixing model. The degree of back-mixing decreased on increase in the flow rate of the liquid phase and found independent of gas flow rate.

Table 2.7 RTD studies on lab scale reactors

System	Tracer used	Model used for simulation	Remarks	References
Horizontal tube for heat exchanger	^{81m}Kr	--	Gas phase velocity, void fraction	[76]
Tank with four stirrers	^{99}Mo	Perfect mixers with recycling model	Mixing time, flow rate, MRT	[56]
Bubble column reactor	^{198}Au nano-particles and ^{82}Br	Tanks-in-series with back-mixing	Similar behavior of two radiotracers, back-mixing in column	[77]

It can be concluded from the literature review that various studies related to radiotracer RTD experiments have been carried out. The studies are classified as industrial-scale RTD, pilot plant RTD and laboratory scale RTD experiments. But, no study is available on pulping digester using radiotracer or any conventional tracer. RTD test acts as a convenient tool for understanding the phenomenon inside the chemical reactors and the RTD obtained from radiotracer technique having more advantages than obtained from using conventional tracers. The literature shows that the various studies have been successfully conducted using the radiotracer which confirms the applicability of the radiotracer including the investigation of mixing efficiency, mean residence time measurement, flow rate measurement, flow behavior of fluid inside reactors, mixing pattern, etc.

Besides the RTD investigation its modeling is equally important to explore different parameters and the hydrodynamics of the system. The available RTD models are

the plug flow model, axial dispersion model, tank-in-series models, compartment model, etc.

2.2 Residence time distribution models

A number of models are available in the literature which are used for RTD modeling [78-80]. In the present time, designing and performance of the reactors also have been investigated using RTD modelling [81-83]. Through RTD modelling, the hydrodynamic behavior of the reactor is predicted by optimizing the model parameters [84]. Some of the basic RTD models are explained below.

2.2.1 Axial dispersion model

As per the available literature on RTD, axial dispersion model (ADM) is described by the following differential equation for an impulse input of tracer [27]:

$$\frac{\partial c}{\partial \theta} = \left(\frac{1}{Pe}\right)\frac{\partial^2 c}{\partial z^2} - \frac{\partial c}{\partial z} \tag{2.2}$$

where, c represents the dimensionless concentration of the tracer in the system, Pe is the peclet number of the system, θ is the dimensionless time (t/τ) and z is the dimensionless distance ($ut + x$)/L. The Peclet number (Pe) is defined as:

$$Pe = \frac{uL}{D} \tag{2.3}$$

where, u is the bulk fluid velocity, L is the characteristics length and D is the dispersion coefficient. The relation between RTD function and dimensionless time with respect to Pe is shown in Figure 2.1, which shows that how the shape of RTD curve changed from asymmetric at high dispersion to the symmetric at low dispersion coefficient. If the value of dispersion number (D/uL) is less than 0.01, the ADM is selected by considering the small extent of dispersion, whereas if D/uL is greater than 0.01, then it considered as large dispersion and the equation is selected accordingly [27]. A number of researchers used ADM for RTD study [32, 85-87]. Various studies [86, 88, 89] indicate that the prediction of axial dispersion component is one of the steps to develop the RTD model.

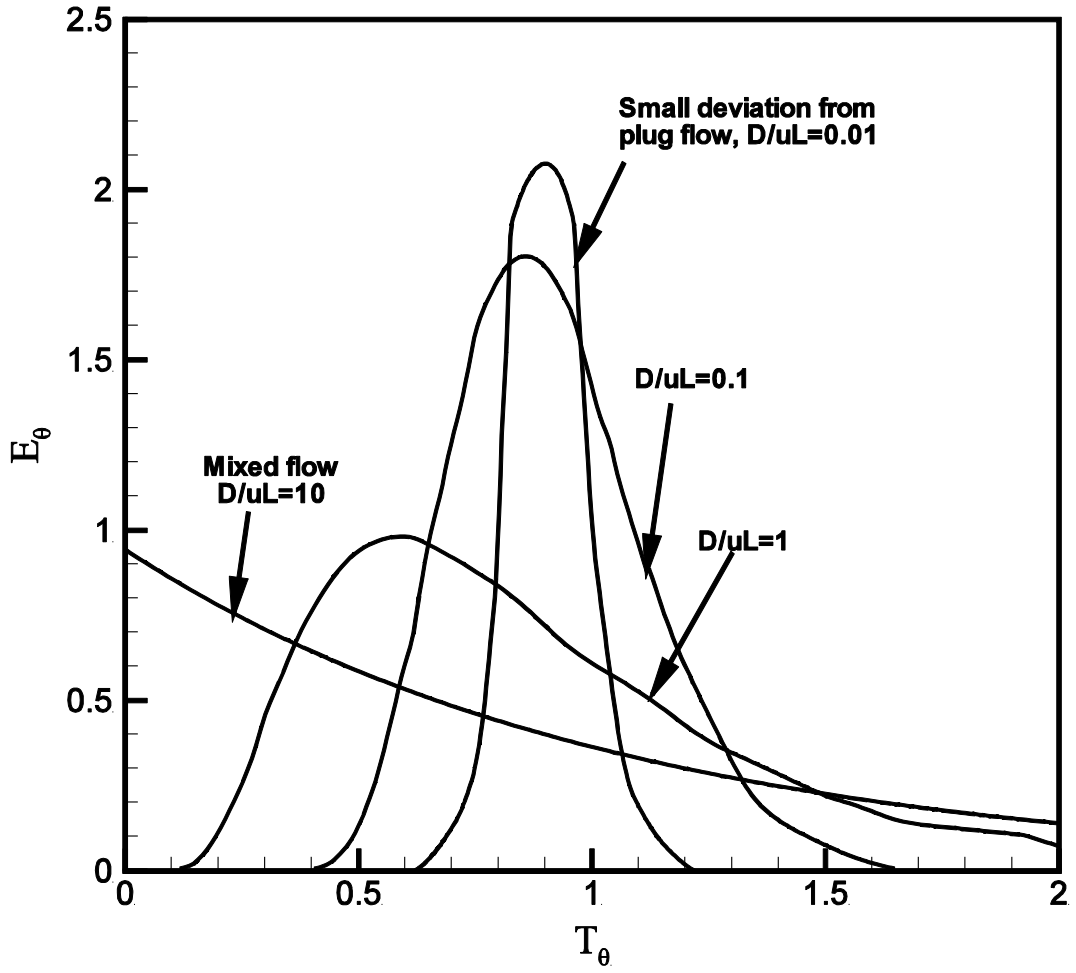

Figure 2.1 General tracer response curve for axial dispersion model [26]

The ADM is generally used in long pipes with laminar flow, tubes having turbulent flow, packed beds, etc. Despite the combination of plug flow and perfect mixers, ADM is also an ideal substitute for generating the conception of RTD for non-ideal reactors [27].

2.2.2 Tank-in-series model

This model represents the *N* number of tanks with equal volume connected in series. For the small value of *N*, even a small deviation in *N* may lead to large deviation in the residence time distribution. Whereas, for a large value of *N*, the large change is insignificant and model behaves like plug flow. In other words, as the number of tanks increased, the degree of mixing decreased. A comparison between axial dispersion and tank-in-series (TIS) at steady state of an enzymatic reactor is given by Abu-Reesh and Abu-Sharkh in 2003 [80]. The relation between Peclet number (Pe) for ADM and number of tanks in series (*N*) for the tanks in the series model at low dimensionless residence time is given by:

$$Pe = 2(N-1) \tag{2.4}$$

ADM and TIS models behave identically at zero dispersion or when *N*=1 (Abu-Reesh and Abu-Sharkh, 2003) [80]. Pulse response for N number of tanks is summarized and is given below [27]:

$$E(t) = \frac{t^{N-1}}{\bar{t}^N} \frac{N^N}{(N-1)!} e^{-\frac{tN}{\bar{t}}} \tag{2.5}$$

At very high back-mixing, the model is not able to predict the absolute results. A number of modifications are developed in the existing models. The model is explained by Saravanathamizhan et al. in 2008 [90] assuming three different cases for 3 CSTRs in series i.e. (i) volume of each tank in CSTR is equal, (ii) volume of each tank of CSTR is unequal and (iii) volume of 1st and 3rd tank is equal and volume of 2nd tank is greater than 1st and 3rd tank. RTD equations are derived for each case.

In another study, a similar type of approach was used to solve the CSTR containing one large tank and two small tanks in series (Yianatosa et. al, 2005) [91]. A CSTR with three tanks in series each having different volume is shown in Figure 2.2.

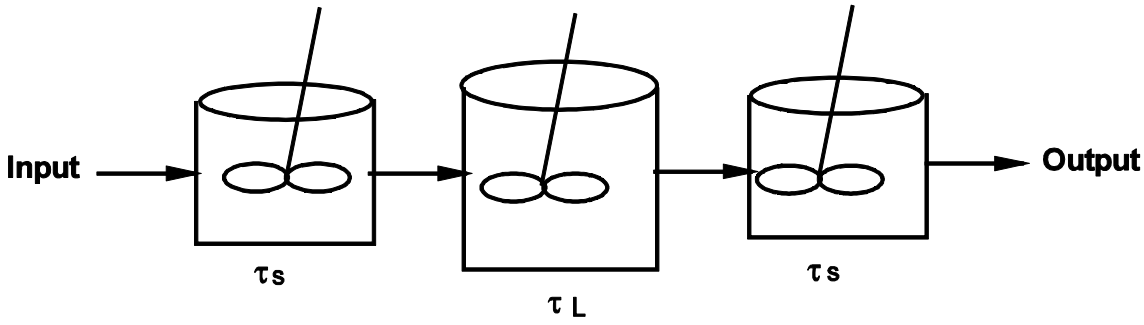

Figure 2.2 CSTR with different volume of tanks

2.2.3 Compartment model

Single parameter models (ADM and TIS) are not able to define the large deviation in the ideal flow. The multi-parameter models are capable to describe the stagnant volume, bypassing or recycling, dead zones, etc. [92] Further, the increase in the parameter may increase the complexity of the model with an improved description of RTD curve. The system which has stagnant or dead volume and involves a stream of fluid exchange between dead volume and stagnant regions is explained by Dagadu et al. [69]. Dead

volume of 15-20% is observed in gold leaching tank and tanks-in-series model with an exchange between stagnant zones and dead volume used to model the experimental data.

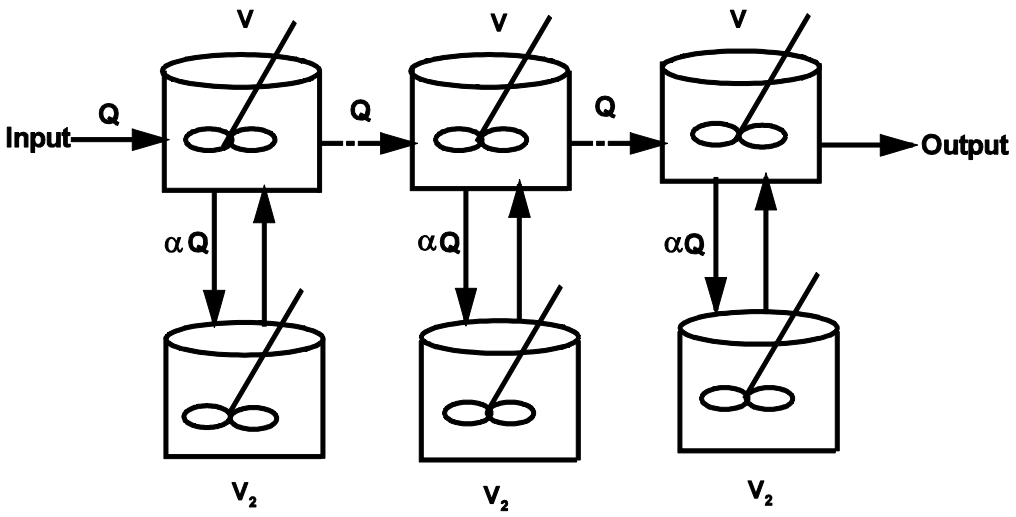

Figure 2.3 Tank-in-series with exchange model (IAEA, 2008) [32]

Similar tank-in-series with exchange model is shown in Figure 2.3, here, V represents the volume of the mainstream, V_2 is the volume of the dead zone, Q is the flow rate of the mainstream and αQ is the flow rate of the exchange stream. The model consists of four parameters i.e. a number of tanks (N), MRT of mainstream (τ), MRT for the exchange between stagnant zone and main flow stream (τ_m) and the ratio of the volume of exchange stream to the volume of the mainstream (K). The solution for this model is given as:

$$\frac{dC_1(t)}{dt} = \frac{1}{\tau}[C_{in}(t) + \alpha C_2(t) - (1-\alpha)C_1(t)] \tag{2.6}$$

$$\frac{dC_2(t)}{dt} = \frac{1}{\tau_m}[C_1(t) - C_2(t)] \tag{2.7}$$

where $\tau_m = V_2/\alpha QN$ is the MRT for the exchange stream.

There are numbers of studies available in the literature showing the various combinations of different models [93, 94]. A comparison of plug flow with recycling, tanks in series with recycling and plug flow in combination with the tanks in series with recycling has been explained by Fu et al. [94]. In Figure 2.4, tank-in-series with recycle

stream has been shown where Q is the inlet and outlet flow rate, αQ is the flow rate of the recycle stream and $(1+\alpha)Q$ is the flow rate of the mainstream.

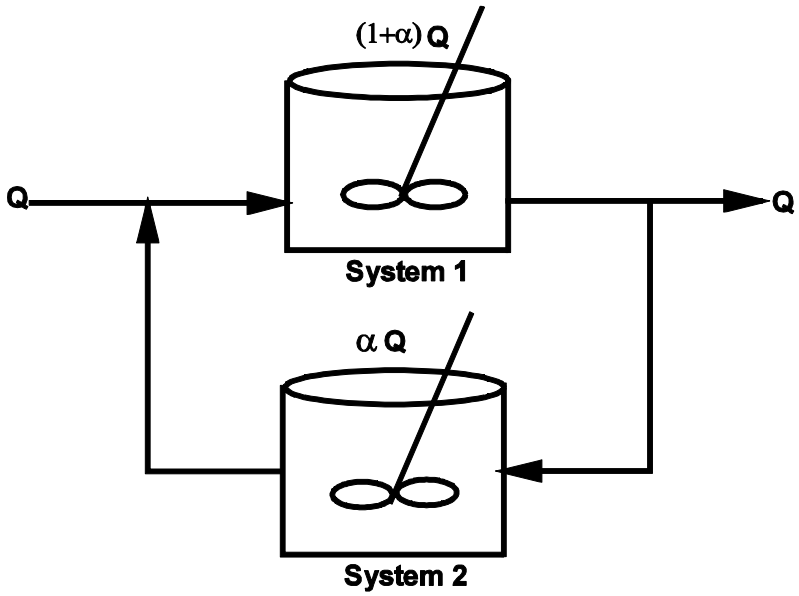

Figure 2.4 Tank-in-series model with recycle stream

The recycle rate is determined using the equation:

$$\alpha = \frac{Q_r}{Q} \tag{2.8}$$

where Q_r is the flow rate of the recycle stream. Another study of Martin shows the comparison of the extended tanks in a series model with the conventional tanks-in-series model and closed dispersion model [95]. Extended tank-in-series model is found superior to the tank-in-series model and differ significantly from closed dispersion model in the range of $0 < Pe < 29$.

Chapter-3 Material and Methods

3.1 Materials

3.1.1 Wheat straw

Agro residue of the wheat crop (wheat straw) was obtained from the farmers of Punjab and Haryana region of India, in the chopped form of pieces 2-4 cm. The chopped wheat straw was cleaned and soaked in water for 48 h for the softening of biomass. Wheat straw is a complex mixture of lignin, cellulose and hemicelluloses as three main components, and a small amount of soluble substrates (also known as extractives) and ash, which is similar as other biomass of ligno-cellulosic composition. The overall chemical composition of wheat straw might slightly differ depending on the type of wheat species, soil, climate and cultivation conditions.

3.1.1.1 Physical and chemical properties of wheat straw

Physical properties of the wheat straw determined as per the procedure mentioned in the later section are given in Table 3.1. The moisture content of the wheat straw has been found to be 2.01 % which is very low as compared to the normally reported values [96]. The moisture content of wheat straw may vary due to the different cultivation and storage conditions. The dry weather condition is also one of the reasons of low moisture content. The available literature shows that the bulk density is a function of wheat straw particle size and cutting/grinding methods [96]. The bulk density of the wheat straw is measured as 180 kg/m^3. The value of wheat straw porosity is obtained as 65.30 % which is similar to the value reported in the literature [96]. The physical properties of the wheat straw used at industrial as well as at pilot scale pulping are shown in Table 3.1.

Table 3.1 Physical properties of wheat straw

Moisture content	2.01 %
Bulk density	180 kg/m^3
Porosity	65.30 %

The chemical composition of wheat straw is shown in Table 3.2. The wheat straw mainly contains 67.3 % holocellulose, out of which 40 % is cellulose, 18.3 % lignin, and 8.2 % ash.

Table 3.2 Chemical composition of wheat straw

Components	Composition (%)
Holocellulose	67.3
Pentose	2.6
Acid soluble lignin	1.3
Acid insoluble lignin	17.0
Ash	8.2
cellulose	40

3.1.2 White liquor

The other main raw material is white liquor which is the solution of sodium hydroxide and some other chemicals such as sodium sulfide, sodium carbonate and sodium chloride are also used in trace amount. The composition of the white liquor is given in Table 3.3. Sodium hydroxide is used for the solution with a purity of 94%. The purity of the sodium hydroxide was determined by dissolving the 2 g of sodium hydroxide in 50 ml of distilled water. The phenolphthalein was added to the solution and titrated against 1N HCl. The percentage purity was determined according to the following formula:

$$\% \, Purity = \frac{B.R. \ * \ 0.04 * 100}{Sample \ weight} \tag{3.1}$$

where B.R. is the burette reading.

Table 3.3 Chemical composition of white liquor

Chemicals	Composition (w/w %)
Sodium hydroxide	8.28
Sodium sulfite	0.44
Sodium carbonate	0.88
Sodium chloride	2.20

3.1.3 Radiotracer

The radiotracers are used to determine the RTD of pulping digesters at industrial scale. According to the selection criteria explained in the Chapter-1, the three radiotracers were found to be most suitable based on their short half-life, activation energy and chemical form used for the specific phase to trace the liquid phase of the digester. These radiotracers are ^{82}Br, ^{198}Au and ^{99m}Tc. These radiotracers were obtained from the Board of Radiation and Isotope Technology (BRIT), Mumbai, under the supervision of a team of scientists from Bhabha Atomic Research Center (BARC), Mumbai. The specifications of the radiotracers are given in Table 3.4.

Table 3.4 Properties of the radioisotopes

Isotope	Half-life	Radiation energy (MeV)	Chemical form	Tracing of the phase
Gold-198	2.7 day	0.41	Chloroauric acid	Solid, aqueous
Bromine-82	36 h	0.55	Ammonium bromide	Aqueous
Technetium-99	6 h	0.14	Sodium pertechnatate	Aqueous

3.2 Equipment

3.2.1 Industrial scale three-tube digester

First phase RTD experiments have been carried out in a three-tube continuous pulping digester at M/s Satia Industries Ltd., Muktsar Sahib, Punjab, India. Satia Industries Ltd. is one of the biggest paper mill using wood and other non-conventional raw materials (wheat straw, veneer waste and *sarkanda*) for pulp production.

The schematic of an industrial scale three-tube continuous pulping digester is shown in Figure 3.1. It consists of three horizontal tubes connected by vertical necks. Each tube of the digester is fitted with helical screw conveyor to facilitate the transport of pulping mixture along with the tube length. These helical screws are driven by three-phase induction motors. The length of individual digester tube is 12 m with an internal diameter of 1.450 m. Wheat straw screw feeder is connected to the inlet of the first tube to provide the feed at high pressure to counter the inside pressure of the digester. The white liquor is fed using white liquor feeding pump at the inlet of the first tube. Connections are provided

on each tube for superheated steam injection. At the outlet of the third tube, the pulp is discharged in a blow tank and sent for the further operations.

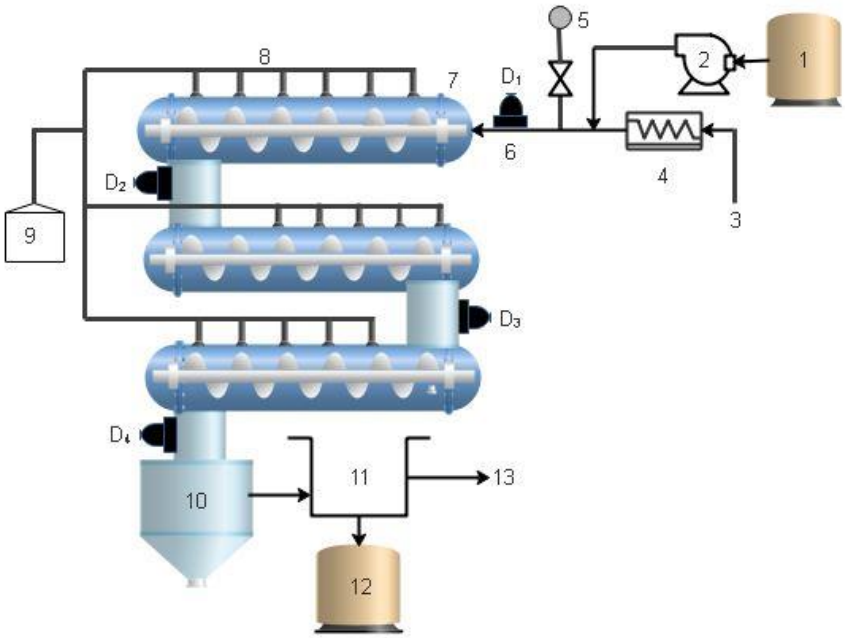

Figure 3.1 Schematic diagram of three-tube continuous digester with experimental setup. 1-white liquor storage tank, 2-liquor feeding pump, 3-washed wheat straw, 4-wheat straw screw feeder, 5-radiotracer injection port, 6- scintillation detectors (D_1, D_2, D_3, D_4), 7-digester tube, 8-steam pipes, 9- boiler, 10-blow tank, 11-pulp washer, 12-black liquor storage tank, 13-pulp.

3.2.2 Industrial scale two-tube digester

The construction of two-tube pulping digester is similar to a three-tube digester; the only difference is the reduced number of tubes. It is also equipped with screw conveyor and multiple steam injection inputs. The raw material feed mechanism is also similar to three-tube pulp digester. The internal diameter of each digester tube is 1.10 m and the length of each tube is 7.7 m. Hence, the effective digester length is 15.4 m. The schematic of the two tube digester is shown in Figure 3.2.

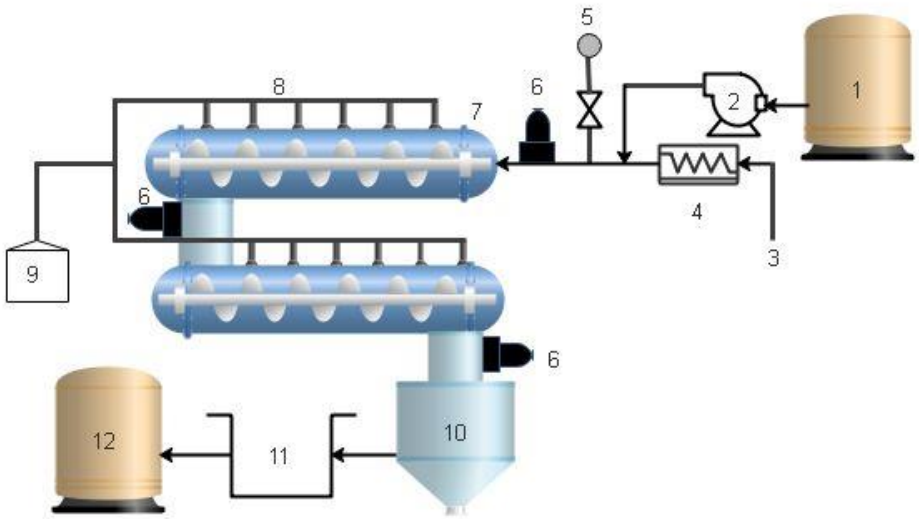

Figure 3.2 Schematic of the two-tube continuous industrial pulping digester. 1-white liquor storage tank, 2-white liquor feeding pump, 3- wheat straw, 4- wheat straw screw feeder, 5- radiotracer injection port, 6- gamma rays detector, 7-digester tube, 8- steam lines, 9- steam generator, 10-blow down tank, 11-pulp washer, 12- pulp storage tank

The feed rate of wheat straw is controlled with the help of screw feeder rpm. The white liquor is stored in a storage tank. The white liquor was fed in the first digester tube by the separate inlet near to the feed point.

The flow rate of white liquor is controlled with the help of a flow controller. Thermocouples and pressure gauges are being installed in each tube to measure the temperature and pressure respectively. Temperature is displayed on the control panel. High-pressure safety valve is also installed on each tube of the digester. The whole set up was operated and controlled through the controlled panel.

3.3 Procedure

3.3.1 Pulping

For industrial scale pulping, wheat straw and white liquor were used as raw materials. The wheat straw obtained from farmers was cleaned by washing to remove dust and other soluble impurities. After washing wheat straw was soaked in water for 36-48 h for softening of the biomass. The soaked wheat straw with the approximate consistency of 45-47% is ideal for the digestion process. Then it is fed to the digester along with white liquor through wheat straw screw feeder. A high-pressure white liquor feeding line injects

the white liquor in the digester near the screw feeder inlet section. The feeding process is crucial in the pulping process because solid/ semi-solid material has to be fed at high pressure of 7 kg/cm^2 and high temperature of 170 °C. To overcome this difficulty, a screw-feeder is used which compresses the biomass and develops a counter pressure of (>7) kg/cm^2. During the feeding process, the screw feeder reduces the moisture content of biomass up to 10%. The high pressure superheated steam is also injected at multiple points in the three-tube continuous digester. The injected steam maintains the operating temperature of 155-170 °C and operating pressure of 5.39-6.45 kg$_f$/cm^2. Additionally, the steam condensate gets mixed with the pulp mixture and fulfills the additional water requirement to maintain the pulp consistency in the digester.

The feed mixture horizontally moves in the three-tube digester with the help of screw conveyor. The speed of screw conveyor is used to increase or decrease the residence time of the material in the digester. During the movement of the feed mixture, wheat straw reacts with white liquor and white liquor absorbs/diffuses into the wheat straw. The diffused white liquor dissolves natural binder lignin and mixed in the liquid phase. After complete dissolving of lignin in the white liquor, the cellulose fibers are disintegrated and form pulp. During the delignification process the composition of the feed mixture and the physico-chemical properties of the mixture changes continuously along the length of the digester, this makes the process more complicated to understand. The digested mixture of pulp and black liquor is obtained from the outlet of the third tube of the digester.

3.3.2 RTD experiments

3.3.2.1 RTD experiments on three-tube digester

First set of experiments were performed on three-tube pulping digester using radiotracer ^{82}Br in Satia Industries Ltd. Muktsar. ^{82}Br in the form of ammonium bromide was identified as a suitable radiotracer to trace the liquid phase. It has similar physiochemical properties with the white liquor. Hence, ^{82}Br is the most suitable radiotracer to trace the white liquor. ^{198}Au was commonly used to trace the solid phase by adsorbing on the surface of solid process material. But, it did not adsorb on the wheat straw surface. Hence, the data from gold radiotracer was also used to trace the liquid phase.

A one-shot impulse tracer introduction technique was used for the determination of RTD of the continuous pulping digester.

In the first set of experiments, the small amount (2-5 ml) of the ^{82}Br as ammonium bromide (depending upon the activity of the time of the experiment) was dissolved in 100 ml of water. This solution was instantaneously injected in the white liquor inlet pipe near the feed point to the digester, and then it moved along with the pulping mixture in the digester. The injection time duration was < 1 s, and the introduced volume was small as compared to the scale of the digester so as not to change the existing flow pattern. Four sodium-iodide scintillation detectors were placed to trace the radioactive material ^{82}Br as shown in Figure 3.1. The detector placed at the inlet of the first tube provided the injection time of the radiotracer. The detectors were also placed at the outlet of each tube as shown in Figure 3.1. These scintillation detectors were coupled with the data acquisition system (DAS) using wired networks [32]. A multichannel DAS was used to record the online data. The DAS was set to record data points with a sampling time of 10 sec. As the radioactive material passed from the digesters, a pulse was observed on the monitor and recorded in the computer connected to DAS. Initially, at first detector, it showed a very sharp peak with high energy. Further, as the material moved along the digester from detector to detector, the peak height reduced and broadness of the peak increased.

3.3.2.2 RTD experiments on two-tube digester

The second phase of industrial RTD experiments was carried out on two identical two-tube pulping digesters in M/s Trident Industries, Barnala using radiotracer ^{99m}Tc. Schematics of the two-tube pulping digester is shown in Figure 3.2. Radiotracer ^{99m}Tc in the form of sodium pertechnetate was used to trace the liquid phase of the two-tube pulping digesters. Detectors were placed at the inlet and outlet of each tube as shown in Figure 3.2. The experimental procedure of the two-tube digester is same that of three-tube digester as explained in the previous section.

3.3.3 Analysis

3.3.3.1 Physical and chemical analysis of wheat straw

Physical properties of wheat straw such as porosity, moisture content, ash content and bulk density were measured by following the methods available in the literature [96]. For moisture content measurement, a fixed amount of wheat straw in a dish was weighed and kept in the oven for overnight at 105 °C. After drying, the dish was again weighed and reduction in weight was measured.

For porosity measurement, a fixed amount of wheat straw was placed in a 100 ml graduated cylinder and cylinder was filled with water up to the level of the sample taken. A mesh screen was placed on the sample to avoid the floating of wheat straw. The porosity was calculated according to the following formula [96]:

$$P(\%) = \frac{V_i - V_f}{V_s} 100 \tag{3.1}$$

where V_i is the volume of the sample and water, V_f is the total volume and V_s is the volume of the sample.

For bulk density measurement, an empty container was weighed. Then container was filled with wheat straw and compacted slightly to remove large voids. The container is again weighed with the sample and the bulk density was measured using the following relation [96]:

$$\rho_w = \frac{W_2 - W_1}{V} \tag{3.2}$$

where W_2 is the combined weight of the sample and container, W_1 is the weight of container and V is the volume of the container.

The chemical composition of the wheat straw was determined according to the Tappi standard. For cellulose and holocellulose measurement T264 om 88 [97], for ash content T 211 om 85 [98], for acid insoluble and acid soluble lignin T 222 om 88 [99-101] were used. For analysis, the sample was prepared using Tappi test method [102].

For sample preparation, extraction of 5-6 g of powdered wheat straw has been carried out using 200 ml of an ethanol-benzene mixture (1:2 ratio) for 8 h. After extraction, the sample was washed with ethanol to remove extra benzene and again extracted with ethanol for 4 h. Then, after removing the solvent, the sample in 500 ml distilled water was kept in a water bath at 100 °C for 1 h. Sample was washed with boiling distilled water and dried in an oven.

Acid insoluble lignin was measured by taking 1 g of above prepared sample and mixing with 15 ml of 72% sulfuric acid. The sample was kept in ice bath at 2 °C and then in a water bath at 20 °C for 2 h. After that 575 ml of water is added to the sample and total reflux was carried out for 4 h. The sample was kept overnight to settle the insoluble material. At last, the sample was filtered and firstly washed with hot distilled water and then with cold distilled water. After drying in the oven, the sample was weighted [99,

102]. In the case of acid soluble lignin, the absorbance of the filtered sample was measured at 205 nm.

For cellulose measurement, 0.5 g sample with a mixture of acetic acid and nitric acid was mixed with the help of cyclo-mixture and then kept in a water bath at 100 °C for 30 min. After cooling at room temperature, the sample was centrifuged for 15 min. The residue of the centrifuge was washed with distilled water, mixed with sulfuric acid and kept for 1 h. 1 ml of this solution was diluted with 100 ml of distilled water. Then 1 ml of this diluted solution was kept in ice bath for 5 min after adding the 5ml of chilled anthrone reagent. The sample was kept in a boiling water bath and then cooled. The color intensity of the sample was measured at 650 nm with a blank of distilled water [100].

Holocellulose content was measured by taking 2 ml of sample with 80 ml of distilled water, 2 g of sodium chloride and 0.5 g of acetic acid. This mixture was heated in a shaking water bath and a mixture of 0.5 ml acetic acid and 1 g of sodium chloride was added after each hour until the white color appears. Then the solution is cooled in ice bath and after filtration washed with distilled water and dried in an oven. Dry sample was weighed [103].

3.3.3.2 Analysis of pulp

The pulp obtained from the digester was analyzed for Kappa number [104]. Kappa number (K) is the measure of the degree of delignification of the solid raw material and determined by the reaction of pulp samples with acidified potassium permanganate solution (Tappi, T-236 om-99) [104]. For better pulp quality the value of kappa number should be low with less variation. The oven-dry sample of the pulp was taken (1g) in a 2 l beaker and 800 ml distilled water was added in the beaker. The beaker was kept on a magnetic stirrer and continuous stirring was done so that the pulp sample was completely disintegrated in the water. A solution of 100 ml of 0.1N $KMnO_4$ and 100 ml of 4N H_2SO_4 was prepared in another beaker and added to the sample solution by maintaining the temperature 25 °C. After 10 minutes, 20 ml of the KI and 2-3 drops of the starch solution was added to stop the reaction. The solution was titrated against 0.1N $Na_2S_2O_3$. The same procedure was also repeated for the blank sample. The Kappa number was calculated using the following relation:

$$K = \frac{P\ F}{W} \tag{3.3}$$

where F is the factor for correction and W is the weight of the sample and P can be calculated as:

$$P = \frac{B - A}{0.1} \tag{3.4}$$

where B is the amount of $Na_2S_2O_3$ consumed in the blank sample and A is the amount of $Na_2S_2O_3$ consumed in the test sample. For efficient delignification and improved digestion process, a low value of K is desired that requires a slightly excess amount of white liquor.

3.3.3.3 Analysis of black liquor

The analysis of the black liquor was done by measuring the amount of residual alkali present in the black liquor (Tappi, T 624 cm-00) [105]. In a beaker 25 ml of 20%, $BaCl_2$ was added with 25 ml of black liquor. This solution was made up 500 ml by adding distilled water. The solution was kept undisturbed for the next 30 minutes. Then 25 ml of the sample was taken from the solution and titrated against 0.1N HCl using phenolphthalein as an indicator.

$$RA = \frac{P * 0.1 * Eq.\ weight}{sample\ weight} \tag{3.5}$$

where P is the titration reading.

3.3.4 Data treatment for radiotracer test

The measured RTD data should be treated for background radiation, dead time correction, radioactive decay correction, tail correction, and smoothing. The data treatment steps are shown in Figure 3.3.

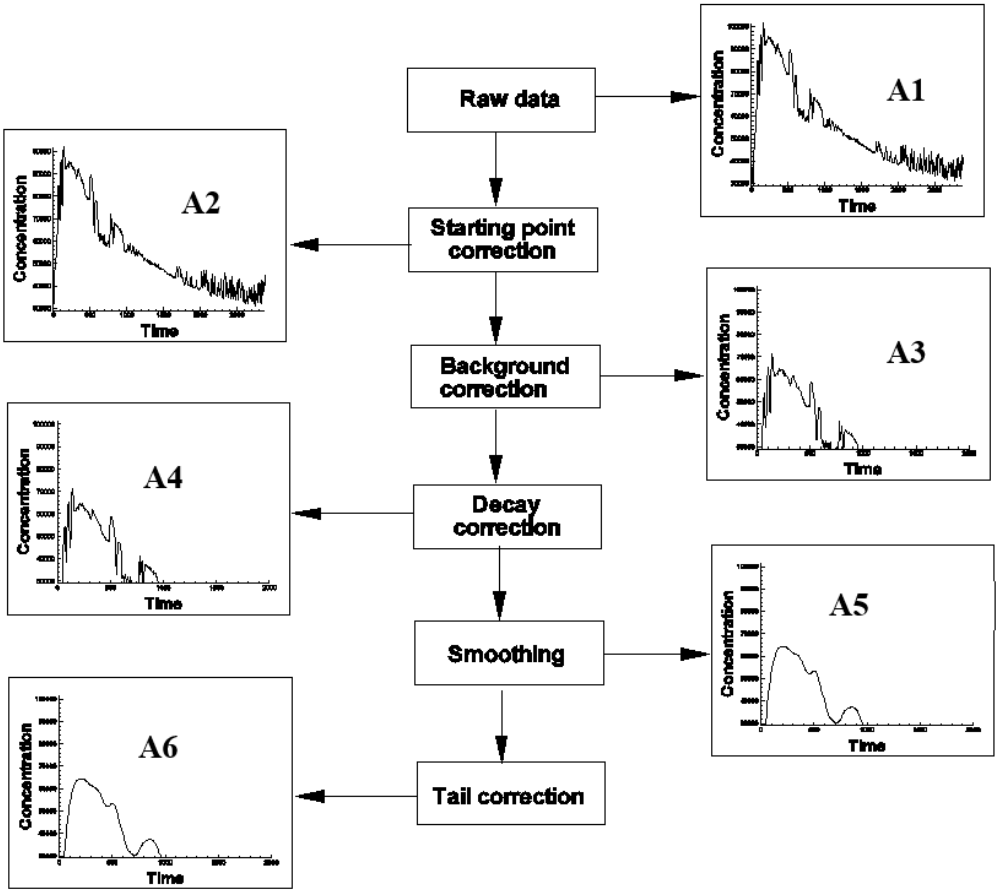

Figure 3.3 Schematic of data treatment

3.3.4.1 Background correction

Before the injection of the tracer in the system, it is essential to count the level of radiation in the background. This background radiation level is deducted from the experimentally measured data. The following equation is used for background correction:

$$C_c = C_m - B_r \tag{3.6}$$

here C_c is the corrected experimental data, C_m is the originally measured data and B_r is the background radiation level.

3.3.4.2 Zero time correction

This step is used to ensure the starting point of the data at zero time. In this step, data before the injection has to be removed to make the starting point at the zero time as shown in Figure 3.3 [32].

3.3.4.3 Radioactive decay correction

Radioisotopes are the compounds which decay exponentially with time, so it is essential to use the decay correction step. To compensate for the radioactive decay, we have to use the following function [56]:

$$C_r(t) = C_m(t)e^{-\lambda t} \tag{3.7}$$

$C_r(t)$ is the corrected concentration after decay correction, $C_m(t)$ is the concentration measured experimentally and λ is the decay constant

and can be defined as:

$$\lambda = \frac{\ln 2}{t_{1/2}} \tag{3.8}$$

where $t_{1/2}$ is the half-life of the radiotracer used.

3.3.4.4 Tail correction

If the concentration of the tracer does not go back to zero after monitoring, then tail correction step is used. Tail correction can be performed by multiplying the tracer concentration with some exponential decaying function. The tail correction step can be performed using the equation given below [56]:

$$C_t(t) = C(t)e^{-t/x} \tag{3.9}$$

where t is the time.

3.3.4.5 Smoothing

This step is used to remove the fluctuations presented due to electrical noise or any other disturbances. It is performed using a finite impulse response (FIR) filter with a transfer function as follows [56]:

$$H(z) = \frac{1 + z^{-1} + z^{-2} + z^{-3} + z^{-4}}{5} \tag{3.11}$$

where $H(z)$ is the frequency response and H is the Z-transform for the impulse response. We have to choose the filter according to the requirement. High order filter has the problem of over-smoothing. The output response of the filter can be presented as follows:

$$C_f(n) = \frac{1}{5}(C(n) + C(n-1) + C(n-2) + C(n-3) + C(n-4)) \tag{3.12}$$

where, $C(n)$ is the input to the filter and C_f is the output concentration obtained after smoothing.

3.4 Residence time distribution modeling method

A number of RTD studies are explained in the literature by different authors [106-109]. RTD analysis is an ideal approach broadly used to describe the non-ideal behavior of the flow in any system/reactor. It is described by using exit age distribution [27] in the form of $E(t)$ and $F(t)$ for a pulse and step input respectively. The age distribution or the RTD function is represented by the following expression [54]:

$$E(t) = \frac{C(t)}{\int_0^\infty C\,(t)dt} \tag{3.13}$$

where, $C(t)$ is the exit concentration of the radiotracer at time *t*. The denominator ($\int_0^\infty C\,(t)dt$) is the area under the C curve. The material, which spent the time between $t = 0$ to $t = \infty$ be equal to 1 [27].

$$\int_0^\infty E(t)dt = 1 \tag{3.14}$$

The mean residence time (MRT) $\bar{t}$ is the first moment of the RTD function which is equal to [27, 32]:

$$\bar{t} = \int_0^\infty t\ E(t)dt \tag{3.15}$$

In general, the first moment is used to determine the MRT of the system. Second moment of the RTD function is termed as variance (σ^2) and it gives the spread of the distribution. The variance is represented using the following equation [54]:

$$\sigma^2 = \int_0^\infty (t-\bar{t})^2\,E(t)dt \tag{3.16}$$

The third moment of RTD function is termed as skewness (λ^3) and it gives the symmetry of the distribution. Skewness is represented by using the following formula [54]:

$$\lambda^3 = \frac{1}{\sigma^{\frac{3}{2}}}\int_0^\infty (t-\bar{t})^3\,E(t)dt \tag{3.17}$$

For most of the cases, these three moments are sufficient to characterize the RTD. The fourth moment is kurtosis (κ^4) [54].

The theoretical MRT of the vessel is represented by τ which is equal to the ratio of the volume of the reactor to the volumetric flow rate of the fluid [27].

$$\tau = \frac{V}{f} \tag{3.18}$$

where V represents the volume of the reactor and f denotes the volumetric flow rate of the fluid. If the theoretical MRT is more than the experimental MRT, then there is a possibility of dead zones or fouling/scaling in the reactor. If the theoretical MRT is less than the experimental MRT, then there may be the chances of bypassing the process fluid.

Once we get the experimental RTD data for any system, we can evaluate the hydrodynamics by fitting the RTD model. RTD modeling has a number of benefits, which are given here [110]:

- The flow rate (Q) is calculated for the systems where flow meters are not installed e.g. in the river, sewage, etc. [111]
- The tracer test provides various information about the process equipment, such as flow dynamics, the presence of dead zones, back mixing and short-circuiting of the materials inside the vessel. The on-line tracer test may lead to corrective action as preponed/postponed of the regular maintenance cycle, which may save manpower, maintenance time and money.
- The RTD models are fitted to the experimental data using the least square curve fitting method with the help of a computer program. In this type of computation, each data point contributes to the accuracy with which the process parameters are determined.
- Abnormal behavior (presence of dead volume, by-passing, back-mixing, etc.) of the process can be predicted by calculating the process parameter which gives the better insight/understanding of the process.
- An established RTD model can predict missing data of the process due to some fault or any technical problem during the experiment.

Plug flow model and perfect mixers are assumed to represent two extremes of the system. Practically, a system behaves in between these two extremes. An RTD test

provides information about the distribution within the process vessel and gives information about the dynamic behavior of the flow [112]. The RTD experiments are conducted when the process/system is at steady state. A trace amount of the tracer injected into the system along with the bulk material. The tracer moves throughout the process vessel and it does not disturb the bulk flow at all. The RTD study is also helpful to know the reason behind any abnormality or low efficiency of the reactor using numerical simulation or CFD. Velocity profile and the detailed flow field are also obtained through RTD flow modeling [54, 56].

3.5 RTD modeling for pulping digester

The numerical modeling is one of the ways to fit the experimental data with available RTD models and their combinations to predict the reactor flow behavior. The available RTD models having their own specific flow characteristics and the fitted models depict the flow behavior of the reactor. Various types of RTD models are available according to the type of reactor or flow behavior. Hence, available RTD models were used to model the present RTD data and flow behavior of pulping digester. The values of the RTD model parameters were identified and used to predict the flow behavior. Modeling of the three-tube digester has been carried out using different models for impulse input.

The sudden injection of the one-shot tracer input provided an ideal impulse signal at the inlet of the pulping digester. Assuming $C(t)$ is the energy concentration of the radiotracer at time, t. At $t = 0$, the sharp peak was observed at the first detector mounted at the inlet of the first tube because of the sudden injection of radiotracer. The subsequent signals were observed at detectors with an increase in time ($t > 0$). The normalization of the signals was done according to the following equation,

$$Normalized\ tracer\ concentration = \frac{C(t)}{\int_0^\infty C(t)dt} \tag{3.19}$$

where the denominator represented the area under the tracer concentration-time curve. The area was computed using the definite integral method.

$$Area = \int_a^b f(x)dx \tag{3.20}$$

3.5.1 Selection of the model

There are various models available for RTD modeling which include plug flow model, perfect mixers, tank-in-series with recycling model, tank-in-series with exchange

model, axial dispersion model, etc. [113-116]. The plug flow model and perfect mixers are assumed to represent two extremes of any industrial reactor. Practically, a system behaves in between these two extremes. A simple approach to select a model is to start from the perfect plug flow model which represents the shift of impulse input to the output. Plug flow merely represents the input with a time lag. Next approach is to select the model with dispersion in which sharp input impulse is spread as it moves along the length of the reactor. Hence, the axial dispersion model was tried, which successfully represented the flow profile of the digester. We also tried the tank-in-series model but it failed to fit the RTD experimental data. Generally, tank in series model is used for CSTRs or the reactor have high local mixing of the fluid has low viscosity. Hence, for our system which have high viscosity fluid with low dispersion, it was not able to represents the data very well.

Further, the tank-in-series model with back-mixing is also selected to model the experimental data and it also provided a good fit with the data.

3.5.1.1 Axial dispersion model (ADM)

To examine the flow characteristics of the liquid phase inside each tube, a plug-flow component followed by ADM was considered for representing the RTD data, though the two processes are happening simultaneously. The ADM has been widely used to represent the flow inside longitudinal pipes and tubes [3, 117]. It is generally applied for small deviations from plug-flow. The open-open boundary conditions were chosen for modeling since there was no abrupt change in the flow conditions at the inlet point of tracer introduction and outlet boundaries for each of the tubes wherein the detectors were placed. The axial dispersion model component for large deviation from plug-flow, i.e., $D/uL > 0.01$, with open-open boundary conditions are used and expression is given by the following equation.

$$E_{ad} = \frac{u}{\sqrt{4\pi(Dt)}} exp\left[-\frac{(L-ut)^2}{4Dt}\right] \tag{3.21}$$

where E_{ad} is the RTD function for the axial dispersion component, D is the axial dispersion coefficient, u is the velocity of the liquid phase, L is the length of the tube and t is independent variable time. A schematic of the axial dispersion model with a plug flow component is shown in Figure 3.4.

The axial dispersion model component for small dispersion, i.e. $D/uL < 0.01$, is used to produce the convoluted signal. The equation used is expressed as:

$$E_{sd} = \sqrt{\frac{Pe\ u^2}{4\pi L}}\ exp\left[-\frac{(L-ut)^2}{4L^2/Pe}\right] \tag{3.22}$$

where E_{sd} is the RTD function of the axial dispersion model used for the small extent of dispersion. The liquid phase dispersion is determined by calculating the dimensionless Peclet number (Pe*)* and it is defined as:

$$Pe = \frac{uL}{D} \tag{3.23}$$

The Peclet number represents the two extremes, which are the plug-flow and the large deviation from plug-flow, i.e. mixed-flow. It can be seen how the spread of the RTD function increases from a sharp asymmetrical signal at low Peclet number, $Pe \rightarrow 1$ to a broad symmetric signal as that for the plug-flow, i.e., at small dispersion, $Pe = \infty$.

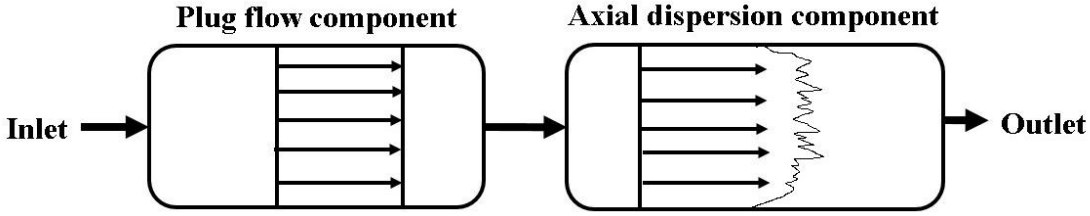

Figure 3.4 Plug flow in series with axial dispersion model

The plug-flow component represented the time delay part of the outlet tracer concentration data. Since the pulse response at the outlet is not observed until the introduced tracer does reach the outlet end, a pure time delay is observed in all the outlet signals which is constant. The model for this component is represented as:

$$E_{pf}(t) = I(t - \tau_{PF}) \tag{3.24}$$

where E_{pf} is the RTD function for the plug-flow model component, *I* is the normalized tracer input signal, *t* is independent variable time, and τ_{PF} is the time delay or the MRT for the plug-flow component.

The ADM with plug flow model in series was directly used for the first tube (D_2) and for the whole digester (D_4) since the introduced tracer signal at the feed point was instantaneous and the first detector D_1 recorded a highly sharp, i.e., an ideal impulse spike or Dirac delta function. Hence, the tracer signal at the outlet of the first tube and at the outlet of the third tube by assuming three-tube digester as a single reactor could be

simulated to an impulse response represented by the Eq. (4.3) for the axial dispersion component. Rather than comparing the variance given by the second moment of the $E(t)$ curve with that of the experimental response, the parameters of the axial dispersion (Pe) was adjusted until the experimental response data fitted the simulated data.

3.5.1.2 Tank-in-series with back-mixing model

The tanks-in-series with back-mixing model (TIBM) was also found suitable for simulating the measured RTD data [118]. The block diagram of the model is shown in Figure 3.5. If an impulse, $x(t)$ of the tracer is injected at the inlet of the first tank, then the tracer balance equations for the model are given as:

For the first tank: $$\tau_1 \frac{dC_1}{dt} = x(t) + \alpha C_2 - (1+\alpha)C_1 \quad (3.25)$$

For nth tank: $$\tau_1 \frac{dC_n}{dt} = (1+\alpha)C_{n-1} + \alpha C_{n+1} - (1+2\alpha)C_n \quad \text{for n = 2,3…N-1} \quad (3.26)$$

For Nth tank: $$\tau_1 \frac{dC_N}{dt} = (1+\alpha)(C_{N-1} - C_N) \quad (3.27)$$

where τ_1: mean residence time in each tank, (V/NQ), V: total volume, α: back flow ratio (q/Q), q: exchange flow rate between the tanks, Q: flow rate through the system, C_1, C_n and C_N concentration of tracer at the outlet of fist tank, nth tank and Nth tank, respectively.

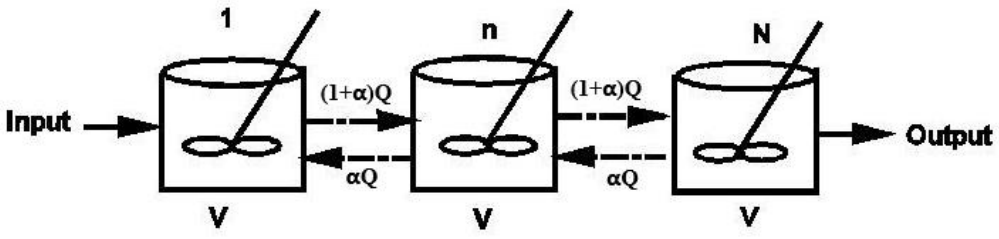

Figure 3.5 Tank-in-series with back-mixing model

3.5.2 Convolution procedure

3.5.2.1 Non-ideal tracer input

There may be several situations where the input signal may get converted into a non-ideal input signal, for example, an ideal input signal is introduced into a long reactor

and reactor is divided into several sections. Only the first section is having the ideal impulse input whereas the following sections will receive the non-ideal pulse input because the ideal input signal gets modified after passing through the first section of the reaction vessel. This change in the input signal happens due to the specific hydrodynamics of the process characterized by RTD of the first section. Hence, the convolution procedure is used to deal with a non-ideal input signal. In case of the digester, second and third tube have non-ideal tracer input and to obtain the RTD of these tubes convolution procedure is used.

3.5.2.2 Convolution integral

Since the impulse signal got distorted as it passed through the tubes, the input signals to the second and third tubes do not replicate an ideal impulse function. This tracer input is rather a non-ideal pulse introduction. Therefore, a modeling procedure is proposed here to obtain the $E(t)$ curve for the second and third tubes, which uses their outlet tracer concentration data measured by the detectors D_2, D_3, and D_4. A schematic of the proposed procedure is shown in Figure 3.6. The parameter of the axial dispersion (D) of the model was adjusted after its convolution with the inlet tracer concentration data of the second and third tubes. The model parameter adjustment was done until the experimental outlet tracer concentration data fitted the data obtained by the convolution of the input tracer concentration data with the model for each tube. The adjusted parameter values yielded the RTD function of individual tubes.

When the non-ideal pulse signal was introduced to the second and third tubes of the system as noted above, it got modified on passing through the vessel to yield an output signal. This modification in the input signal occurred due to the specific hydrodynamics of the process characterized by its RTD. The output response signal data C_{out} can be computed by convoluting the input concentration versus time signal data C_{in} with the RTD data obtained from the assumed values of model parameters substituted into the model RTD function, $E(t)$. The convolution integral, in general, is given by the following cross-correlation product of C_{in} and the RTD function:

$$C_{out}(t) = \int_0^t C_{in}\,(t - t')E(t')dt' \tag{3.28}$$

In case the input signal was known in a discrete form, a discrete output signal can be computed numerically by the following discretized form of the above integral:

$$C_{out}(t_i) = \Delta t \sum_{j=1}^{i-1} C_{in}(t_{i-j}) E(t_j) \tag{3.29}$$

where Δt is the time step. t_i is the sampling time instant. t_j is the difference between the sampling time and the time instant of the input considered.

3.5.3 Theoretical and experimental mean residence time

The theoretical mean residence time (τ) of the liquid phase for digester having volume V with an average volumetric flow rate Q is defined by the following equation [27].

$$\tau = \frac{V}{Q} \tag{3.30}$$

Each tube has a diameter of 1.45 m and a length of 12 m. in case of three-tube digester and 1.1 m dia with a length of 7.7 m in the case of two tube digester. As it is known that the volumetric flow rate is different for each experiment, hence, the MRT for each case also will be different. The theoretical MRT should be equal to the MRT obtained from RTD experiments. If we obtained the experimental MRT is higher than the theoretical MRT, then there is some anomaly in the flow and if experimental MRT is less than the theoretical MRT, then there is the possibility of the dead zone inside the reactor [68]

The simple RTD data treatment is the calculation of moments. The moments are used to characterize the RTD function in terms of statistical parameters such as mean residence time and standard deviation. In this study, only the first moment around the origin is determined by means of the following relation [27],

$$\tau_{AD} = \int_0^\infty t \; E(t) dt \tag{4.13}$$

where τ_{AD} is the mean residence time for RTD model.

.

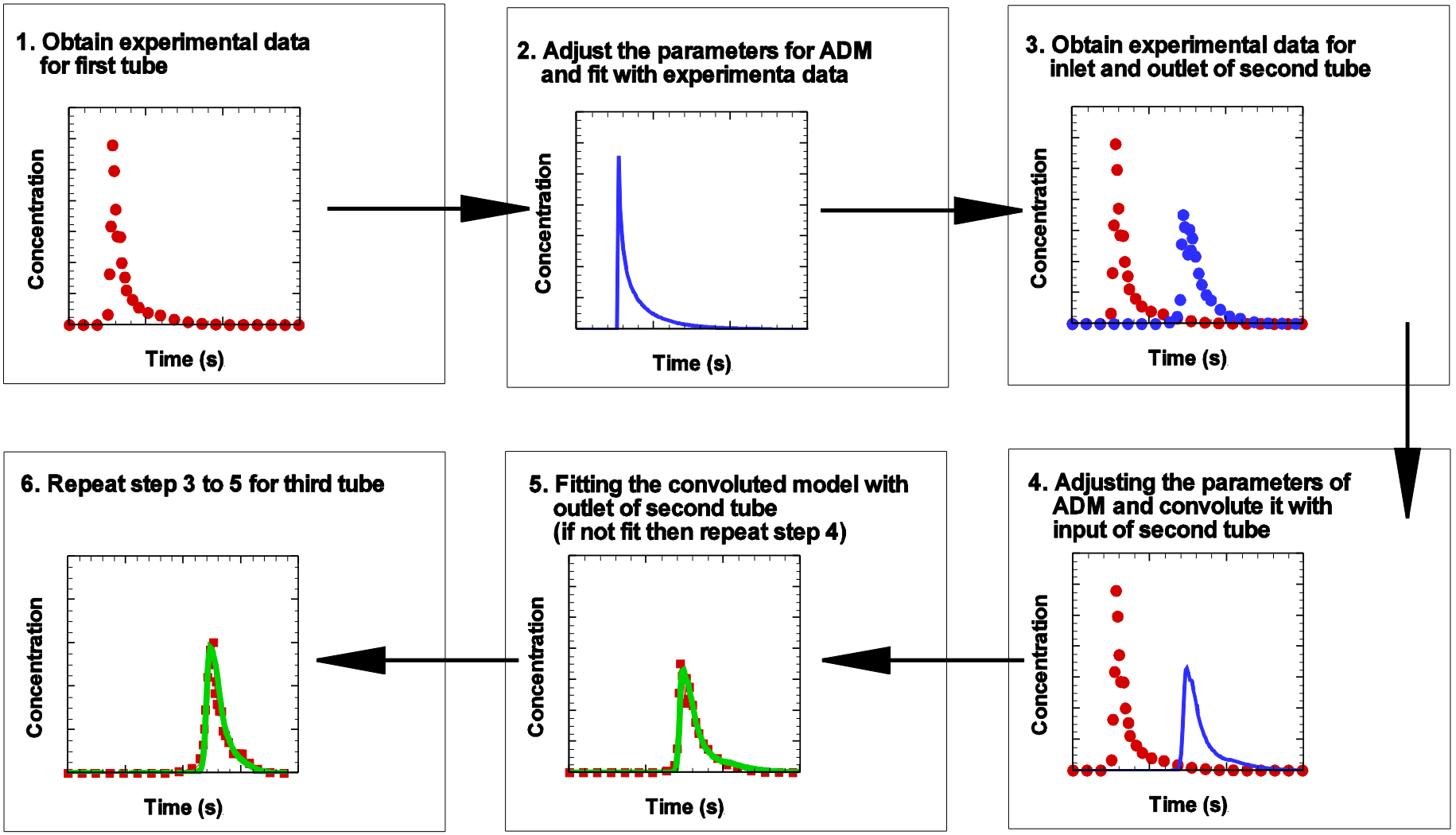

Figure 3.6 Procedure of the numerical modeling and convolution process for three-tube digester

The MRT for the plug flow component (τ_{PF}) is determined from the experimental data. The time taken by the tracer component before the curve start rising is measured as MRT of the plug flow component. From the graphs shown in Figure 3.6, it is shown by the straight horizontal values of concentration before the concentration starts increasing. The total MRT for the whole digester can be calculated as,

$$\tau_T = \tau_{AD} + \tau_{PF} \tag{3.31}$$

where τ_T is the total mean residence time for three-tubes (whole digester). Rather than using the direct equation for τ_T, it was computed using Eq. (3.30), using the adjusted RTD data obtained by carrying out the RTD modeling procedure after getting the RTD function.

3.5.4 Estimation of model parameters

The values of model parameters were estimated using a least-square curve fitting method. For an impulse input, the model equations were solved and directly fitted to the experimentally measured RTD curves, and the obtained corresponding parameters were used to best fit the experimental data. The quality of the data fitting is judged by the root mean square (RMS) value of the sum of the squares of the differences between the data and model. The minimum value of RMS value (equation 3.32) is considered as a fitting quality of data, i.e., minimum RMS value is desirable. The values of the model parameters corresponding to the minimum RMS value were chosen as the best set of parameters.

$$RMS = \sqrt{\frac{1}{N_P}\sum_{i=1}^{N_P}\left[E_m(t) - E_{exp}(t)\right]^2} \tag{3.32}$$

where N_P is the number of data points.

Chapter-4 RTD Study of Three-Tube Pulping Digester

4.1 With radiotracer ^{82}Br

RTD experiments have been carried out in a three-tube continuous horizontal pulping digester (Figure 3.1) to optimize the operating conditions and to diagnose the flow behavior inside the digester. The radiotracer ^{82}Br is used in the form of ammonium bromide to carry out the RTD experiments at different operating conditions and selected experiments are chosen to represent this work. The operating conditions of the digester are shown in Table 4.1. The screw speed of the wheat straw feeder has been varied from 55 to 65 rpm (5.3-6.2 m^3/min). The white liquor flow rate has been varied from 300-365 l/min.

Table 4.1 Operating conditions of three-tube digester using ^{82}Br

Exp. No.	Screw speed (RPM)	White liquor flow rate (l/min)	Steam flow (Ton/h).	Steam pressure ($kg_f/cm^{2)}$	Temp (^oC)	
					Tube 1	Tube 2 & 3
1	55	300	15.00	6.65	157	162
2	55	310	18-19	5.98	167	165
3	55	320	18-19	6.04	165	161
4	65	350	16-17	5.39	163	161
5	65	355	16	6.26	165	163
6	65	360	15-16	6.08	165	168
7	65	365	17	6.32	160	166

The effect of operating parameters on the pulping process was observed for the experiments performed. The values of output parameters (Kappa number and residual alkali) were estimated for each experimental conditions and are tabulated in Table 4.2. In the first set of experiments (Exp. 1-3) with rpm 55 (feed rate 5.3 m^3/min), the Kappa numbers are observed as 14.2, 13.4 and 12.8 for the corresponding white liquor flow rates of 300, 310 and 320 l/min respectively. The Kappa number decreases with gradual increase in white liquor flow rate from 300 to 320 l/min. Conversely, the observation of Table 4.2 shows that the amount of residual alkali also increases in product stream with increasing the white liquor flow rate which is not required. For an optimum pulping process, the value of Kappa number and residual alkali should be minimum with less

variation in these parameters. At high white liquor flow rate, the amount of residual alkali may be higher than that required for sufficient delignification. This may be the reason for the high value of residual alkali at a high white liquor flow rate.

Table 4.2 Output parameters for experiment conducted using ^{82}Br

Exp. No.	Kappa number of pulp	Residual alkali in black liquor (g/l)
1	14.2	4.60
2	13.4	6.14
3	12.8	11.2
4	14.0	5.17
5	12.8	5.33
6	17.9	6.40
7	12.8	5.01

In the second set of the experiments (Exp. 4-7) with 65 rpm screw speed, the Kappa number shows a similar trend as in the first set of experiments except for Exp. 6. The Kappa number in experiment 4 is 14 and it decreased to 12.8 in Exp. 5 which is the indication of improved digestion process with an increase in white liquor flow rate. In Exp. 6 the Kappa number suddenly increased from 12.8 to 17.9 and residual alkali increased from 5.33 to 6.40 g/l, which was unexpected and it shows malfunctioning of the system. The reason behind the increase in the Kappa number may be due to the increased white liquor flow rate which may result in channeling. Furthermore, in Exp. 7, the Kappa number decreased to 12.8 with residual alkali of 5.01 g/l. In every situation, sufficient chemicals are required to carry out the pulping process for completion but in actual, a slight excess amount of the chemicals are used to maintain the driving force for delignification process. But if the chemicals are present in lesser amount than the requirement, then the dissolved lignin starts precipitating on the fibers, which is undesirable.

Based on the above discussion, Exp. 7 was the optimum one with lowest Kappa number (desired delignification) and residual alkali. The residual alkali is also low for Exp. 5. Exp. 5 can also be taken as second optimum digestion process with little increase in residual alkali.

4.1.1 Raw data of RTD experiments

The obtained raw data after RTD experiments for three-tube pulping digester is shown in Figure 4.1. The data shown in the figure represents the concentration of the tracer versus time at the outlet of first, second and third tubes of the digester.

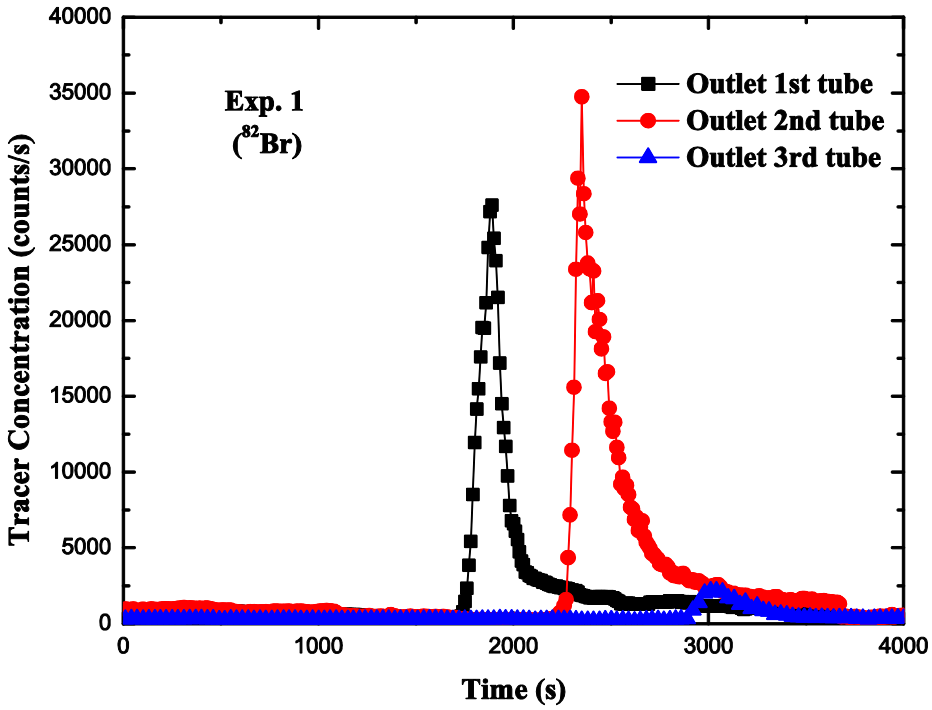

Figure 4.1 Typical raw data obtained after different RTD experiments using ^{82}Br

4.1.2 Pretreated data

The obtained RTD experimental data is pretreated for starting point correction, background correction and tail correction and the pretreated data after these treatments are shown in Figure 4.2, Figure 4.3 and Figure 4.4 respectively.

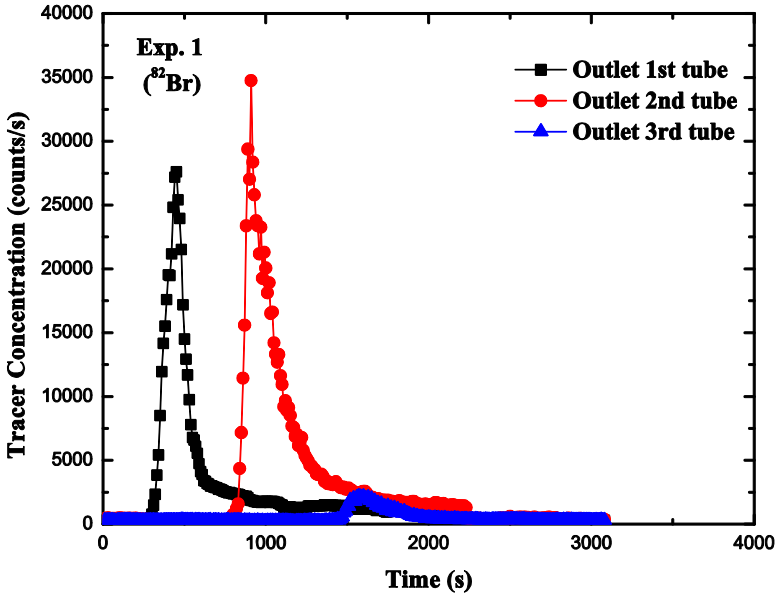

Figure 4.2 Data obtained after dead time correction

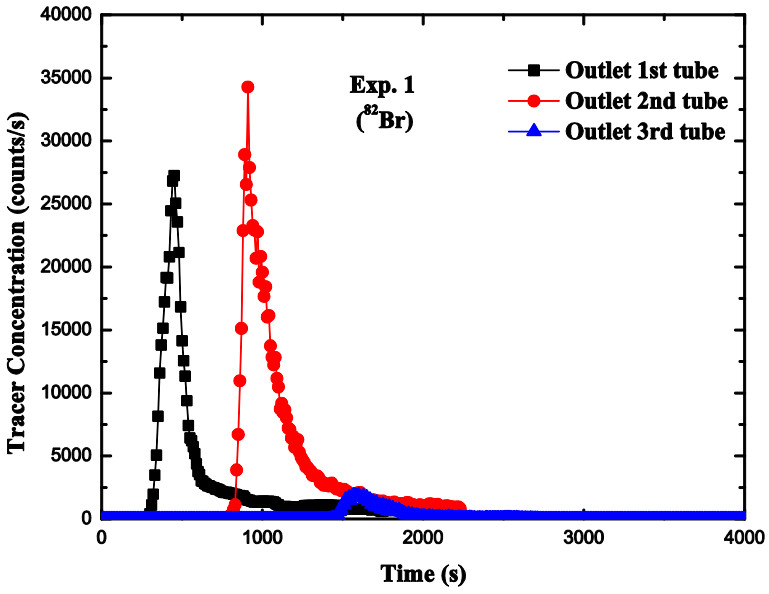

Figure 4.3 Data obtained after background correction

Generally, we set the DAS before injecting the radiotracer and it starts taking readings. In starting point correction, we eliminate the counts present before injecting the radiotracer. The average data for 800-900 s was removed in each case based upon the white liquor flow rate. It was the sum of the time before injecting the radiotracer and time taken by radiotracer to reach up to first detector D_1. After removing this dead time, the concentration recorded by detector D_2, D_3 and D_4 at that time is considered as background

radiation. In background correction counts presented due to noise, electrical disturbance or any other background sources are subtracted.

It is assumed that in a continuous system after completing the experiment, concentration goes back to zero. But in some cases this does not happen, hence we have to perform the tail correction step, in which an exponential function is multiplied with the tail part concentration sequence. In smoothing, data fluctuations are removed [8].

As due to the decaying property of the radioisotopes, the energy of emitting radiation decreases continuously. For a chemical process which has long residence time, it is required to carry out the decay correction to compensate for the low radiation energy. As the pulping in the continuous digester is short term process, the decay correction is not required. The data obtained after RTD test is already smooth, hence smoothing is also not required.

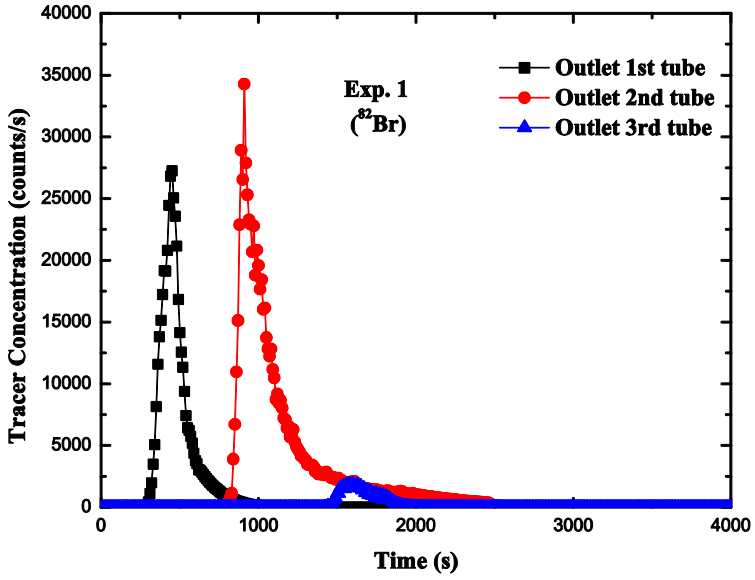

Figure 4.4 Data obtained after tail correction

4.1.3 Modelling of the first tube and whole digester

In order to investigate the overall flow behavior of the digester, the curves recorded for the first tube and for the whole digester were simulated using the models discussed in Chapter-3 and the results are given in Table 4.3 and Table 4.4 respectively. The impulse input is injected at the inlet of the first tube and the response is recorded at the outlet of first, second and third tubes. The modelling of the experimental data recorded at the outlet of the first tube is carried out by directly optimizing the model parameters and comparing

the response with the experimental data. The modeling of the digester is also carried out by assuming it a single system as it also has impulse input.

Table 4.3 Model parameters of first tube

Exp. No.	τ_{PF1} (min)	ADM		TIBM		
		τ_{ADM1} (min)	Pe_1	τ_{TIBM1} (min)	N_1	α_1
1	5	2	4	2.7	7	1.2
2	3.4	1	1.5	1.4	2	8
3	4.2	1.4	2	2	4	3
4	4.9	2.1	2	2.5	3	2
5	3.7	2	8	2.8	11	3
6	4.3	0.8	1	1.3	2	5
7	4.1	1.4	4	2	4	1

The plug flow component for the first tube is ranging from 3.7-5 min. as shown in Table 4.3. The value of Pe_1 was obtained between 1 and 8. The low value of Pe_1 shows that there is a high dispersion inside the first tube. The high value of Pe_1 and N_1 are obtained only in case of Exp. 5 as compared to other cases which represents the low value of dispersion or mixing in the first tube. Very high dispersion is observed in Exp. 6. For TIBM, the value of N_1 varied from 2 to 11 and the value of back-mixing ratio (α_1) varied from 1 to 8. In every experiment, the MRT for the TIBM component is slightly higher than the MRT of the component of ADM which may be due to the high back-mixing. The fitting of the model for the first tube is shown in Figure 4.5 for different experiments. From the figure, it is observed that the tail part of the experimental data was best fitted by the TIBM. The shape of the model shows a sudden increase in concentration and then decreased slowly with a long tail which indicate the high dispersion. Figure 4.5 also shows the model data for the first tube at very high dispersion. The shape of the model data for the first tube indicates high dispersion (Pe=2).

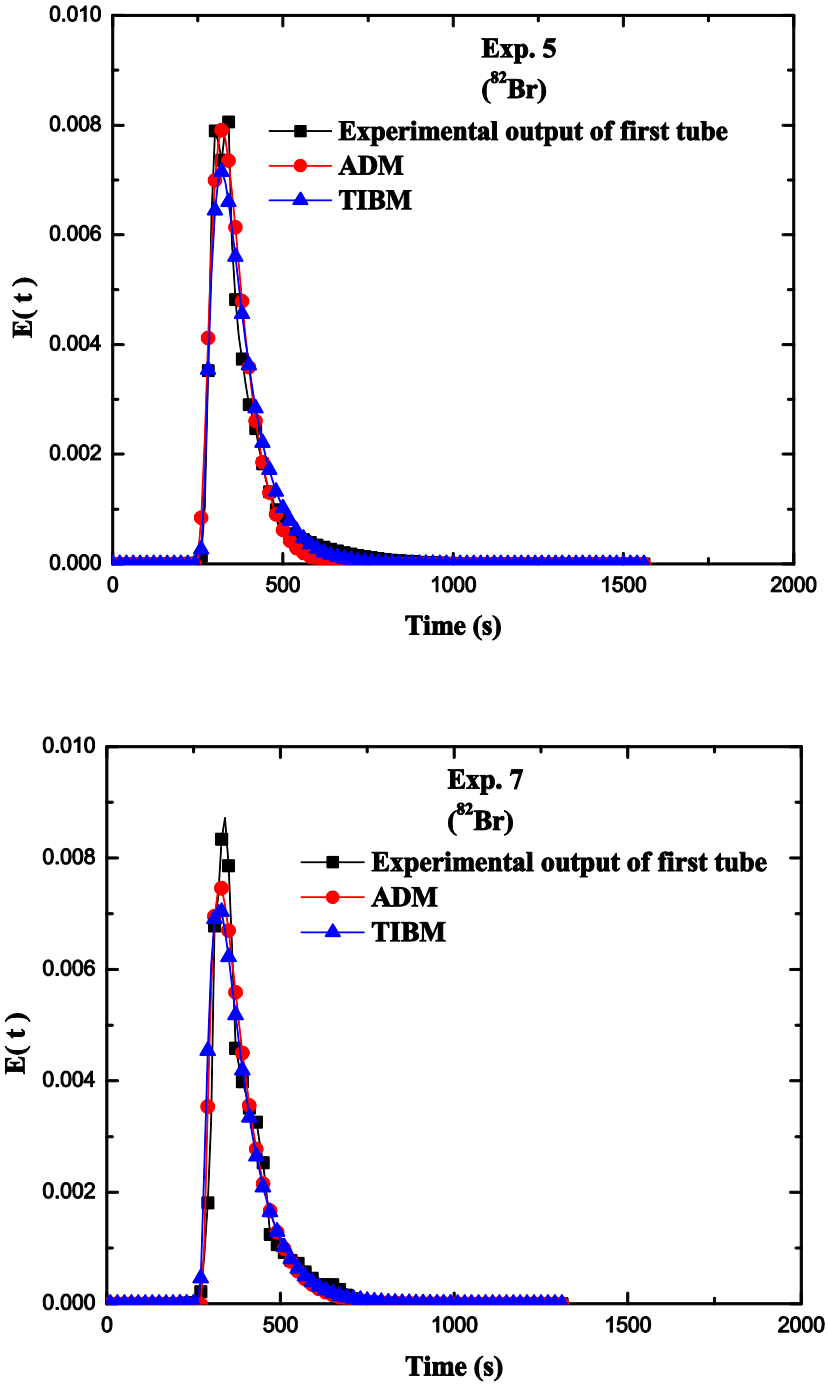

Figure 4.5 Model adjustment for the first tube with different experiments using ^{82}Br

The plots showing the comparison of experimental and model simulated RTD curves for the whole digester are shown in Figure 4.6.

In the case of the whole digester, the time spent by the liquid phase in the plug flow component ranged from 18 to 29 min. For ADM, the values of model parameter, i.e., $Pe_{(1\text{-}3)}$ and $\tau_{ADM(1\text{-}3)}$ ranged from 3 to 9 and 1.8 to 10 min, respectively, indicating high to an intermediate degree of axial mixing. The high value of Pe represents the low axial

dispersion. However, in case of TIBM, the values of model parameters i.e. $N_{(1-3)}$ and $\alpha_{(1-3)}$ ranged 8-17 and 0.7-4 respectively, indicating slightly low mixing flow behavior of liquid phase with moderate back-mixing in the digester except for Exp. 3. Highest back-mixing is observed in case of Exp. 7 represented by the value of α=4. It is observed that the time spent by the liquid phase in the axially dispersed component is much shorter than the mean residence time of the liquid in plug flow component. The MRT of ADM component is equal to the MRT of TIBM component except in case of Exp. 2. The highest MRT is observed in case of Exp. 4.

The maximum axial mixing of the liquid phase is observed in tube 1. The graph shown in Figure 4.6 shows smaller tail with somewhat bell shaped curve which indicate less dispersion as compared to the first tube. Also, from the Figure 4.6, it is clearly shown that the TIBM is better representing the experimental RTD data as compared to the ADM.

Table 4.4 Model parameters of whole digester

Exp. No.	$\tau_{PF(1-3)}$ **(min)**	**ADM**		**TIBM**		
		$\tau_{ADM(1-3)}$ **(min)**	**Pe**$_{(1-3)}$	$\tau_{TIBM(1-3)}$ **(min)**	**N**$_{(1-3)}$	$\alpha_{(1-3)}$
1	23	6	8	6	17	1
2	23	1.8	4	2.3	11	3
3	20	3	7	3	15	0.7
4	29	10	3	10	8	2
5	24	4	6	4	13	2
6	18	3	9	3	17	3
7	25	7	6	7	11	4

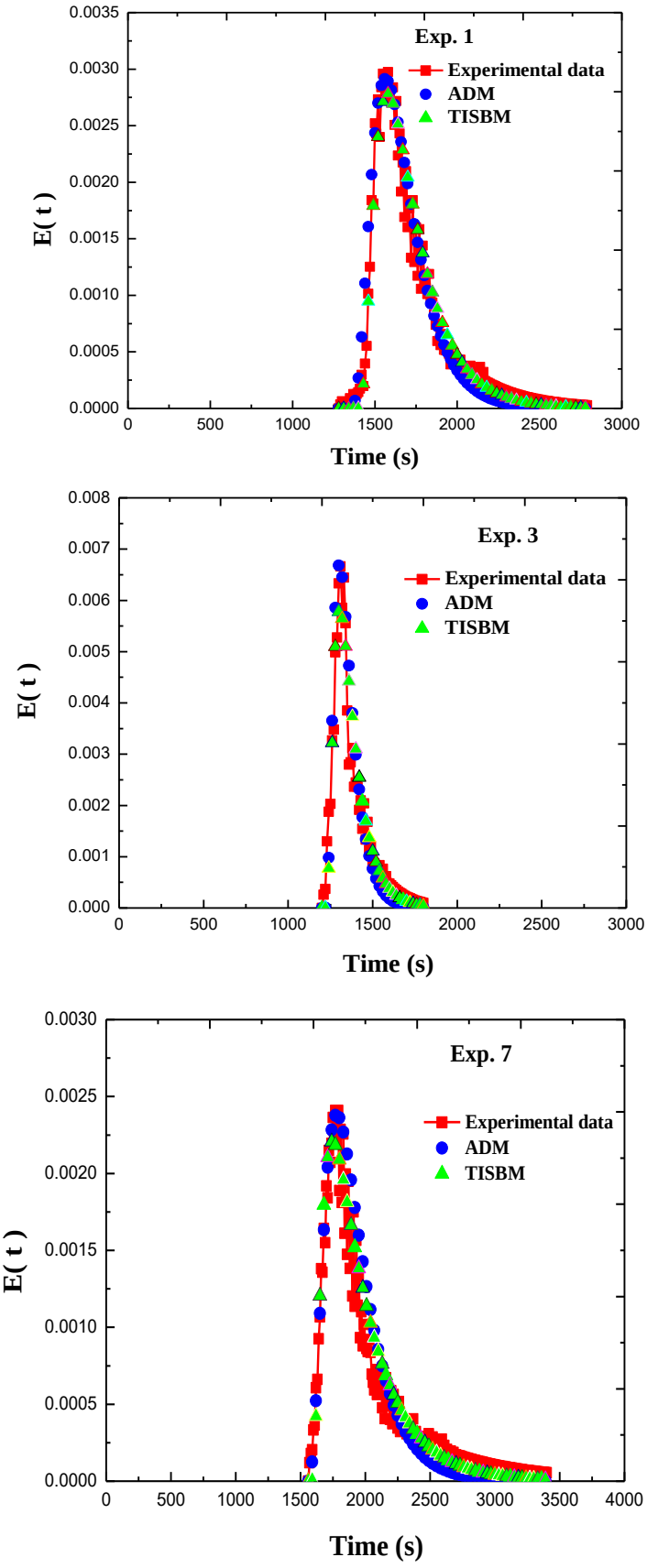

Fig. 4.6 Comparison of experimental and model simulated RTD curves for whole digester

4.1.4 Modelling of second and third tubes

The output signal of the first tube is the input signal for the second tube which is a non-ideal input signal. The direct model fitting for the experimental data of the second tube does not give the true RTD of the system. Hence, the non-ideal input signal was convoluted with model data and compared with the experimental output. The axial dispersion model and tank-in-series with back-mixing models each connected with a plug flow component in series are used for data fitting. The model parameters for second and third tubes are calculated during optimization and shown in Table 4.5 and Table 4.6 respectively. The convolution procedure is explained in Chapter-3 in detail.

Table 4.5 Model parameters of second tube

Exp. No.	τ_{PF2} (min)	ADM		TIBM		
		τ_{ADM2} (min)	Pe_2	τ_{TIBM2} (min)	N_2	α_2
1	3.6	0.8	3.5	3.2	5	1.5
2	5.9	0.7	5.5	1.4	7	1
3	3	1	4	1.6	8	0.4
4	4.5	0.4	5	1	9	0.9
5	4.2	0.7	4.8	1.2	9	1
6	5.2	0.7	4	1.3	7	1
7	4.0	0.6	3.4	1	6	1

Table 4.6 Model parameters of third tube

Exp. No.	τ_{PF3} (min)	ADM		TIBM		
		τ_{ADM3} (min)	Pe_3	τ_{TIBM3} (min)	N_3	α_3
1	6.3	2.8	18	3	18	0.3
2	10.4	1	21	1.2	22	0.09
3	8	1.8	17	2	10	0.08
4	10.4	3.7	18	4	18	0.2
5	7	3.1	13	4.2	12	0.04
6	5.7	2.3	21	2.6	20	0.07
7	6.6	2.8	23	3	24	0.1

The observations of Table 4.3, 4.5 and 4.6 show that Pe has increased from digester tube 1 to tube 3 and the maximum value of Pe is observed for the third tube (Table 4.6), which indicate very low dispersion. The fitting of models using convolution for the second and third tube are shown in Figure 4.7 and Figure 4.9 respectively.

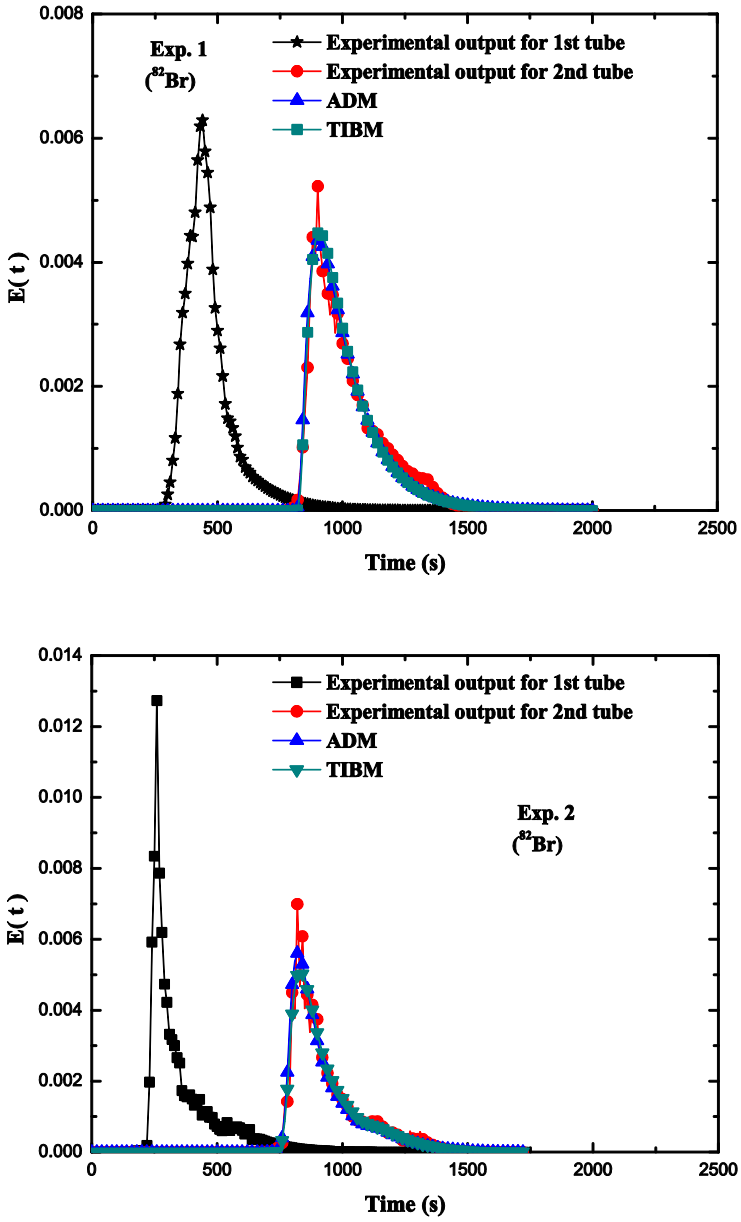

Figure 4.7 Model adjustment for the second tube with different experiments

At the initial stage, the liquid phase has low viscosity and specific gravity. At high temperature and pressure, liquor starts to diffuse in the wheat straw. The low value of Pe in the first tube also shows the highly dispersed flow (Table 4.3). The E(t) curve represented by the outlet of the first tube, Pe=2, (Figure 4.8), shows that the concentration increases

suddenly and then starts decreasing slowly with a long tail. This type of curve represented highly dispersed flow behavior.

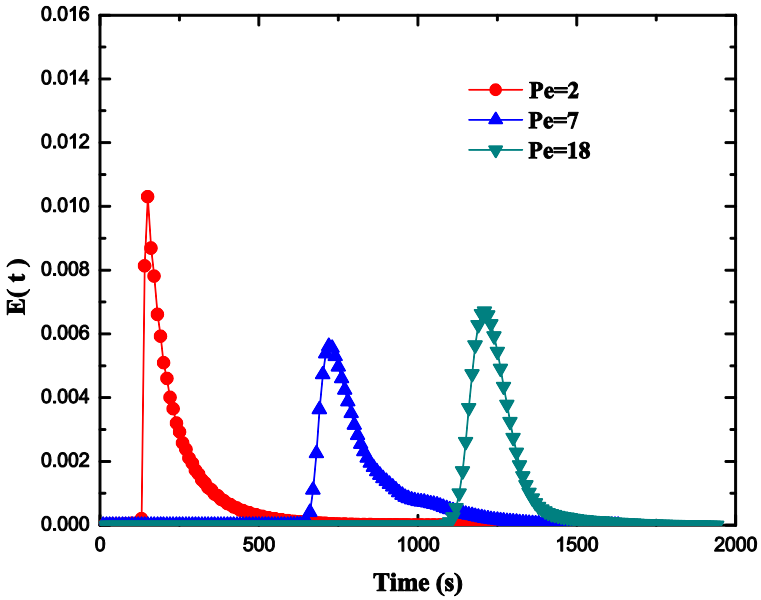

Figure 4.8 E(t) curves predicted for axial dispersion model at different deviations from plug flow for each tube

Along the length of the digester, as the delignification proceeded, the lignin dissolve in the liquor phase and viscosity of the liquor phase increased continuously. The higher value of Pe for the second tube as compared to the first tube shows reduced degree of dispersion. In Figure 4.8, the E(t) curve represented the intermediate dispersion for the second tube (Pe=7) and plug flow behavior inside the third tube (Pe=18).

RTD modeling for the third tube is carried out using a similar procedure which is used for the second tube. The outlet signal of the second tube acts as an input signal for the third tube. This non-ideal input signal was convoluted with the model data and compared with the experimental output for the third tube. The model fitting for the third tube is shown in Figure 4.9 where the non-ideal input data of the third tube is shown, which is convoluted after optimizing the model parameters and the obtained results are compared with the experimental RTD output of the third tube. Up to the third tube, whole biomass is transformed into the pulp slurry which flows like a plug flow in the third tube. The high viscosity of the liquor is the reason behind the low dispersion in the third tube. At high viscosity, liquid phase come across high hindrance from solid particles which may be the reason of low dispersion. The symmetry of the graph at the outlet of the third tube also supports this explanation (Figures 4.9). The highest value of Pe for the third tube also

demonstrates this fact. At high white liquor flow rate, liquor covers the wheat straw rapidly and dispersion decreases due to a reduced amount of interaction between the phases. Inside the third tube, the low dispersion is obvious due to the high viscosity of the liquid phase due to dissolved lignin and other components of wheat straw. The high viscous fluid encounters high hindrance from solid particles which may further decrease the dispersion.

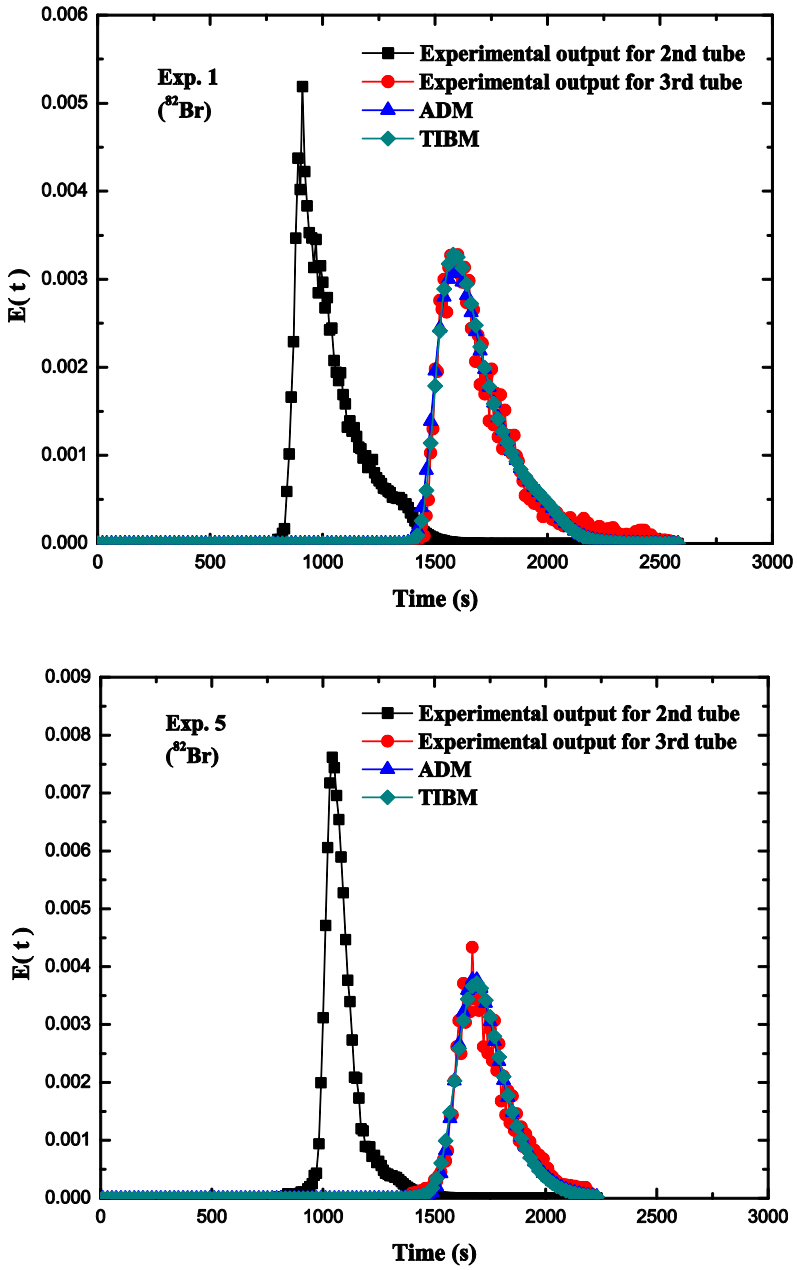

Figure 4.9 Model adjustment for the third tube with different experiments

MRT for the plug flow component, axial dispersion component and tank-in-series with back-mixing component are higher for the third tube as compared to the first and

second tube. At high viscosity, liquid flows with low velocity due to increased friction forces which resulted in higher MRT of the third tube (Table 4.6). The MRT of the plug flow component is very high as compared to the MRT of ADM and TIBM. The low back-mixing may be reason behind the high MRT of plug flow component.

4.2 With radiotracer ^{198}Au

We tried to adsorb the gold radiotracer on the surface of wheat straw so that we can trace the solid phase also. But, it did not adsorb on the surface of wheat straw, hence, we used it to trace the liquid phase of the three-tube pulping digester. The operating conditions for RTD experiments are shown in Table 4.7. The earlier optimized conditions (RTD experiments using ^{82}Br) are chosen to carry out the experiments.

Table 4.7 Operating conditions of three-tube digester using ^{198}Au

Exp. no.	Screw speed (RPM)	White liquor flow rate (l/min)	Steam Flow (Ton/h).	Steam pressure ($kg_f/cm^{2)}$	Temp (°C)	
					Tube 1	Tube 2-3
1	65	350	16	6.21	162	164
2	65	365	16-17	6.11	163	164

Only two experiments were performed using radiotracer ^{198}Au. The wheat straw screw feeder rpm was kept constant and the flow rate was varied from 350-365 l/min. The performance of the digester was evaluated by measuring the Kappa number of pulp and residual alkali of black liquor. The output parameters are shown in Table 4.8.

Table 4.8 Output parameters for experiments conducted using ^{198}Au

Exp. No.	Kappa number of pulp	Residual alkali of black liquor (g/l)
1	14.0	5.12
2	12.9	4.80

The observation of Table 4.8 shows that the Exp. 2 has low Kappa number which means the delignification is better in this case. The temperature and pressure were almost constant for both the experiments, which means that the low white liquor flow rate resulted in poor delignification.

4.2.1 Raw data of RTD experiments

The same three-tube digester is investigated for its flow behavior using radiotracer ^{198}Au. The similar procedure opted for radiotracer injection and detection as explained in the previous section. The raw data obtained after RTD experiments are shown in Figure 4.10 where the concentration versus time curve for first, second and third tubes are shown.

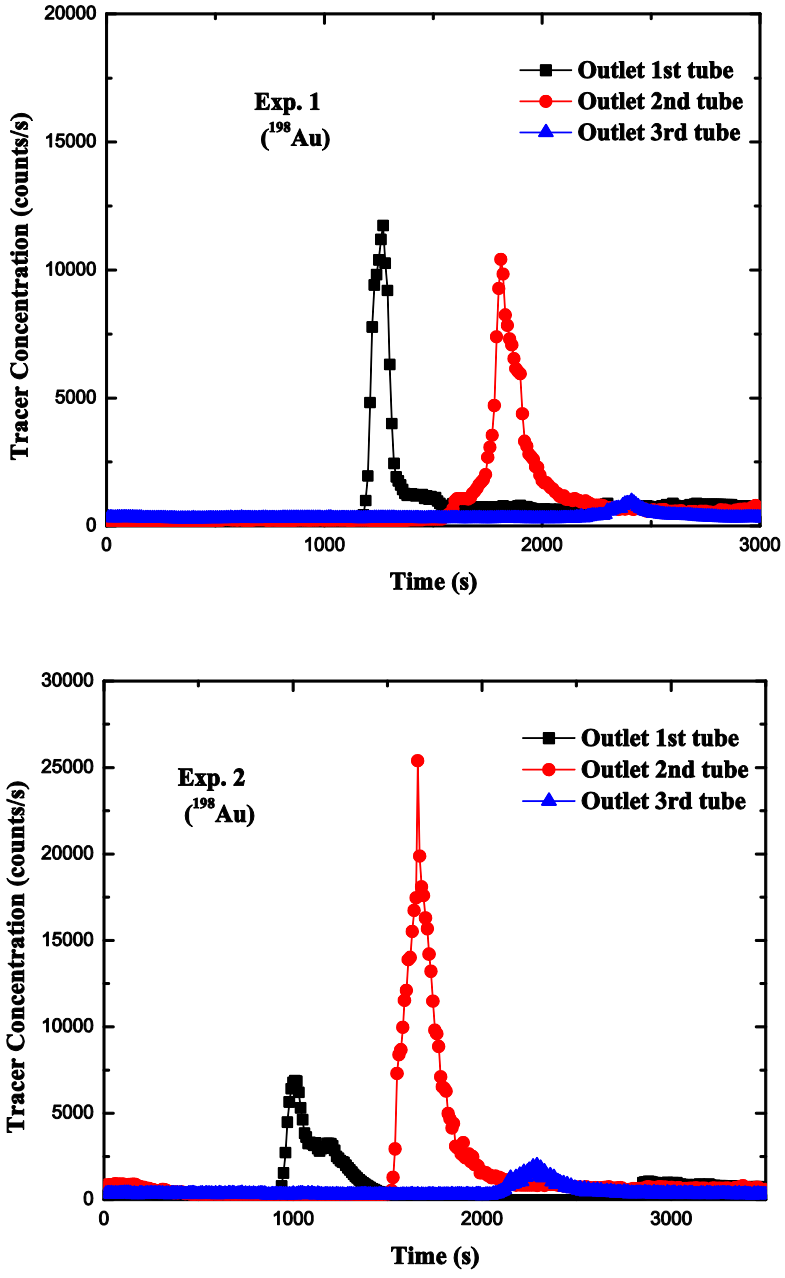

Figure 4.10 Typical raw data obtained for different RTD experiments using ^{198}Au

4.2.2 Treated data

The raw data are treated for starting point correction, background correction and tail correction. The treated data are shown in Figure 4.11.

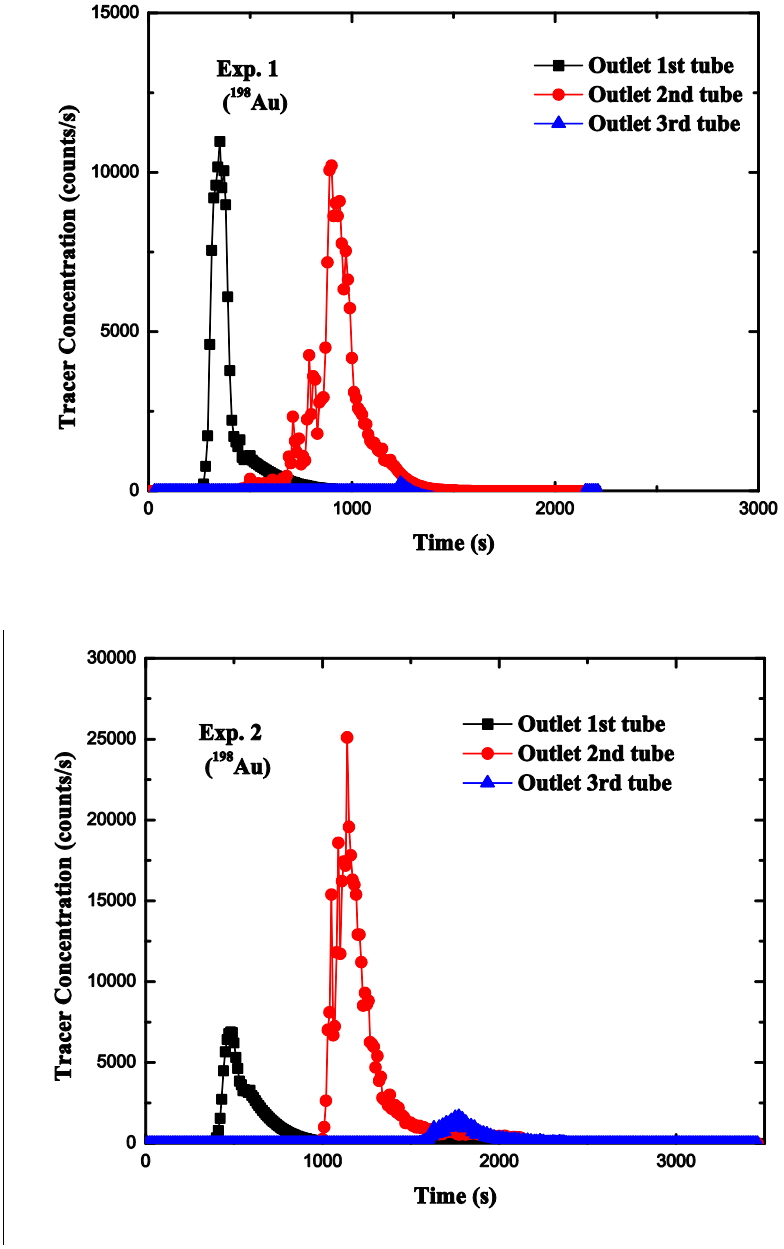

Figure 4.11 Pretreated concentration vs time curves for experiments using ^{198}Au

4.2.3 RTD modeling of first tube and whole digester

The ADM and TIBM are used for RTD modeling. The dispersion of white liquor inside the tube of the digester has been determined using the Pe. Pe gives the dispersion of the material or solute alongside the flow's longitudinal direction. The low value of Pe for

the first tube shows very high dispersion in the first tube. The model parameters for both experiments for the first tube and whole digester are given in Table 4.9.

Table 4.9 Model parameters of first tube and whole digester

Exp. No.		Plug flow component (min)	TIBM			ADM	
			No. of tanks (N)	Back-mixing ratio (α)	τ (min)	Pe	τ (min)
1	1st tube	6.3	4	3.2	3	2	2.3
	whole digester	23.8	31	1.3	6.3	16	5.8
2	1st tube	3.8	7	5.2	1.2	3.5	0.9
	whole digester	20	26	2.8	6	13	5.6

4.2.4 Modelling of second and third tubes

The model parameters for both experiments for the second and third tube are given in Table 4.10.

Table 4.10 Model parameters of second and third tubes

Exp. No.		Plug flow component (min)	TIBM			ADM	
			No. of tanks (N)	Back-mixing ratio (α)	Value of τ (min)	Pe	τ (min)
1	2nd tube	8	17	1.8	2.3	9	2.2
	3rd tube	10	28	0.6	2	29	1.5
2	2nd tube	7.8	20	2.3	2.8	11	3
	3rd tube	8.3	29	0.9	1.6	26	1.8

The observations of Table 4.9 and Table 4.10 show that the dispersion is decreasing as the material passes from the inlet to the outlet of the digester. The maximum value of Pe is observed inside the third tube which represents the plug flow behavior or negligible dispersion inside the third tube. The complete transition of the flow from high dispersion to low dispersion due to an increase in the viscosity of the liquid phase. The viscosity of the liquid phase has increased due to dissolved lignin. The curve obtained at the outlet of the first tube (Figure 4.12), shows a sudden increase in the concentration and having a long tail for both experiments. The behavior of these types of curves represents

mixed flow with high dispersion coefficient. Modeling for the first tube is presented in Figure 4.12. Along the length of the digester, dispersion decreases from the inlet to outlet.

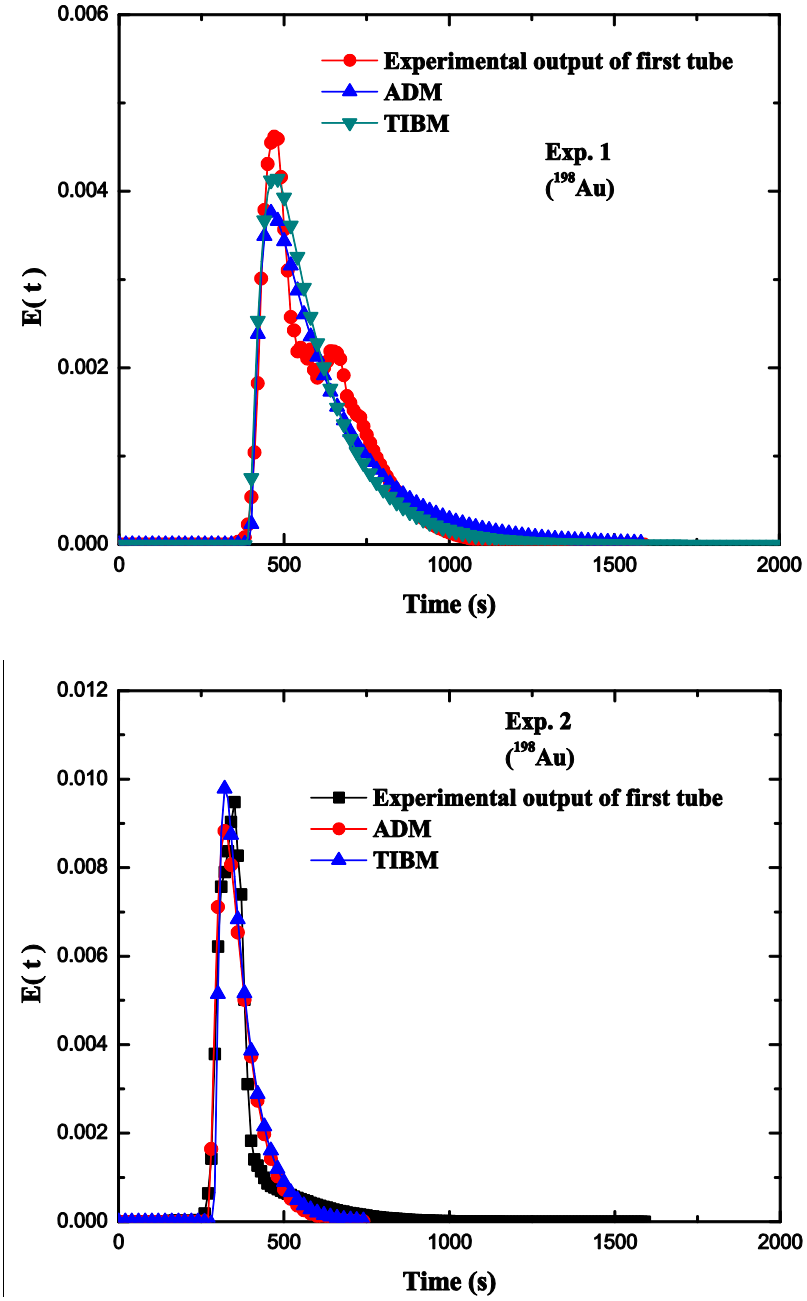

Figure 4.12 RTD modelling of first tube for Exp. 1 and Exp. 2

In Figure 4.14, the *E*(*t*) curves for both experiments represent low dispersion in the second tube. Similarly, for the third tube (Figure 4.15) the dispersion further decreased to a minimum value. The symmetric shape of the curve represented the plug flow behavior inside the third tube. Overall dispersion inside the digester is almost equal that represented by the second tube. The modeling for the whole digester by assuming it a single reactor is represented by Figure 4.13.

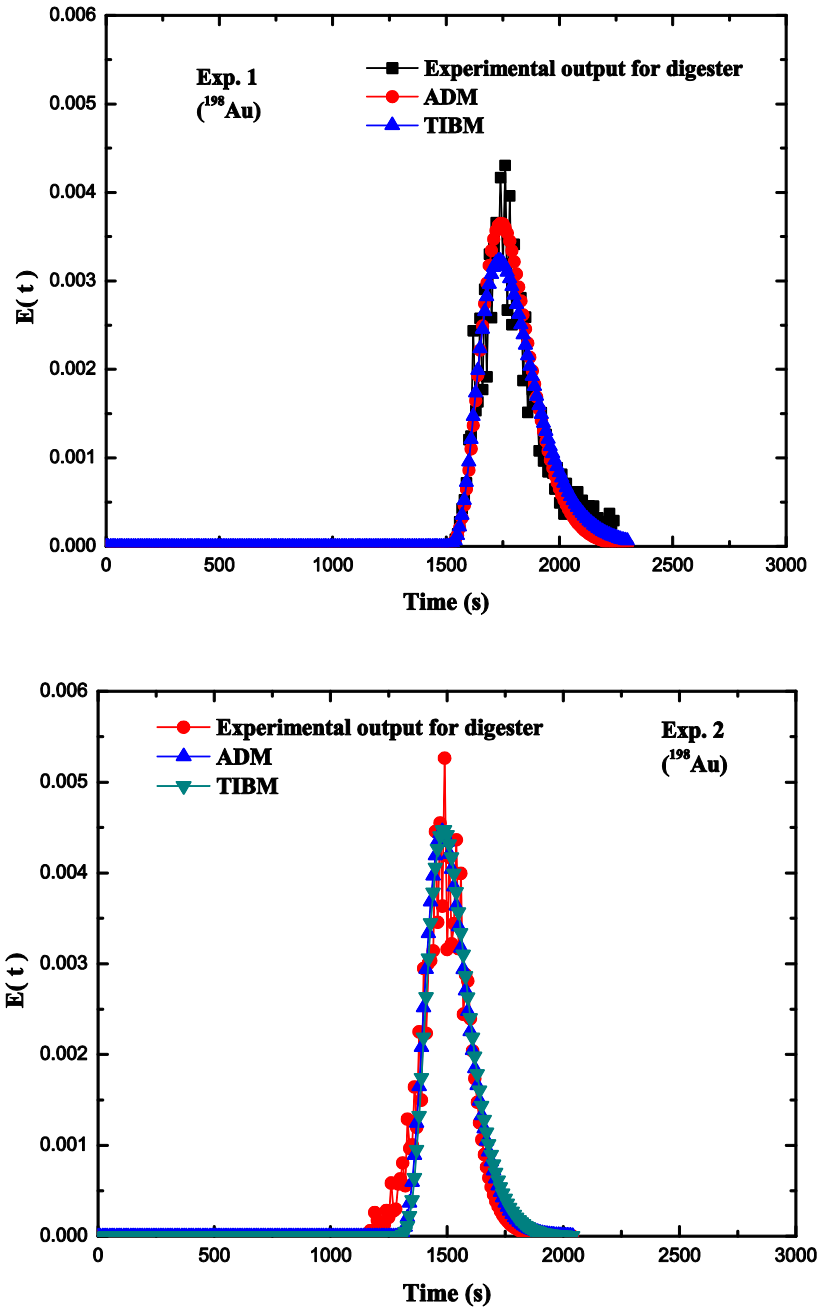

Figure 4.13 RTD modelling of whole digester by assuming it a single reactor

The mean residence time in the first tube for both the experiments is shown in Table 4.10. The main difference is observed in the MRT of the first tube. MRT of experiment 2 is lower than the MRT of experiment 1. The decrease in the MRT is observed due to the high white liquor flow rate.

In the second and third tubes, MRT is almost similar in both the experiments. Inside the first tube, the liquor viscosity is low which results in high dispersion. As the

viscosity increases in the second tube, fluid starts to flow with less turbulence. High velocity inside the first tube resulted in the high back-mixing as shown in Table 4.9.

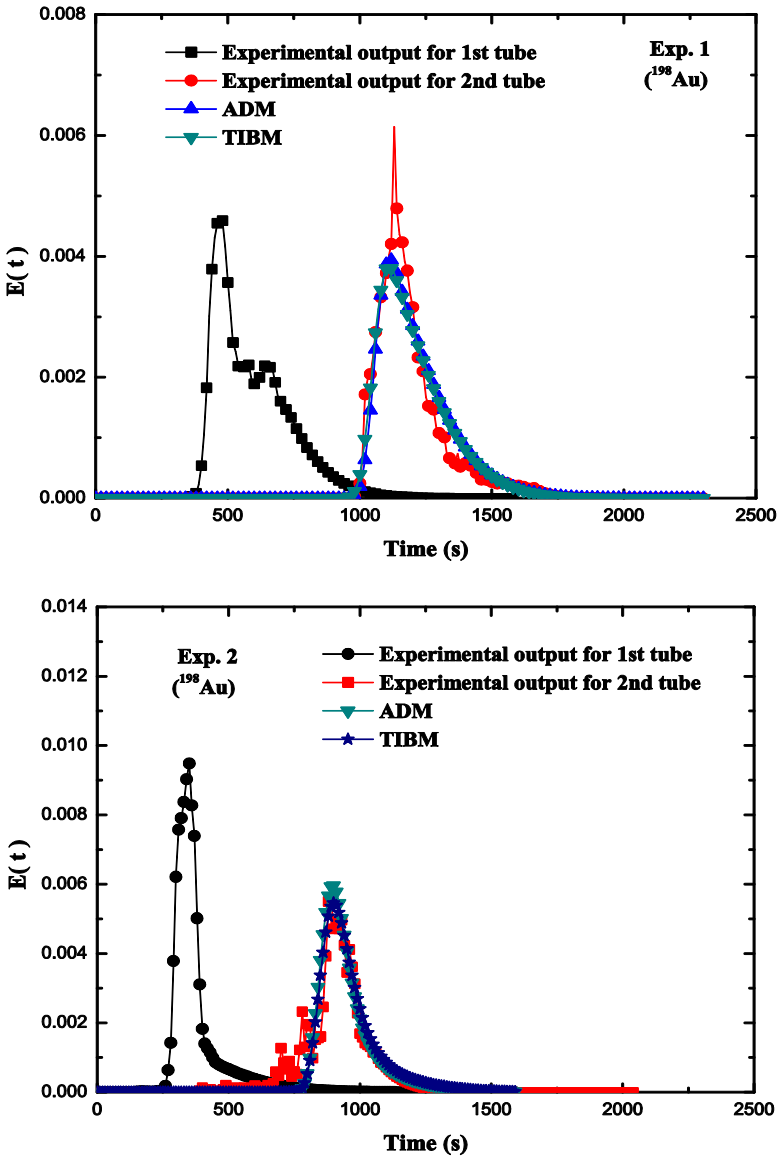

Figure 4.14 RTD modelling of second tube using convolution

As the viscosity increased inside the second tube, back-mixing also decreased. Very low back-mixing was observed in the third tube. It was also observed that the number of tanks in the tank-in-series with the back-mixing model was almost double the value of Pe. We know that the axial dispersion model represents the plug flow stream overlapped with some amount of back-mixing. These results also verified this fact.

The two separate phases converted into the pulp slurry at high temperature and pressure which flows like a plug flow in the third tube. From a hydrodynamic point of

view, a transition flow behavior is observed for the whole digester. The concept of transition flow can be applied only for the case when the whole digester is assumed as a single reactor.

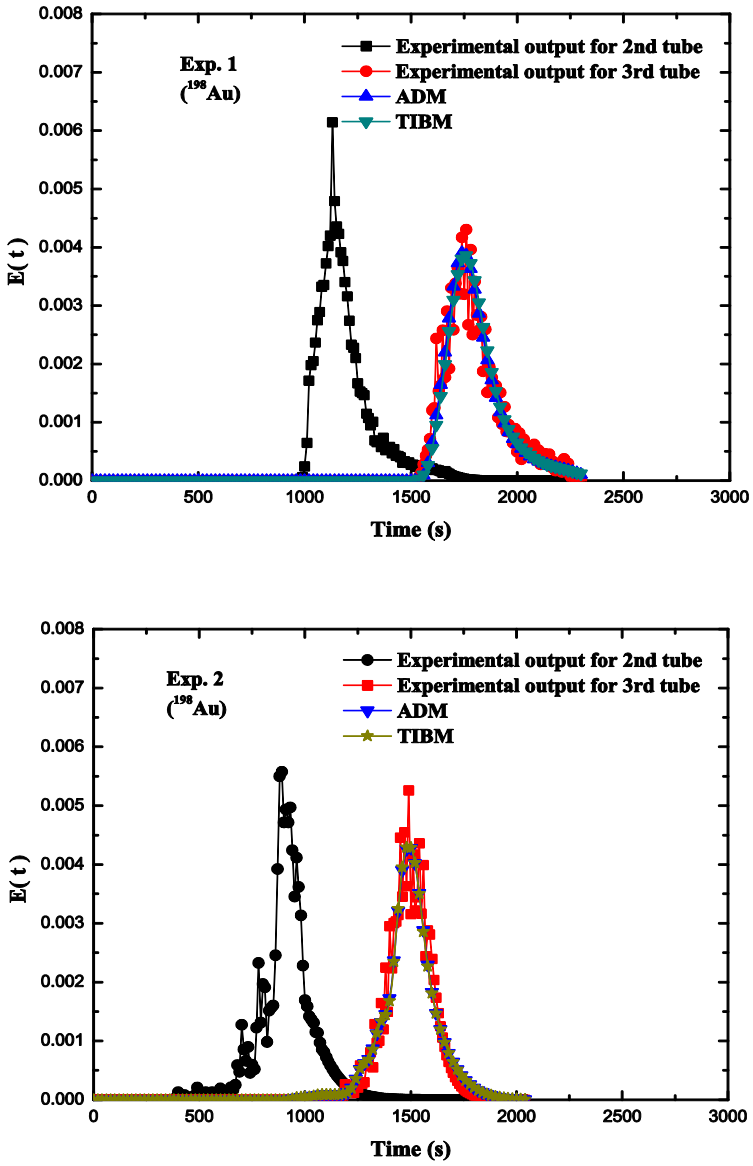

Figure 4.15 RTD modeling of third tube using convolution

For this case, we assumed that the viscosity is constant at each point in the digester which is equal to the viscosity of the pulp. But in actual, the viscosity and specific gravity are continuously changing from inlet to outlet. Inside the first tube of the digester, the liquid phase has low specific gravity and viscosity. At these conditions, the high dispersion of white liquor in the wheat straw is observed. As the dispersion increases at high temperature and pressure, the cellulose fibers start to separate from lignin. The lignin gets dissolved in the liquid phase which results in a high viscosity of the liquid phase. Also, the

dissolved lignin and other chemicals turned the liquor black. Inside the third tube, the liquid phase has high viscosity and density with plug flow behavior.

4.3 Conclusions

RTD experiments using Radiotracer Bromine (^{82}Br) as ammonium bromide and gold (^{198}Au) as chloroauric acid were performed to investigate the flow behavior of three-tube continuous flow pulping digesters in the paper industry in India. The experimental data were obtained at the outlet of each tube using γ-ray scintillation detectors. The data were pretreated for dead time correction, starting point correction and tail correction. Axial dispersion model and tank-in-series with back-mixing model each preceded by a plug flow component were used to simulate the experimental data. For the second and third tubes, a convolution procedure is used for simulating the experimental data due to non-ideal injection. The model parameters were calculated for each experiment and the dispersion was found to decrease as the material passed through the first to the third tube of the digester. This suggests that the highly dispersed flow of the process material in the first tube is transformed into a flow having negligible dispersion in the third tube. In the third tube, both phases converted in a slurry-like single phase with high viscosity. Inside the third tube, the liquid phase encounters high hindrance or obstruction from the solid particles due to high viscosity. This hindrance is further responsible for the plug flow behavior inside the third tube. The MRT of each tube is different in spite of having the same dimensions which is due to the complex flow behavior resulting in different dispersions in each tube.

Chapter-5 RTD Study of Two-Tube Pulping Digester

5.1 RTD study of two-tube digester

The second phase of RTD experiments has been carried out in two identical two-tube continuous pulping digesters at M/s Trident Industries Ltd., Barnala, Punjab, India. The radiotracer ^{99m}Tc in the form of sodium pertechnetate is used to trace the liquid phase of both the digesters. The injection and detection procedure is explained in Chapter-1. The wheat straw feed rate and white liquor feed rate are the main process variables. The operating conditions of digester 1 (D1) and digester 2 (D2) are given in Table 5.1.

Table 5.1 Operating conditions during RTD measurements of digesters D1 and D2

Experiment No.	Temperature (°C)		Pressure (kg_f/cm^2)	Wheat straw feeder RPM	White liquor flow rate (l/min)	Steam flow rate (kg/min)
	Tube 1	Tube 2				
Digester 1 (D1)						
1	174.2	172.3	7.4	5	215.0	88.3
2	171.5	172.6	7.8	5.5	245.8	106.6
3	169	169.5	6.99	5.5	261.8	95.0
4	165.8	163.8	6	6	235.0	100.0
5	168.8	165.3	7.3	6	278.2	93.3
6	172	169.9	7.35	6.2	264.6	108.3
Digester 2 (D2)						
1	170.7	170	7.19	5	229.3	88.3
2	164.3	164.8	7.1	5.5	265.8	115
3	161.8	160.6	6.58	5.5	280.8	100
4	162.7	162.7	6.81	6	259.5	101.6
5	167.6	167.7	7.19	6	282.2	102.8
6	164.1	163.7	7.08	6.2	292.5	108.3

The operating parameters for pulping digester are varied in a prescribed limit so that it does not affect the normal industrial scale operation. The biomass feed rate is varied using

wheat straw screw feeder rpm which was kept in the range of 5-6.2 rpm (2.5-3.6 m^3/min). The white liquor flow rate is varied from 215-292.5 l/min.

The obtained pulp is analyzed for the output product quality as Kappa number and black liquor is analyzed to obtain its residual alkali and these output parameters are tabulated in Table 5.2. The value of Kappa number is the measurement of the extent of delignification process and it indicates the amount of residual lignin in the pulp. The lower value of the Kappa number shows the better quality of pulp and its vise-versa.

Table 5.2 Output parameters of digesters D1 and D2

Experiment No.	**D1**		**D2**	
	Kappa number of pulp	**Residual alkali (g/l)**	**Kappa number of pulp**	**Residual alkali (g/l)**
1	15	5.4	14.3	5.5
2	15.1	6.7	16	6.5
3	15.2	5.7	16.5	6.7
4	15.5	6.1	16.7	7
5	15	5.9	15.7	6.9
6	16.5	5.8	15	5.8

Output product quality of both the digesters is considered as the measurement of performance. Initially, the RTD experiments were performed in digester D1 as per operating conditions are given in Table 5.1. The value of the output parameter Kappa number was found in the range of 15-16.5 and the value of another output parameter (residual alkali in black liquor) was obtained in the range of 5.4-6.7. These output values are in the satisfactory range except Exp. 2 and Exp. 6. In the case of Exp. 2, there may be some material stuck inside the digester which gives long residence time. The high value of residual alkali in this case also indicates some kind of abnormal behavior.

Specifically, in the case of Exp. 6, the high steam flow rate has caused the dilution of white liquor inside the digester, which led to inefficient delignification. This inefficient delignification resulted in high Kappa number. It was observed that the steam flow rate higher than 100 kg/min caused the poor delignification resulted in high Kappa number or high value of residual alkali.

In case of digester D2, low value of Kappa number and low value of residual alkali were observed only in Exp. 1 which are shown in Table 5.2. Other than Exp. 1 and 5, Experiments. 2-6 are having a high value of Kappa number and residual alkali, which represent poor delignification. The values of feed screw rpm for digester D2 were kept in the same range as in case of digester D1. However, the flow rate of white liquor was kept higher for each experiment as compared to digester D1. Even at a high ratio of white liquor to feed screw rpm, the output products are of lower quality with a high value of Kappa number and high value of residual alkali (5.8-7 g/l) which indicates poor delignification. This may be due to the low effective volume or less retention time of the process material inside the digester which is estimated after observing the RTD results. Hence, the results show that the digester D2 is not performing well as compared to digester D1.

5.1.1 Raw data of RTD experiments

Schematic of the two-tube pulping digester is shown in Figure 3.2. The injection and detection procedure of the radiotracer was same that used for the three-tube digester. Total of six experiments were selected to represent or analyze the performance of both the digesters. The experimental RTD data obtained for digesters D1 and D2 are shown in Figure 5.1 and 5.2 respectively.

5.1.2 Treated data

The raw data were treated for dead time correction, background correction, tail correction and data smoothing. In dead time correction, the counts before radiotracer injection are removed. Depending upon the gap between the times of DAS started getting reading and radiotracer injection, 500-900 s are removed. Background correction was done to remove the counts present due to electrical noise or any other disturbance. Tail correction was done so that the concentration of tracer reached to zero after completion of RTD experiment. The data smoothing was done to remove the fluctuations. The pulping digester has small residence time, hence decay correction is not required. Pretreated data for different experiments are shown in Figure 5.3 and Figure 5.4 for digester D1 and D2 respectively.

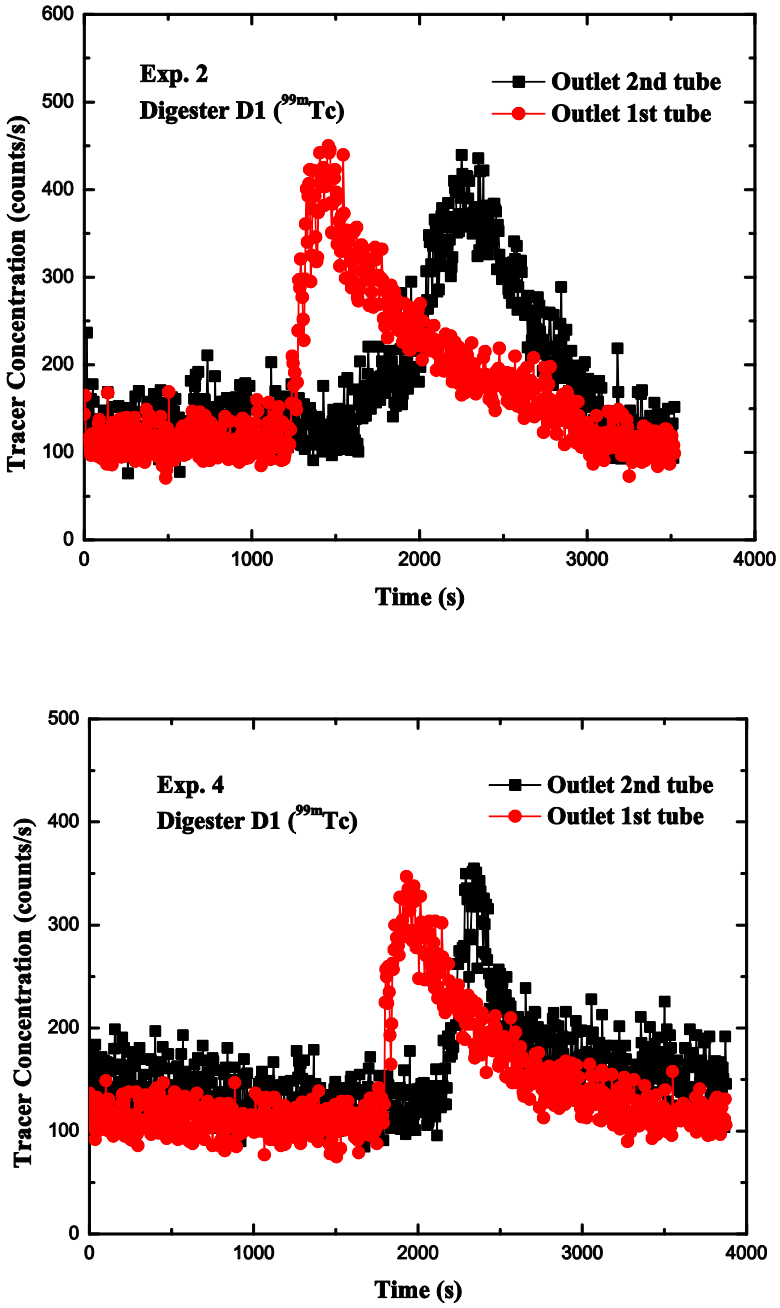

Figure 5.1 Typical raw RTD data obtained for two-tube digester D1

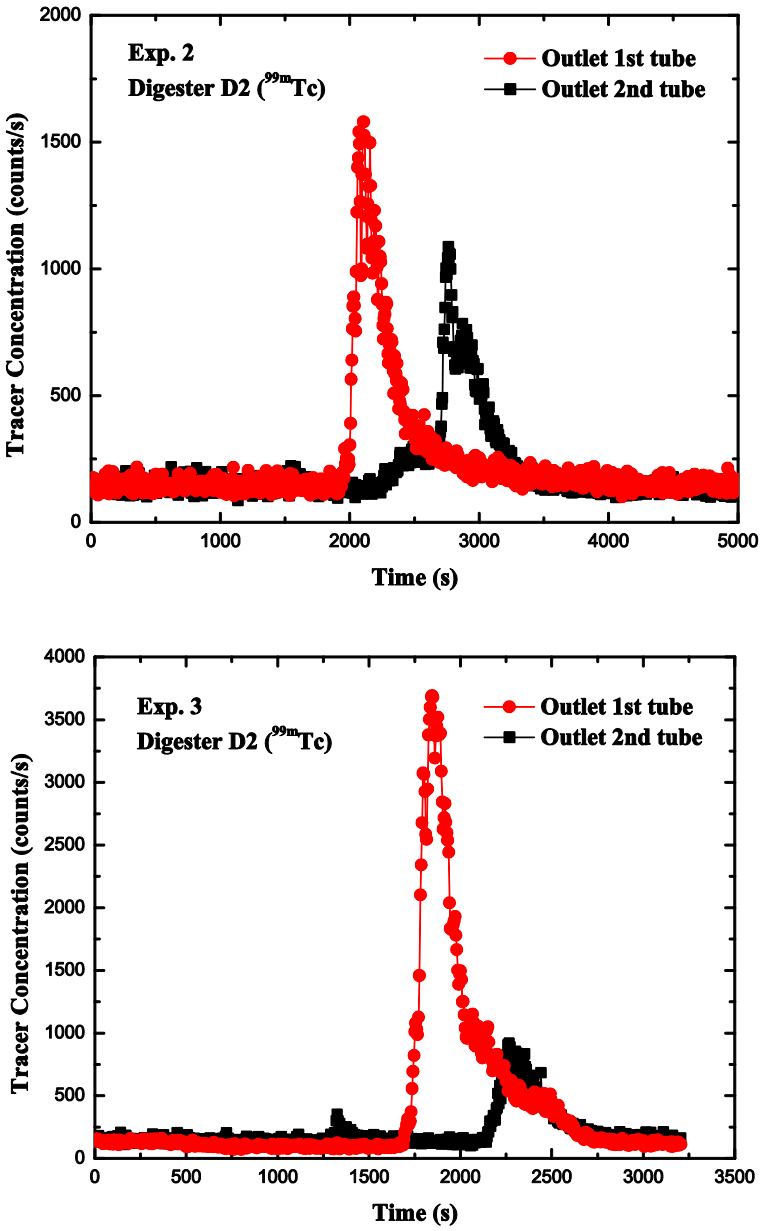

Figure 5.2 Typical raw RTD data obtained for two-tube digester D2

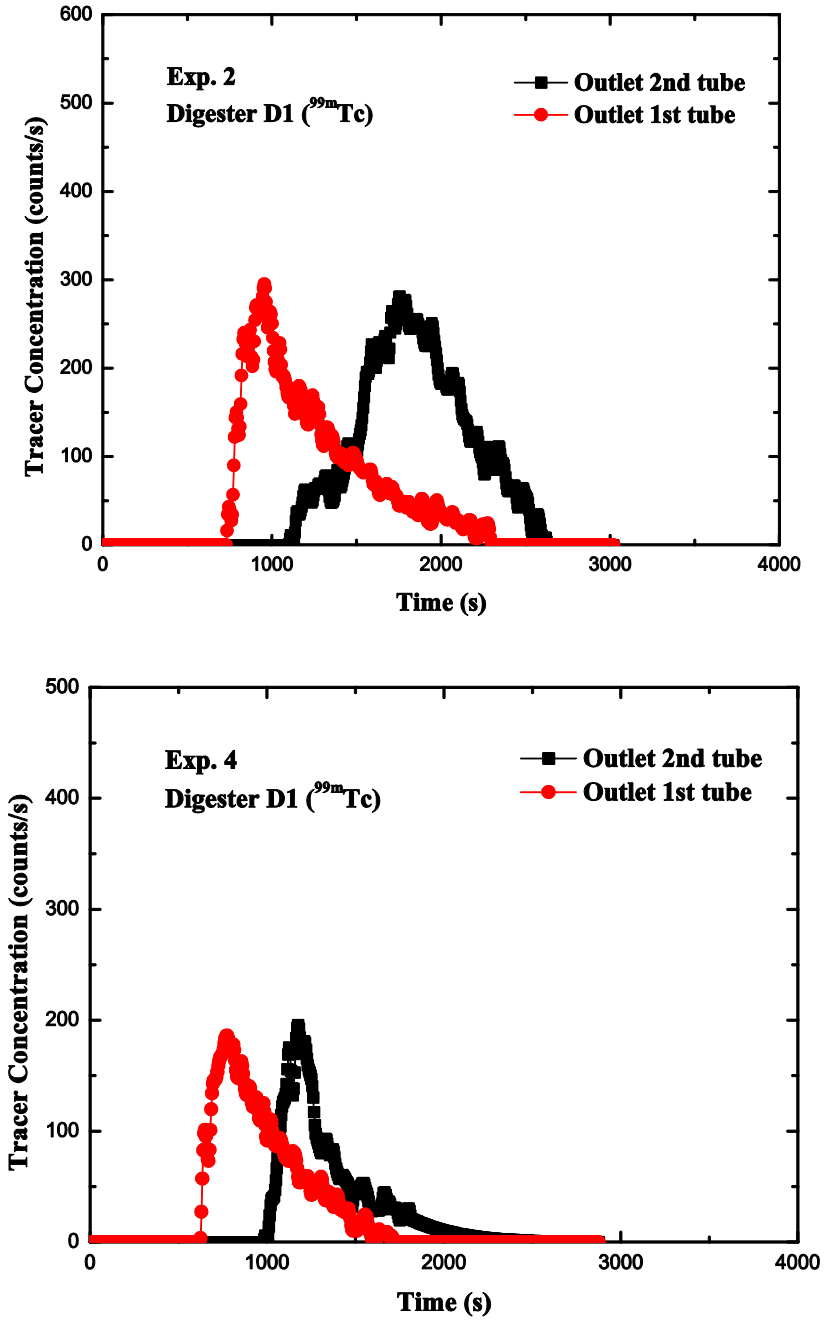

Figure 5.3 Pretreated RTD data for two-tube digester D1

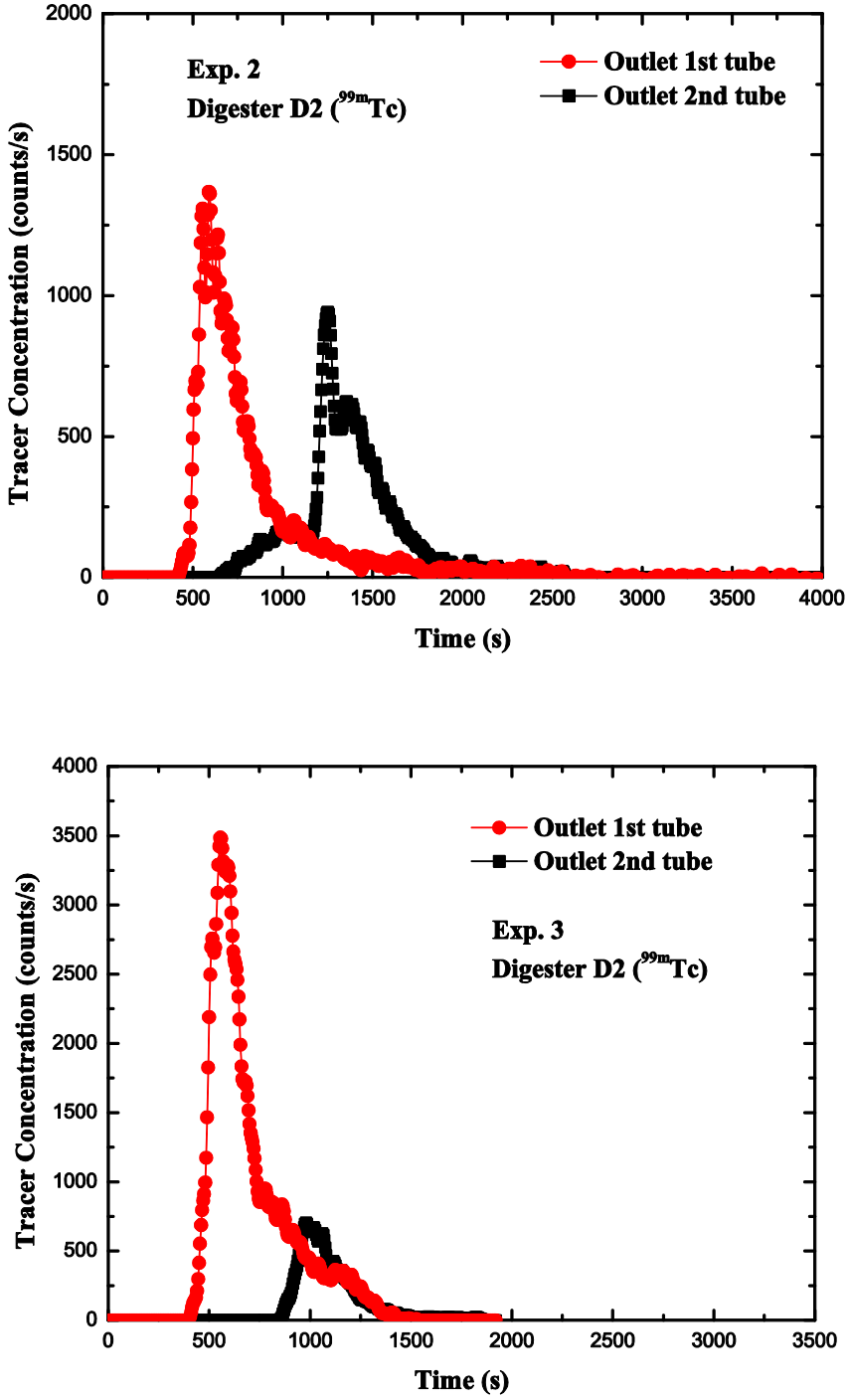

Figure 5.4 Pretreated RTD data for two-tube digester D2

5.1.3 RTD modeling of first tube and whole digester

RTD modeling of the whole digester by assuming it a single reactor has been completed using ADM and TIBM models, each model preceded by a plug flow component. The modelling was completed by keeping the plug flow component constant for each digester. The modeling parameters of the whole digester are shown in Table 5.3 for both the digesters D1 and D2.

Table 5.3 Model parameters of digesters D1 and D2 as separate single reactor

Exp. No.	$\tau_{pf(1-2)}$ (min)	ADM		TIBM		
		$Pe_{(1-2)}$	$\tau_{ADM(1-2)}$ (min)	$N_{(1-2)}$	$\alpha_{(1-2)}$	$\tau_{TIBM(1-2)}$ (min)
Digester 1 (D1)						
1	16.6	8	11.2	16	2	11.5
2	16.6	16	14.8	32	2	15
3	16.6	2.1	5.5	5	1	5.6
4	16.6	2.5	5.8	5	2	6.0
5	16.6	4	6.1	8	1.5	6.3
6	16.6	3	6.0	6	2	6.2
Digester 2 (D2)						
1	11.6	5	5.6	10	2	5.7
2	19.0	5	4.5	10	2	4.6
3	13.3	8	4.8	16	1.5	4.9
4	13.3	4	5.8	8	2	6.0
5	13.3	5.5	5.1	11	1.5	5.2
6	13.3	8	5.0	16	2	5.1

During the fitting of RTD models, the plug flow component was kept constant to reduce the number of variables. Table 5.3 shows that the plug flow component of digester D1 is 16.6 min for all experiments. For digester D2, the plug flow component is obtained as 11.6 min and 19 min for Exp. 1 and Exp. 2 respectively. However, for other experiments (Exp. 3 to Exp. 6) the plug flow component is obtained as 13.3 min. After obtaining the plug flow component, the remaining 2 parameters were varied during the optimization of the ADM model. The optimum values of these parameters are given in

Table 5.3. Table 5.3 also shows the value of $Pe_{(1-2)}$ in the range of 3-16 and value of $N_{(1-2)}$ in the range of 5-32 with a back-mixing ratio of 1-2. This shows moderate mixing or dispersion in inside the pulping digester. However, the high value of $Pe_{(1-2)}$ in case of digester D2 indicates low dispersion as compared to the digester D1.

For both the digesters, the comparisons of experimental RTD data, ADM, and TIBM are shown in Figure 5.5 and 5.6 for various experiments.

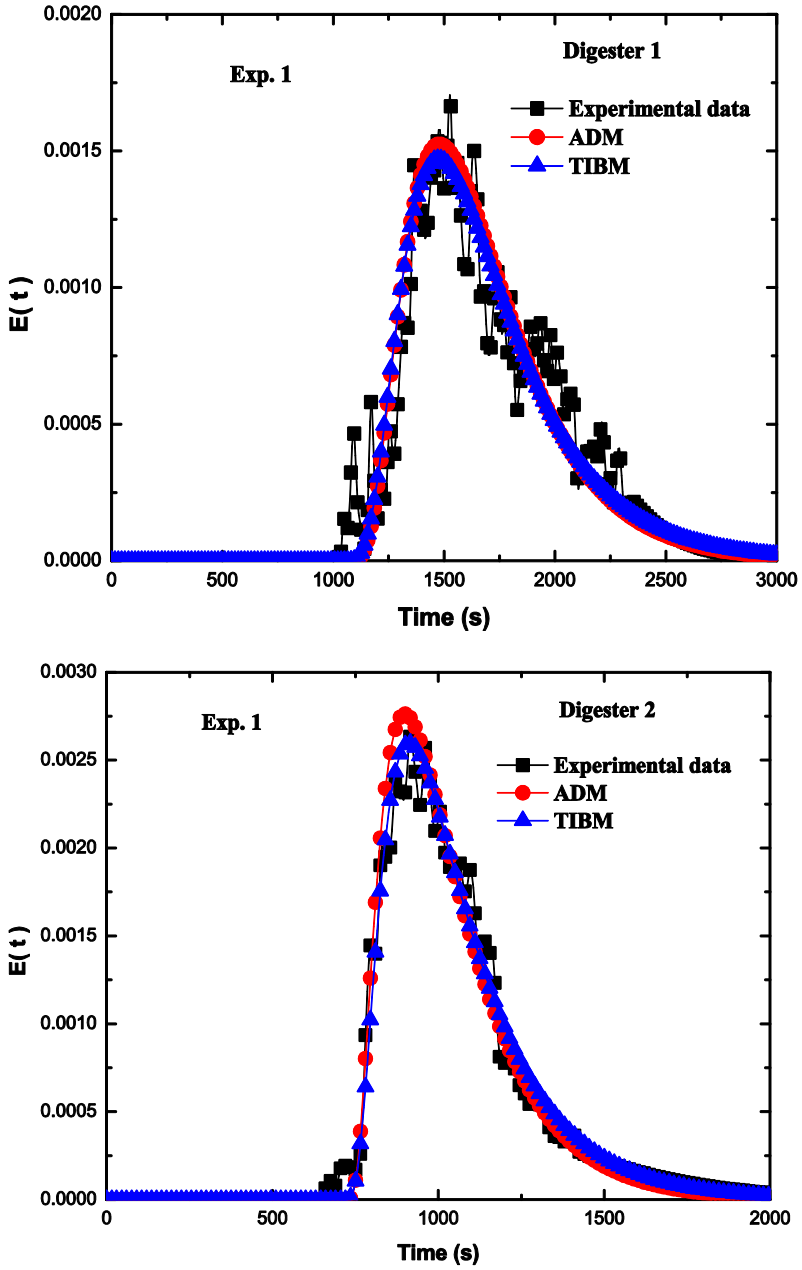

Figure 5.5 RTD models of whole digesters experiment 1 (D1 and D2)

Figures 5.5 and 5.6 are showing the satisfactory match between the experimental data and the proposed models (ADM and TIBM). TIBM shows a better match with experimental values as compared to ADM. Hence, it can be concluded that both the models are suitable for RTD modelling of the pulping digester and TIBM is more appropriate among both models.

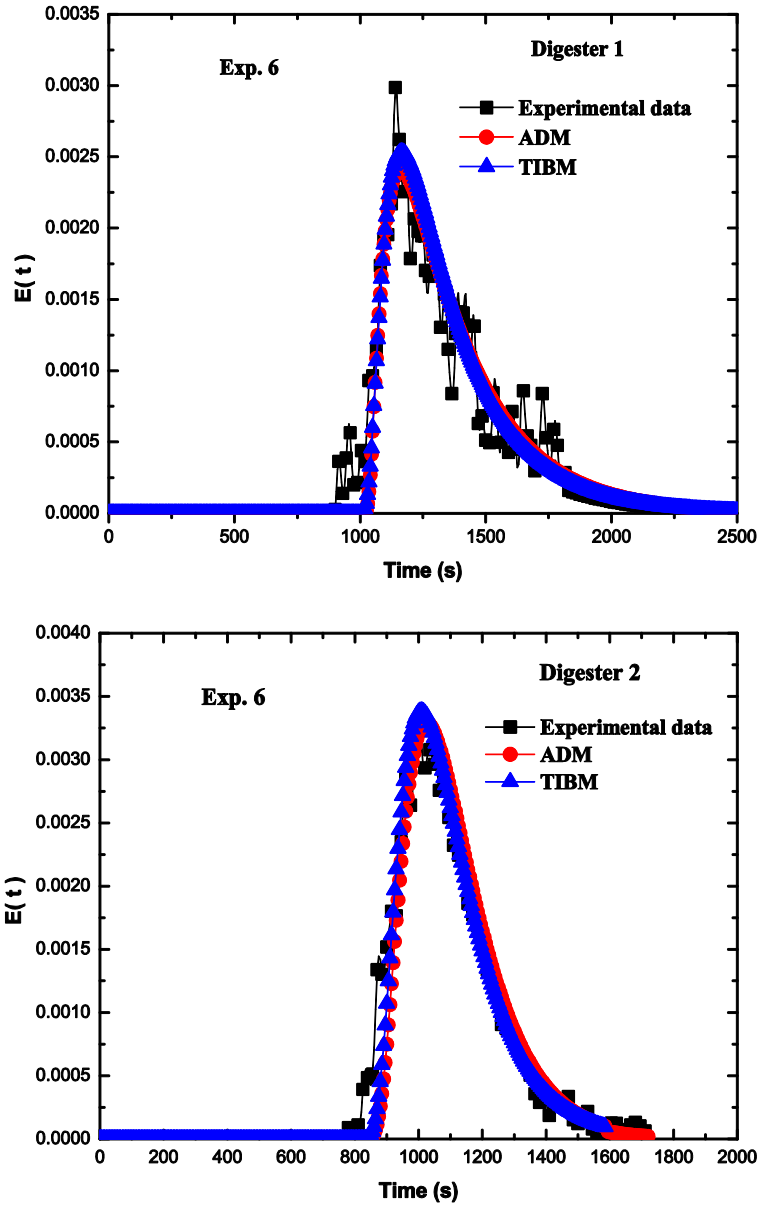

Figure 5.6 RTD modelling of whole digester experiment 6

Additionally, the modeling of the individual digester tubes is also performed to see the local flow behavior inside each tube. The modeling of the first tube

for both the digesters was completed using a similar procedure which is used for the modeling of the whole digester (as explained in the previous section). Table 5.4 shows that the value of Pe1 varied from 1.5 to 4 and the value of N1 varied from 4 to 10 which indicate the high dispersion or mixing inside the first tube. Whereas the value of α1 varied from 2.5-12 which indicates the high back-mixing inside the first tubes of both the digesters. The high back-mixing may be caused by the high flow rate and low viscosity of the white liquor.

Table 5.4 Model parameters of first tube in D1 and D2

Digester 1 (D1)						
Exp. No.	**τ_{pf1}(min)**	**(ADM)**		**(TIBM)**		
		Pe_1	**τ_{ADM1}(min)**	N_1	α_1	**τ_{TIBM1}(min)**
1	10	3	6.3	10	9	6.8
2	12	3	7.6	6	3	7.8
3	10	3	7.3	9	5	7.6
4	10	3	6.5	4	6	6.7
5	10	1.5	7.4	8	12	7.6
6	10	1.5	7.85	4	8	8.0
Digester 2 (D2)						
1	8.0	4	6.0	9	3	6.7
2	7.5	3	4.9	7	2.5	5.3
3	7.3	4	3.7	9	3.5	4.2
4	7.5	4	6.9	4	7	7.3
5	7.0	3	7.1	5	6	7.4
6	7.5	4	5.6	10	4	5.9

The comparison of experimental data with the models for the first tube of both the digesters is shown in Figure 5.7. From Figure 5.7, it is concluded that the presence of high dispersion and back-mixing are present inside the first tube. The curve shows that concentration increases suddenly and then decreases with a long tail. This type of behavior indicates the high dispersion inside the first tube. Values of Pe_1 and α_1 in Table 5.4 also demonstrate this fact. Dispersion and back-mixing are higher inside the first tube

in case of D1 as compared to D2 as shown in Table 5.4. TIBM represents the experimental data better than the ADM in the first tube due to the high back-mixing ratio as shown in Figure 5.7.

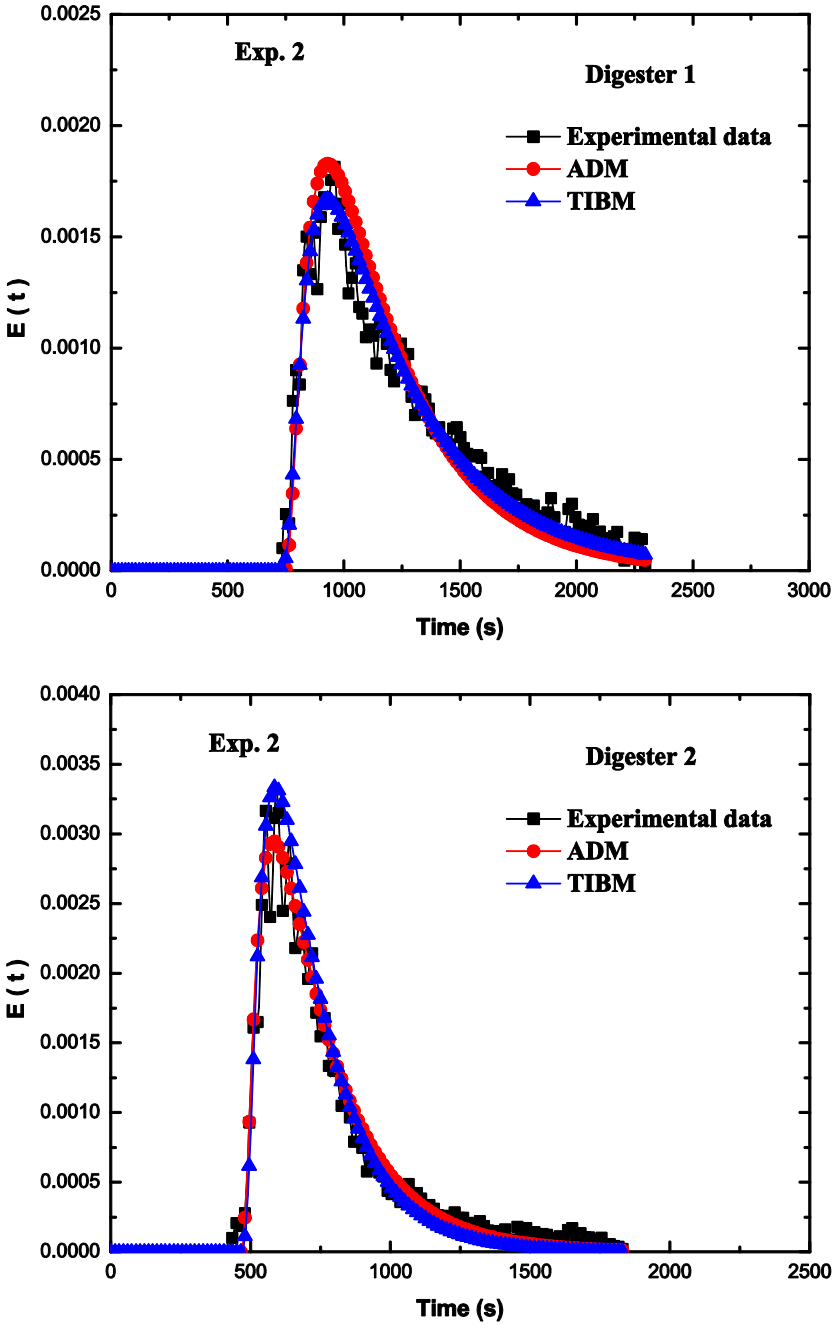

Figure 5.7 RTD modelling of first tube experiment 2

5.1.4 RTD modelling of second tube

Modeling parameters for the second tube are presented in Table 5.5. During the optimization process, the obtained value of the Pe_2 is in the range of 8-13 and the value of N_2 is in the range of 10-24 which indicates the low dispersion inside the second tube.

The back-mixing ratio inside the second tube is also low which is shown from the value of α_2 (0.08-0.8) in Table 5.5. High back-mixing is observed in case of Exp. 2 in D1. The comparison of experimental and models data is shown in Figure 5.8 and it was observed that the TIBM model gave better fit with the experimental data.

Table 5.5 Model parameters of second tube in D1 and D2

Digester 1 (D1)						
Exp. No.	**τ_{pf2}(min)**	**ADM**		**TIBM**		
		Pe_2	**τ_{ADM2}(min)**	α_2	N_2	**τ_{TIBM2}(min)**
1	7.5	8	3.9	0.2	10	4.1
2	7.5	12	13	1.3	21	13
3	5.9	11	2.1	0.8	24	2.2
4	4.1	9	1.9	0.4	19	2.0
5	4.1	8	1.7	0.5	13	1.8
6	4.1	11	1.1	0.5	21	1.2
Digester 2 (D2)						
1	1.6	9	1.0	0.08	13	1.0
2	10.0	13	1.0	0.7	18	1.2
3	5.0	9	2.4	0.5	14	2.5
4	4.1	7	1.3	0.5	11	1.5
5	4.1	11	0.9	0.4	20	1.0
6	4.1	12	1.2	0.6	16	1.3

Inside the second tube, wheat straw was converted into pulp which flowed at low velocity due to high viscosity. At high viscosity, liquid particles encounter equal hindrance from solid particles which resulted in low dispersion inside the second tube.

It is observed that the first tube of each digester has high dispersion with the high back-mixing ratio. However, the second tube has very low dispersion as compared to the first tube with the little back-mixing ratio.

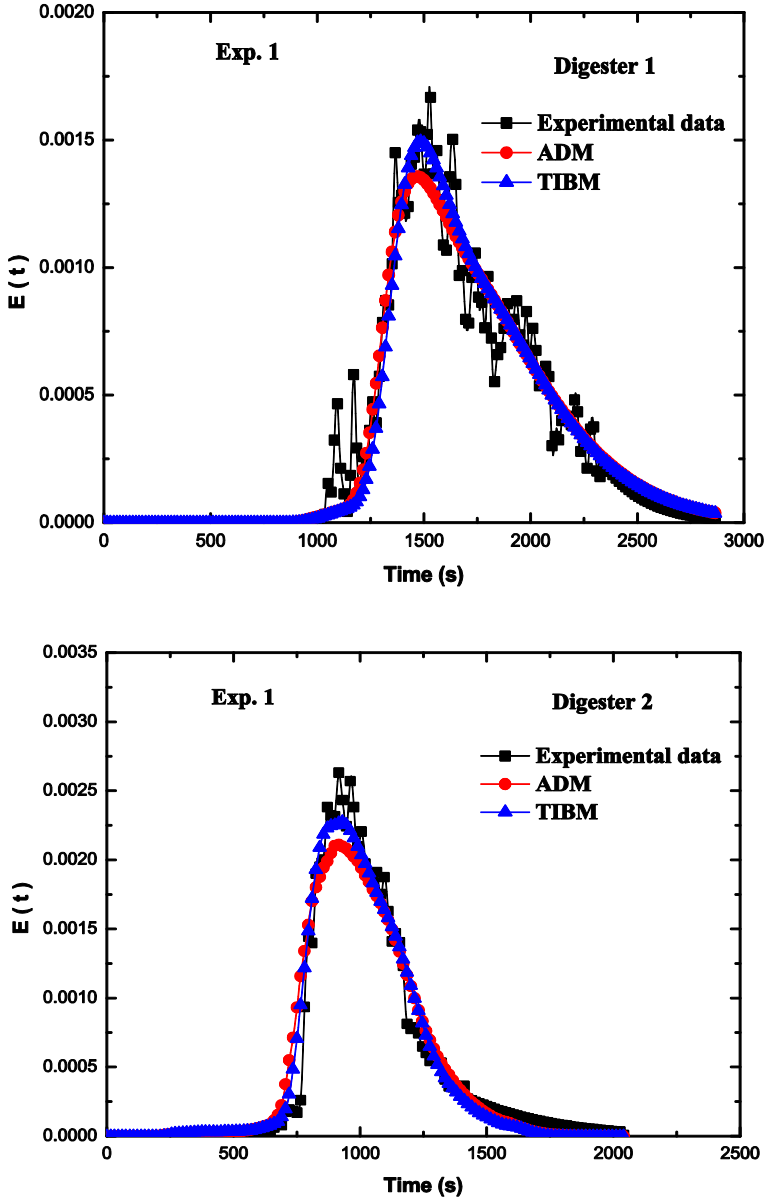

Figure 5.8 RTD modeling of second tube

5.1.5 Mean residence time (MRT)

MRTs for each experiment for the whole digester, D1 are shown in Table 5.3. For Exp. 1, the MRT for the plug flow component is 16.6 min and MRT for the ADM component is 11.2 min and the MRT for Exp. 2 was suddenly increased to 14.8 min, which is very high as compared to other experiments. This may be due to higher recycling

ratio of the liquid material at a higher flow rate (245 l/min) with respect to wheat straw feed rate. Further, in Exp. 3, the low value of MRT is observed as the feed rate was increased. Little increase in the MRT was observed as we increased the feed rate in Exp. 4 and Exp. 5, MRT increased. Further in Exp. 6, the MRT again decreased. A similar pattern was also observed in the case of digester D2. However, the MRT values were found very low as compared to D1 in each experiment.

The MRTs of individual digester tubes are also obtained and shown in Table 5.4 and 5.5. These tables show that MRTs of the first tube is higher than the MRTs of the second tube in both the digesters. The reason for high MRT in the first tube may be the high back-mixing ratio. MRT of each tube depends on the speed of the helical screw inside tubes which is driven by the connected motor for providing optimum delignification time. The speed of these helical screws is kept constant for all the experiments and identical for both the digesters. A little difference in total MRT is observed when the MRTs of the first and second tube was added. It may be due to unavoidable experimental or simulation errors.

The experimentally measured MRTs of both the digesters are different even having similar geometry and operating conditions. In the case of D1, the average value of the experimentally measured MRT is 24 min. The output product quality of the digester D1 is also better than digester D2. Hence, the digester D1 is working well. However, in the case of D1, the experimental MRT values are very low (average 18 min) as compared to theoretical MRT. D2 has lower MRT in all the experiments than that in D1, which may be due to channeling or scaling inside the digester. The low MRT indicates that the D2 has very less effective volume. The 24% reduction in MRT of digester D2 was observed which may be the reason for the decrease in the efficiency of the digester D2. Due to less effective volume in D2, the low retention time is available for the process material which is not sufficient to carry out the proper delignification. The improper delignification results in the poor quality product. Overall, the present RTD analysis and modeling show that the digester D1 was performing well and the digester D2 was underperforming and needed serious maintenance.

5.2 Conclusions

RTD experiments were carried out in two identical two-tube pulping digesters using radiotracer ^{99m}Tc in the form of sodium pertechnetate. The wheat straw screw speed

rpm was varied in the range of 5-6.2 rpm. At low wheat straw feed rate, the recycling of white liquor was observed and it affected the delignification reaction which resulted in high residual alkali in black liquor and Kappa number of pulp. The irregular flow and high back-mixing were observed inside the first tube of digesters. In the second tube of digesters, the low dispersion was observed. The ADM and TIBM each connected with a plug flow component in the series are found suitable to model the experimental RTD data. The TIBM has predicted more accurate results than ADM and represented the pulp digester flow behavior better than the ADM. The lower value of MRTs than the theoretical MRTs in the second digester, show the lower effective volume of the digester than the theoretical value. The second digester has 24% lower MRT than the first digester which is probably due to channeling and reduced effective volume. The low effective volume may be the reason behind the inefficient delignification and poor quality pulp (high Kappa number).

Chapter-6 Conclusions and Recommendations

6.1 Conclusions

RTD experiments have been carried out in a three-tube continuous pulping digester at M/s Satia Industries Ltd., Muktsar Sahib, Punjab (India), to optimize the operating conditions and to diagnose the flow behavior inside the digester. Radiotracer ^{82}Br as ammonium bromide and ^{198}Au as chloroauric acid have been used to trace the liquid phase of the digester. Data obtained from RTD experiments has been pre-treated for background correction, starting point correction, tail correction and data smoothing. As the pulping in the continuous digester is a short term process, the decay correction is not required.

The mean residence time and flow patterns of liquid phase in different sections as well as in entire digester were estimated at different operating conditions. Flow channeling or parallel flow paths were observed in the first and second tube of the digester. To predict the flow behavior, modeling was done using different RTD models available. Value of the model parameters gives the insight to predict the nature of the flow. The axial dispersion model (ADM) and tanks-in-series with back mixing model (TIBM) with a plug flow component connected in series were found suitable to describe the flow of liquid phase in the digester. The RTD curves showed channeling in the first tube. The results of model simulations indicated plug flow behavior ofthe liquid phase in the third tube. The degree of delignification i.e. Kappa number was found to be minimum (12.8) for screw speed of 65 rpm and white liquor flow rate of 355 l/min. The residual alkali was also found optimum (5.33 g/l) in this case. Therefore, a screw speed of 65 rpm and white liquor flow rate of 355 l/min are considered as an optimum flow condition for operating the pulping digester. The industry has now implemented this finding and getting benefit in terms of product quality and ease of operation.

For the second and third tubes, a convolution procedure was used for simulating the experimental data due to non-ideal impulse injection. It is observed that the dispersion is decreasing as the material passes through the first to the third tube of the digester. This suggests that the highly dispersed flow of the process material is transformed into a flow having negligible dispersion as it passes from the inlet to the outlet of the digester. Inside the third tube, the liquid phase encounters equal hindrance or obstruction from the solid particles as both phases flow like a single phase as a slurry. This hindrance is further responsible for the plug flow behavior inside the third tube. The MRT of each tube is

different despite having same dimensions which is due to the complex flow behavior resulting in different dispersions in each tube. MRT of the plug flow component is increased from the first tube to the third tube.

^{99m}Tc in the form of sodium pertechnetate was also used to analyze the two identical two-tube pulping digesters (old and new) at M/s Trident Industries Ltd. Barnala, Punjab (India). Two continuous digesters have similar operating conditions but the output product quality of the first digester is poor as compared to the second digester. Output product quality of both the digesters is considered as the measurement of performance. The wheat straw screw speed was varied in the range of 5-6.2 screw rpm. At low wheat straw feed rate, the recycling of the white liquor was observed and it affected the delignification reaction which resulted in high residual alkali and Kappa number (poor delignification). The irregular flow and back-mixing were observed inside the first tube of both digesters. Inside the second tube of both the digesters, the low dispersion was observed. The ADM and TIBM each connected with a plug flow component in the series are found suitable to model the experimental RTD data. The results predicted by the TIBM were fitted more closely than the ADM. TIBM gave the best fit with the tail part of the experimental data. The 24% lower value of MRTs in the second digester (old one) than the theoretical MRTs indicates the lesser effective volume for the pulping digester. The second digester has 24% less effective volume. This less effective volume may be due to the channeling and/or scaling inside the second digester, which may be the reason for poor product quality (poor delignification).

6.2 Recommendations for future work

The following recommendations are proposed for future work in the related field.

- The mathematical modeling of Pandean type digester is not available in the literature to the best of our knowledge. This work can be done as an extension.
- The computational fluid dynamic (CFD) study of the three-tube continuous pulping digester is missing in the available body of literature and can be carried out as an extension of this work.
- The RTD of the digester can be obtained by CFD analysis and obtained results can be compared with the existing experimental values. It will provide deeper insight of the process and hydrodynamics of the delignification process for the continuous digester.

- Method to obtaining concentration time curve from count vs time data from radiotracer experiments. Generally, when we carried out the RTD experiment on any reactor, we obtained the data in the form of concentration versus time. RTD experiment using radiotracer gives us the data in the form of counts of radiation emitted per unit time versus time. Hence, we can try to find some method which will be able to convert the counts/s in terms of concentration.
- As delignification reaction proceeds, the material properties of the reactive mixture changes continuously and there is no mechanism available to deal it theoretically and numerically. We can measure the rheological properties of the fluid whose viscosity changes continuously.
- The reaction kinetics of wheat straw soda pulping is not available in the literature. We can carried out the pulping reaction at different temperature-pressure conditions for different time interval and can measure the rate of the reaction and other kinetic parameters. So, it can be extended as future work.
- Different models like laminar flow model and compartment model can be selected for modeling the data obtained from RTD experiments conducted on pulping digester. Different kind of observation and parameters can be obtained through different models which will be very beneficial in the analysis of the behavior of pulping digester

References

1. D. Hunter, *Papermaking: the History and Technique of an Ancient Craft*, Courier Corporation (1978).
2. S. Nomura, E. Hutchins, B.E. Holder, The uses of paper in commercial airline flight operations, *Proceedings of the 20th Anniversary Conference on Computer Supported Cooperative Work, ACM*. (2006), 249-258.
3. Investec-Paper Industry Report, Indian Paper Sector, 6th August, 2018. Investec Securities, Investec Bank plc (UK),
4. IPPTA, Technical advancements in manufacturing of packaging grades of paper, IPPTA, *55th Anual General Meeting and Seminar*, 8-9th march, 2019 (Ahmedabad, Gujarat).
5. L.D. Shackford, A comparison of pulping and bleaching of kraft softwood and eucalyptus pulps, *36th International Pulp and Paper Congress and Exhibition*, Sao Paul Brazil. (2003).
6. M.B. Roncero, A.L. Torres, J.F. Colom T.T.C.F. Vidal, TCF bleaching of wheat straw pulp using ozone and xylanase. Part A: paper quality assessment, *Bioresource Technology*. 87(2003), 305-314.
7. A. Ashori, Nonwood fibers - A potential source of raw material in papermaking. *Polymer-Plastics Technology and Engineering*. 45(2006), 1133-1136.
8. K. Saijonkari-Pahkala, *Non-wood plants as raw material for pulp and paper*, MTT Agrifood Research Finland, Plant Production Research (2001).
9. G.A. Smook, *Handbook for Pulp & Paper Technologists*, Second Edition. Angus Wilde Publications, Vancouver, Bellingham (1992).
10. K. Pahkala, and M. Pihala, Different plant parts as raw material for fuel and pulp production, *Industrial Crops and Products*. 11(2000), 119-128.
11. R.W. Hurter, Nonwood plant fiber characteristics, *Agricultural Residues*. 1 (1997), 1-4.
12. H. Singh, A.K. Singh, H.L. Kushwaha, and A. Singh, Energy consumption pattern of wheat production in India. *Energy*. 32(2007), 1848-1854.
13. B.S. Dedhia, L. Csoka, and V.K. Rathod, Xylanase and ultrasound assisted pulping of wheat straw, *Applied Biochemistry and Biotechnology*. 168(2012), 731-741.
14. S.A. Rydholm, *Pulping Processes*. Interscience Publishers, New York (1965).

15. P. Bajpai, *Bleach Plant Effluents from the Pulp and Paper Industry, Pulp and Paper Making Process.* Heidelberg, Springer (2013), 7-11.
16. J.E. Berg, *Wood and fibre mechanics related to the thermomechanical pulping process*, Doctoral Dissertation, Mid Sweden University (2008).
17. H. Sixta, *Handbook of Pulp*, edited by H. Sixta, Volume 1, WILEY-VCH Verlag GmbH & Co. KGaA, Weinheim (2006).
18. J. Gierer, Chemical aspects of kraft pulping, *Wood Science and Technology*. 14(1980), 241-266.
19. F.S. Chakar and A.J. Ragauskas, Review of current and future softwood kraft lignin process chemistry. *Industrial Crops and Products*. 20(2004), 131-141.
20. I.G. Epelde, C. Lindgren, M.E. Lindstrom, Kinetics of wheat straw delignification in soda and kraft pulping, *Journal of Wood Chemistry and Technology*. 18(1998), 69-82.
21. S.I. Mussatto, G. Dragone, G.J. Rocha, I.C. Roberto, Optimum operating conditions for brewer's spent grain soda pulping, *Carbohydrate Polymers*. 64(2006), 22-28.
22. J.N. McGovern, *Semichemical pulp*. Madison, Wis-US Dept. of Agriculture, Forest Service, Forest Products Laboratory (1945).
23. F.J. Doyle III, and F. Kayihan, Reaction profile control of the continuous pulp digester, *Chemical Engineering Science*. 54(1999), 2679-2688.
24. P.A. Wisnewski, F.J. Doyle III, F. Kayihan, Fundamental continuous-pulp-digester model for simulation and control. *AIChE Journal*. 43(1997), 3175-3192.
25. E.B. Nauman. Residence Time Theory, *Industrial & Engineering Chemistry Research*. 47 (2008), 3752-3766.
26. K.A. Hweij, and F. Azizi, Hydrodynamics and residence time distribution of liquid flow in tubular reactors equipped with screen-type static mixers, *Chemical Engineering Journal*. 279 (2015), 948-963.
27. O. Levenspiel, *Chemical Reaction Engineering*. 4th edition, *Wiley*, India (2004).
28. H.J. Pant, V.K. Sharma, M.V. Kamudu, S. Prakash, S.K. Moorthy, G. Anandam, N. Ramani, G. Singh, Measurement of circulation rates of coal particles in standpipe of a circulating fluidized bed system (CFBS) using radiotracer technique, *Journal of Radioanalytical and Nuclear Chemistry.* 280 (2009), 47-56.

29. G.K. Veluswamy, R.K. Upadhyay, R.P. Utikar, M.O. Tade, G. Evans, M.E. Glenny, S. Roy, V.K. Pareek, Hydrodynamic study of fluid catalytic cracker unit stripper, *Industrial & Engineering Chemistry Research*. 52(2013), 4660-4671.

30. R. Samstag, J.J. Ducoste, A. Griborio, I. Nopens, D.J. Batstone, J.D. Wicks, S. Saunders, E.A. Wicklein, G. Kenny, J. Laurent, CFD for wastewater treatment: an overview. *Water Science and Technology*. 74 (2016), 549-563.

31. H.S. Kim, M.S. Shin, D.S. Jang, S.H. Jung, J.H. Jin, Study of flow characteristics in a secondary clarifier by numerical simulation and radioisotope tracer technique, *Applied Radiation and Isotopes*. 63 (2005), 519-526.

32. I.A.E.A. Radiotracer Residence Time Distribution Method for Industrial and Environmental Applications, Training course series 31, *International Atomic Energy Agency*, Vienna. (2008).

33. I.A.E.A. Tecdoc-291, Tracer methods in isotope hydrology, *Proceedings of an Advisory Group Meeting* organized by the International Atomic Energy Agency, Vienna. (27 September to 1 October 1982).

34. V.N. Yelgaonkar, K.C. Jagadeesan, V. Shivarudrappa, V.K. Sharma, S. Chitra, Production of ^{41}Ar and ^{79}Kr gaseous radiotracers for industrial applications. *Journal of Radioanalytical and Nuclear Chemistry*. 274 (2) (2007), 277-280.

35. S.H. Jung, K.I. Kim, J.H. Ryu, S.H. Choi, J.B. Kim, J.H. Moon, J.H. Jin, Preparation of radioactive core-shell type ^{198}Au@ SiO_2 nanoparticles as a radiotracer for industrial process applications, *Applied Radiation and Isotopes*, 68 (2010), 1025-1029.

36. I.A.E.A. Safety standards for protecting people and environment, Radiation Protection and Safety of Radiation Sources: *International Basic Safety Standards*, Interim Edition, General Safety Requirements Part 3, *International Atomic Energy Agency*, Vienna. (2011).

37. H.J. Pant, V.K. Sharma, M.V. Kamudu, S. Prakash, S. Krishanamoorthy, G. Anandam, P.S. Rao, N. Ramani, G. Singh, R.R. Sonde, Investigation of the flow behavior of coal particles in a pilot-scale fluidized bed gasifier (FBG) using radiotracer technique, *Applied Radiation and Isotopes*. 67 (2009), 1609-1615.

38. L.N. Plummer, Dating of young groundwater, *Isotopes in the Water Cycle, Springer*. (2005), 193-218.

39. H. Constant-Machado, J.P. Leclerc, E. Avilan, G. Landaeta, N. Anorga, O. Capote, Flow modeling of a battery of industrial crude oil/gas separators using ^{113m}In tracer

experiments, *Chemical Engineering and Processing: Process Intensification*. 44(2005), 760-765.

40. W. Mook, and K. Rozanski, *Environmental isotopes in the hydrological cycle*, International Atomic Energy Agency, Vienna (2000), 39.
41. T. Vitvar, P.K. Aggarwal, J.J. McDonnell, A review of isotope applications in catchment hydrology, *Isotopes in the Water Cycle, Springer*. (2005),151-169.
42. J. Charlton, J. Heslop, P. Johnson, Industrial applications of radioisotopes. *Physics in Technology*, 6(1975), 67.
43. S.M. Rao, Injected radiotracer techniques in hydrology, *Proceedings of the Indian Academy of Sciences-Earth and Planetary Sciences*. 93(1984), 319-335.
44. J. Thyn, and R. Zitny, Radiotracer applications for the analysis of complex flow structure in industrial apparatuses, *Nuclear Instruments and Methods in Physics Research Section B: Beam Interactions with Materials and Atoms*. 213(2004), 339-347.
45. H.J. Pant, V.K. Sharma, G. Singh, V.K. Raman, J. Bornare, R.R. Sonde, Radiotracer investigation in a rotary fluidized bioreactor, *Journal of Radioanalytical and Nuclear Chemistry*. 294(2012), 59-63.
46. V.K. Sharma, H.J. Pant, D. Tandon, M.O. Garg, Radiotracer investigations in pilot-scale soakers, *Applied Radiation and Isotopes*. 107(2016), 57-63.
47. F. Ditroi, F. Tarkanyi, S. Takacs, Wear measurement using radioactive tracer technique based on proton, deuteron and α-particle induced nuclear reactions on molybdenum. *Nuclear Instruments and Methods in Physics Research Section B: Beam Interactions with Materials and Atoms*. 290(2012), 30-38.
48. I. Meric, G.A. Johansen, S.D.B. Melo, E.A. Lima, J.M. Jimenez, C.C. Dantas, Monitoring of scale deposition in petroleum pipelines by means of photon scattering: a preliminary study. *INAC 2013: International Nuclear Atlantic Conference*, Recife, PE (Brazil), 24-29 Nov, 2013.
49. R. Thorn, G.A. Johansen, B. Hjertaker, Three-phase flow measurement in the petroleum industry. *Measurement Science and Technology*. 24(2012), 012003.
50. P. Vaz, Radiological protection, safety and security issues in the industrial and medical applications of radiation sources, *Radiation Physics and Chemistry*. 116(2015), 48-55.
51. I.A.E.A. *Safety standards for protecting people and environment, Safety fundamentals SF No-1*, International Atomic Energy Agency, Vienna (2006).

52. I.A.E.A. *Safety standards for protecting people and environment, Radiation Protection and Safety of Radiation Sources: International Basic Safety Standards, Interim Edition, General Safety Requirements Part 3*, International Atomic Energy Agency, Vienna (2011).

53. U.C. Mishra, Regulation of nuclear radiation exposures in India, *Journal of Environmental Radioactivity*. 72(2004), 97-102.

54. H.S. Fogler, Essentials of Chemical Reaction Engineering. *Pearson Education*, (2010).

55. J. Thereska, B. Dida, E. Plasari, T. Cuci, Determination of gas flow distribution in a SO_2-oxidation industrial reactor by radiotracer technique, *Journal of Radioanalytical and Nuclear Chemistry*. 154(1991), 241-248.

56. H. Kasban, O. Zahran, H. Arafa, M. El-Kordy, S.M.S. Elaraby, F.E.A. El-Samie, Laboratory experiments and modeling for industrial radiotracer applications, *Applied Radiation and Isotopes*. 68 (2010), 1049-1056.

57. J. Behin, and M. Aghajari, Influence of water level on oil-water separation by residence time distribution curves investigations, *Separation and Purification Technology*. 64(2008), 48-55.

58. H.J. Pant, A. Kundu, and K.D.P. Nigam, Radiotracer applications in chemical process industry, *Reviews in Chemical Engineering*. 17(2001), 165-252.

59. R.D. Abellon, Z.I. Kolar, W. Den Hollander, J.J.M. De Goeij, J.C. Schouten, C.M. Van Den Bleek, A single radiotracer particle method for the determination of solids circulation rate in interconnected fluidized beds. *Powder Technology*. 92(1)(1997), 53-60.

60. H.J. Pant, V.K. Sharma, A.G.C. Nair, B.S. Tomar, T.N. Nathaniel, A.V.R. Reddy, G. Singh, Application of ^{140}La and ^{24}Na as intrinsic radiotracers for investigating catalyst dynamics in FCCUs, *Applied Radiation and Isotopes*. 67(2009), 1591-1599.

61. G.U. Din, I.R. Chughtai, M.H. Inayat, I.H. Khan, Study of axial mixing, holdup and slip velocity of dispersed phase in a pulsed sieve plate extraction column using radiotracer technique, *Applied Radiation and Isotopes*. 67(2009), 1248-1253.

62. S. Sugiharto, Z. Suud, R. Kurniadi, W. Wibisono, Z. Abidin, Radiotracer method for residence time distribution study in multiphase flow system, *Applied Radiation and Isotopes*. 67(2009), 1445-1448.

63. R. Kumar, H.J. Pant, V.K. Sharma, S. Mohan, S. Mahajani, Investigation of hydrodynamic behaviour of a pilot-scale trickle bed reactor packed with hydrophobic and hydrophilic packings using radiotracer technique, *Journal of Radioanalytical and Nuclear Chemistry*. 294(2012), 71-75.

64. R.M. Moreira, A.M.F. Pinto, R. Mesnier, J.P. Leclerc, Influence of inlet positions on the flow behavior inside a photoreactor using radiotracers and colored tracer investigations, *Applied Radiation and Isotopes*. 65 (2007) 419-427.

65. H.J. Pant, V.K. Sharma, Radiotracer investigation in an industrial-scale oxidizer, *Applied Radiation and Isotopes*. 99(2015), 146-149.

66. H. Ben Abdelouahed, N. Reguigui, N.E. Abbes, Phosphate slurry RTD-effect of the radiotracer choice, *Applied Radiation and Isotopes*. 115(2016), 1-3.

67. H. Ben Abdelouahed, and N. Reguigui, Radiotracer investigation of phosphoric acid and phosphatic fertilizers production process, *Journal of Radioanalytical and Nuclear Chemistry*. 289(2011), 103-111.

68. H.J. Pant, V.N. Yelgoankar, Radiotracer investigations in aniline production reactors, *Applied Radiation and Isotopes*. 57(2002), 319–325.

69. C.P.K. Dagadu, E.H.K. Akaho, K.A. Danso, Z. Stegowski, L. Furman, Radiotracer investigation in gold leaching tanks, *Applied Radiation and Isotopes*. 70(2012), 156-161.

70. Z. Stegowski, and L. Furman, Radioisotope tracer investigation and modeling of copper concentrate dewatering process, *International Journal of Mineral Processing*. 73(2004), 37-43.

71. F.P. Ramırez, and M.E. Cortes, The determination of residence times in a pilot plant, *Nuclear Instruments and Methods in Physics Research Section B: Beam Interactions with Materials and Atoms*. 213(2004), 144-148.

72. V. Santos, and C. Dantas, Transit time and RTD measurements by radioactive tracer to assess the riser flow pattern, *Powder Technology*. 140(2004), 116-121.

73. P. Gupta, M.H. Al-Dahhan, M.P. Dudukovic, B.A. Toseland, Comparison of single-and two-bubble class gas–liquid recirculation models-application to pilot-plant radioactive tracer studies during methanol synthesis, *Chemical Engineering Science*. 56(2001), 1117-1125.

74. H.J. Pant, S. Goswami, J. Samantray, V.K. Sharma, N. Maheshwari, Residence time distribution measurements in a pilot-scale poison tank using radiotracer technique. *Applied Radiation and Isotopes*. 103(2015), 54-60.

75. H.J. Pant, V.K. Sharma, K. Shenoy, T. Sreenivas, Measurements of liquid phase residence time distributions in a pilot-scale continuous leaching reactor using radiotracer technique, *Applied Radiation and Isotopes*. 97(2015), 40-46.

76. J. Oriol, J.P. Leclerc, P. Berne, G. Gousseau, C. Jallut, P. Tochon, P. Clement, Characterization of two-phase flow regimes in horizontal tubes using 81mKr tracer experiments, *Applied Radiation and Isotopes*. 66(2008),1363-1370.

77. S. Goswami, H.J. Pant, J. Biswal, J.S. Samantray, V.K. Sharma, A. Dash, Synthesis, characterization and application of $^{Au}198$ nanoparticles as radiotracer for industrial applications, *Applied Radiation and Isotopes*. 111(2016), 18-25.

78. V. Papangelakis, and G. Demopoulos, Reactor models for a series of continuous stirred tank reactors with a gas-liquid-solid leaching system: Part I. Surface reaction control, *Metallurgical Transactions B*. 23(1992), 847-856.

79. B. Bitsch, C. Barner-Kowollik, S. Zhu, Modeling the effects of reactor backmixing on RAFT polymerization, *Macromolecular Reaction Engineering*. 5(2011), 55-68.

80. I.M. Abu-Reesh, and B.F. Abu-Sharkh, Comparison of axial dispersion and tanks-in-series models for simulating the performance of enzyme reactors, *Industrial & Engineering Chemistry Research*. 42(2003), 5495-5505.

81. W.D. Deckwer, K. Nguyen-Tien, B.G. Kelkar, Y.T. Shah, Applicability of axial dispersion model to analyze mass transfer measurements in bubble columns, *AIChE Journal*. 29(1983), 915-922.

82. S. Degaleesan, and M.P. Dudukovic, Liquid backmixing in bubble columns and the axial dispersion coefficient. *AIChE Journal*. 44(1998), 2369-2378.

83. S. Degaleesan, S. Roy, S.B. Kumar, M.P. Dudukovic, Liquid mixing based on convection and turbulent dispersion in bubble columns, *Chemical Engineering Science*. 51(1996), 1967-1976.

84. F.F. Rivera, M.R. Cruz-Díaz, E.P. Rivero, I. Gonzalez, Analysis and interpretation of residence time distribution experimental curves in FM01-LC reactor using axial dispersion and plug dispersion exchange models with closed–closed boundary conditions, *Electrochimica Acta*. 56(2010), 361-371.

85. O.S. Sudah, A.W. Chester, J.A. Kowalski, J.W. Beeckman, F.J. Muzzio, Quantitative characterization of mixing processes in rotary calciners, *Powder Technology*. 126(2002), 166-173.

86. P.M. Portillo, A.U. Vanarase, A. Ingram, J.K. Seville, M.G. Ierapetritou, F.J. Muzzio, Investigation of the effect of impeller rotation rate, powder flow rate,

and cohesion on powder flow behavior in a continuous blender using PEPT, *Chemical Engineering Science*. 65(2010), 5658-5668.

87. S. Mahmoudi, J.P.K. Seville, J. Baeyens, The residence time distribution and mixing of the gas phase in the riser of a circulating fluidized bed, *Powder Technology*. 203(2010), 322-330.
88. A. Vikhansky, Effect of diffusion on residence time distribution in chaotic channel flow, *Chemical Engineering Science*. 63(2008), 1866-1870.
89. A. Kumar, G.M. Ganjyal, D.D. Jones, M.A. Hanna, Digital image processing for measurement of residence time distribution in a laboratory extruder, *Journal of Food Engineering*. 75(2006), 237-244.
90. R. Saravanathamizhan, R. Paranthaman, N. Balasubramanian, C. Ahmed Basha, Tanks in series model for continuous stirred tank electrochemical reactor, *Industrial & Engineering Chemistry Research*. 47(2008), 2976-2984.
91. J.B. Yianatos, L.G. Bergh, F. Diaz, J. Rodriguez, Mixing characteristics of industrial flotation equipment, *Chemical Engineering Science*. 60(2005), 2273-2282.
92. J.P. Leclerc, S. Claudel, H.G. Lintz, O. Potier, B. Antoine, Theoretical interpretation of residence-time distribution measurements in industrial processes. *Oil & Gas Science and Technology*. 55(2000), 159-169.
93. A. Battaglia, P. Fox, F.G. Pohland, Calculation of residence time distribution from tracer recycle experiments, *Water Research*. 27(1993) 337-341.
94. B. Fu, H. Weinstein, B. Bernstein, A.B. Shaffer, Residence time distributions of recycle systems - Integral equation formulation, *Industrial & Engineering Chemistry Process Design and Development*. 10(1971), 501-508.
95. A.D. Martin, Interpretation of residence time distribution data. *Chemical Engineering Science*. 55(2000) 5907-5917.
96. Y. Zhang, A. Ghaly, B. Li, Physical properties of wheat straw varieties cultivated under different climatic and soil conditions in three continents, *American Journal of Engineering and Applied Sciences*. 5(2012), 98-106.
97. M. Schwanninger and B. Hinterstoisser, Comparison of the classical wood extraction method using a Soxhlet apparatus with an advanced extraction method, *European Journal of Wood and Wood Products*. 60(2002), 343-346.
98. TAPPI, Ash in wood and pulp, *Tappi Test Methods T 211 om-85*, Atlanta, GA, 1991.

99. TAPPI, Acid-insuluble lignin in wood and pulp, *Tappi Test Methods T 222 om-88*, Atlanta, GA, (1994-1995).

100. D.M. Updegraff, Semimicro determination of cellulose inbiological materials, *Analytical Biochemistry*. 32(1969), 420-424.

101. A.G. Schoning, Absorptiometric determination of acid-soluble lignin in semichemical bisulfite pulp and in some wood and plants, *Svensk Papperstidn*. 68(1965), 607-613.

102. B. Xiao, X. Sun, R. Sun, Chemical, structural, and thermal characterizations of alkali-soluble lignins and hemicelluloses, and cellulose from maize stems, rye straw, and rice straw, *Polymer Degradation and Stability*. 74(2001), 307-319.

103. L.E. Wise, Chlorite holocellulose, its fractionation and bearing on summative wood analysis and on studies on the hemicelluloses, *Paper Trade*. 122(1946), 35-43.

104. TAPPI, Kappa number of pulp, *Tappi Test Method T 236 om-99*, USA (1985).

105. TAPPI, Preparation and analysis of caustic soda liquor, *Tappi test method T 624 cm-00*, USA (2000).

106. T.M. Werner and R.H. Kadlec, Wetland residence time distribution modeling, *Ecological Engineering*. 15(2000), 77-90.

107. J.M. Commenge, T. Obein, G. Genin, X. Framboisier, S. Rode, V. Schanen, P. Pitiot, M. Matlosz, Gas-phase residence time distribution in a falling-film microreactor, *Chemical Engineering Science*. 61(2006), 597-604.

108. A.P. Torres, and F.A.R. Oliveira, Residence time distribution studies in continuous thermal processing of liquid foods: a review, *Journal of Food Engineering*. 36(1998), 1-30.

109. J.T. Adeosun, and A. Lawal, Numerical and experimental studies of mixing characteristics in a T-junction microchannel using residence-time distribution, *Chemical Engineering Science*. 64(2009), 2422-2432.

110. A. Harris, J. Davidson, R. Thorpe, A novel method for measuring the residence time distribution in short time scale particulate systems, *Chemical Engineering Journal*. 89(2002), 127-142.

111. G.C. Synman, S.W. Smith, *Mathematical models for the evaluation of radioactive tracer tests carried out in South Africa*, Atomic Energy Board, Republic of South Africa. (No. PEL-249), (1975).

112. J. Puaux, G. Bozga, and A. Ainser, Residence time distribution in a corotating twin-screw extruder, *Chemical Engineering Science*. 55(2000), 1641-1651.
113. V.K. Pareek, Z. Yap, M.P. Brungs, A.A. Adesina, Particle residence time distribution (RTD) in three-phase annular bubble column reactor, *Chemical Engineering Science*. 56(2001), 6063-6071.
114. A. Alvarado, S. Vedantam, P. Goethals, I. Nopens, A compartmental model to describe hydraulics in a full-scale waste stabilization pond, *Water Research*. 46(2012), 521-530.
115. H.T. Liao and C.Y. Shiau, Analytical solution to an axial dispersion model for the fixed-bed adsorber, *AIChE Journal*. 46(2000), 1168-1176.
116. F. Wei, Z. Wang, Y. Jin, Z. Yu, W. Chen, Dispersion of lateral and axial solids in a cocurrent downflow circulating fluidized bed, *Powder Technology*. 81(1994), 25-30.
117. M.H. Roemer, and L.D. Durbin, Transient response and moments analysis of backflow cell model for flow systems with longitudinal mixing, *Industrial & Engineering Chemistry Fundamentals*. 6(1967), 120-129.
118. TAPPI, Solids content of black liquor, *Tappi Test Methods T650 om-09*, (1995).

LIST OF PUBLICATIONS

PUBLICATIONS

- **IN PEER REVIEWD JOURNALS**

1. Meenakshi Sheoran, Sunil Goswami, Harish J. Pant, Jaishree Biswal, Vijay K. Sharma, Avinash Chandra, Haripada Bhunia, Pramod K. Bajpai, S.M. Rao, Ashutosh Das. Measurement of residence time distribution of liquid phase in an industrial-scale continuous pulping digester using radiotracer technique, *Applied Radiation and Isotopes*, 111 (2016) 10-17.
2. Meenakshi Sheoran, Avinash Chandra, Haripada Bhunia, Pramod K. Bajpai, Harish J. Pant, Residence time distribution studies using radiotracers in chemical industry – a review. *Chemical Engineering Communication,* 205, 6, (2018), 739-758.
3. Meenakshi Sheoran, Avinash Chandra, Sanjeev Ahuja, Haripada Bhunia, Harish J. Pant, RTD measurement, modelling, and analysis of liquid phase of three-tube industrial pulp digester. *International Journal of Chemical Reactor Engineering*, 17(4), (2018)-0192.
4. Meenakshi Sheoran, Avinash Chandra, Haripada Bhunia, Pramod K. Bajpai, Harish J. Pant, Industrial scale RTD measurement using gold radiotracer, *Iranian Journal of Chemistry & Chemical Engineering,* (2020), doi: 10.30492/ijcce.2020.39047.
5. Sunil Goswami, Harish J. Pant, Meenakshi Sheoran, Avinash Chandra, Vijay K. Sharma, Haripada Bhunia. Residence time distribution measurements in an industrial-scale pulp digester using technetium-99m as radiotracer. *Journal of Radioanalytical and Nuclear Chemistry.* 323, (2020), 1373–1379.
6. Meenakshi Sheoran, Avinash Chandra, Haripada Bhunia, Pramod K. Bajpai, Harish J. Pant, S. Madhukar Rao. Investigation the flow behavior of continuous pulping digester using radiotracer technique to optimize the operating conditions, *IPPTA Journal,* 28(3), (2016), 33-40.

- **IN CONFERENCES/SYMPOSIA**

A. International

1) Meenakshi Sheoran, Avinash Chandra, Haripada Bhunia, Harish J. Pant, Pramod K. Bajpai, S. Madhukar Rao. Radioactive tracing of an industrial scale three-tube continuous pulping digester, *International Conference on Applications of Radiation Science and Technology,* Vienna, Austria, 24^{th} -28^{th} April 2017.

2) Meenakshi Sheoran, Avinash Chandra, Haripada Bhunia, Harish J. Pant, Pramod K. Bajpai, Radiotracer application for RTD investigation of pulping digester, *NAARRI International Conference Advanced applications of Radiation Technology (NICSTAR),* Mumbai, India, 3-5 March, 2018

3) Meenakshi Sheoran, Avinash Chandra, Sunil Goswami, Vijay K. Sharma, Harish J. Pant, Haripada Bhunia, Arvind K. Gautam, Identification of flow abnormalities in pulp digesters using radiotracers, *8th International Conference on Tracers and Tracing Methods (Tracer 8)*. Vietnam. 26th-28th February (2019).

B. <u>National</u>

4) Meenakshi Sheoran, Avinash Chandra, Haripada Bhunia, Harish J. Pant, Pramod K. Bajpai, S. Madhukar Rao. RTD investigation of an industrial three-tube pulping digester using radiotracer, *National Symposium on Application of Radioisotopes and Radiation Technology in Industry Healthcare and Agriculture (ARRTIHA-2016),* November 28-29, 2016.
5) Meenakshi Sheoran, Avinash Chandra, Haripada Bhunia, Pramod K. Bajpai, Harish J. Pant, S. Madhukar Rao. Investigating the flow behavior of continuous pulping digester using radiotracer technique to optimize the operating conditions. ***IPPTA*** – *Zonal Seminar*, August 4-5, 2016.

REPRINT OF PUBLISHED ARTICLES

Applied Radiation and Isotopes 111 (2016) 10–17

Contents lists available at ScienceDirect

Applied Radiation and Isotopes

journal homepage: www.elsevier.com/locate/apradiso

Measurement of residence time distribution of liquid phase in an industrial-scale continuous pulp digester using radiotracer technique

Meenakshi Sheoran [a], Sunil Goswami [b], Harish J. Pant [b,*], Jayashree Biswal [b], Vijay K. Sharma [b], Avinash Chandra [a], Haripada Bhunia [a], Pramod K. Bajpai [a], S. Madhukar Rao [c], A. Dash [b]

[a] Department of Chemical Engineering, Thapar University, Patiala 147004, Punjab, India
[b] Isotope Production and Applications Division, Bhabha Atomic Research Centre, Mumbai 400085, India
[c] Satia Industries Limited, Sri Muktsar Sahib 152101, Punjab, India

HIGHLIGHTS

- Radiotracer experiments were conducted to measure RTD of liquid phase in a pulp digester
- Mean residence times of white liquor were measured
- Axial dispersion and tanks-in-series models were used to investigate flow patterns
- Parallel flow paths were observed in first section of the digester
- Optimized flow rates of biomass and liquor were obtained

ARTICLE INFO

Article history:
Received 8 December 2015
Received in revised form
25 January 2016
Accepted 25 January 2016
Available online 26 January 2016

Keywords:
Pulp digester
Radiotracer
Bromine-82
Residence time distribution
Mean residence time
Plug flow component
Axial dispersion model
Tanks-in-series with back-mixing model

ABSTRACT

A series of radiotracer experiments was carried out to measure residence time distribution (RTD) of liquid phase (alkali) in an industrial-scale continuous pulp digester in a paper industry in India. Bromine-82 as ammonium bromide was used as a radiotracer. Experiments were carried out at different biomass and white liquor flow rates. The measured RTD data were treated and mean residence times in individual digester tubes as well in the whole digester were determined. The RTD was also analyzed to identify flow abnormalities and investigate flow dynamics of the liquid phase in the pulp digester. Flow channeling was observed in the first section (tube 1) of the digester. Both axial dispersion and tanks-in-series with backmixing models preceded with a plug flow component were used to simulate the measured RTD and quantify the degree of axial mixing. Based on the study, optimum conditions for operating the digester were proposed.

1. Introduction

The Indian paper industry is one of the leading industries in the world with an approximate share of 2.6% of the global production. Currently, there are 813 paper mills in India based on different types of raw material such as wood, bagasse, agro residue (wheat straw, rice straw, etc.) (Jain, 2015). Traditionally, wood was the only raw material used for paper production but due to the excessive exploitation of forest and environmental concern, wood may not be the right choice for paper production. Hence the alternatives of wood are bagasse, cotton, reed, hemp, agro residue etc. In India, around 14 paper mills are using wood out of 850 paper mills (Bajpai et al., 2004a). The worldwide demand of paper is increasing day by day at the rate of 4-5% per anum and the estimated demand in 2025 would be 21.94 million tons in India (Jain, 2015). The paper production rate in 2006-2007 was 5.9 million tons against the installed capacity of 7.6 million tons (Szabo et al., 2009).

The paper manufacturing process requires wood chips or agro residue raw material. The washed and dust free raw material is directly fed to a pulp digester and converted in to pulp using

* Corresponding author.
E-mail address: hjpant@barc.gov.in (H.J. Pant).

http://dx.doi.org/10.1016/j.apradiso.2016.01.025
0969-8043/

CHEMICAL ENGINEERING COMMUNICATIONS
https://doi.org/10.1080/00986445.2017.1410478

Residence time distribution studies using radiotracers in chemical industry—A review

Meenakshi Sheoran[a], Avinash Chandra[a], Haripada Bhunia[a], Pramod K. Bajpai[a], and Harish J. Pant[b]

[a]Department of Chemical Engineering, Thapar Institute of Engineering & Technology, Patiala, Punjab, India; [b]Isotope and Radiation Application Division, Bhabha Atomic Research Centre, Mumbai, India

ABSTRACT

Use of radiotracer in residence time distribution (RTD) studies in industrial as well as lab scale systems has been emphasized in this review. The advantages of radiotracer over conventional tracers are discussed. The injection and detection protocols of the radiotracers are explained. The pretreatment of RTD data obtained and RTD modeling are explained using industrial- and laboratory-scale studies. The detailed RTD studies in (i) oil and gas, (ii) pharmaceuticals and bioprocesses, (iii) fertilizers and pesticides, (iv) polymer, plastic and fiber, (v) mineral processing, organic and inorganic chemicals, (vi) laboratory scale, (vii) pilot plant scale, and (viii) wastewater treatment processes are considered for this review. The case studies are also explained with RTD experiments. The current trend on the application of radiotracer technology in industry is also explained.

KEYWORDS

Mean residence time; modeling; radiotracer; residence time distribution (RTD); troubleshooting

Introduction

Most of the large-scale chemical processes are based on continuous flow reactors including plug flow reactor (PFR) or continuous stirred tank reactor (CSTR). In practice, no system behaves ideally and always shows deviation from the ideal state. Hence, the real systems behave in between plug flow reactor (PFR) and continuous stirred tank reactor (CSTR). There are numerous reasons for the deviation from the actual behavior which includes improper design, fluctuating operating conditions, scale-up effects, different raw material sources, nonuniform heating/cooling, etc. These deviations may cause malfunctioning or failure of the process and may lead to inferior/nonuniform quality product (Hweij and Azizi, 2015).

The flow irregularities and hydrodynamics of any continuous flow system/reactor can be described with the help of fluid mechanics fundamentals and residence time distribution (RTD) theory. The RTD theory is well suited to predict nonideal flow behavior of the system/process and can be explained as the probability distribution function of the material flowing inside the process equipment or reactors (Levenspiel, 2004). Furthermore, it can be used to estimate the process efficiency, mixing time, bypassing, channeling, dead zone, etc. (Pant et al., 2009c). The improper design of the reaction vessel can be evaluated through RTD analysis even at the designing stage itself by determining the hydrodynamic flow behavior at a wide range of operating conditions. Though the RTD provides only global information about the flow behavior, it cannot provide the local information about flow. For the localized or spatial flow distribution, one can use the advanced computational tools [computational fluid dynamics (CFD)]. In some studies, the RTD results are also used to verify the CFD results (Kim et al., 2005).

There are numerous studies available in the literature on the RTD investigation of various flow reactors (Torres and Oliveira, 1998; Bedmar, 1983). Different types of tracers are used to trace different phases (solid, liquid, and gas). Broadly, a unique property of tracer is used to measure the RTD in a system. The process may be physical, chemical, or biological with very short or long residence time. This property may be nuclear, physical, chemical, and biological. A small amount of tracer

CONTACT Avinash Chandra avichiitk@yahoo.com Department of Chemical Engineering, Thapar Institute of Engineering & Technology, Patiala, Punjab 147004, India.

Meenakshi Sheoran[1] / Avinash Chandra[1] / Sanjeev Ahuja[1] / Haripada Bhunia[1] / Harish J. Pant[2]

RTD Measurement, Modeling, and Analysis of Liquid Phase of Three-Tube Industrial Pulp Digester

[1] Department of Chemical Engineering, Thapar Institute of Engineering & Technology (Deemed University), Patiala, Punjab 147004, India, E-mail: avichiitk@yahoo.com. https://orcid.org/0000-0001-9647-2421.
[2] Isotope Application Division, Bhabha Atomic Research Centre, Mumbai 400085, India

Abstract:
Residence-time distribution (RTD) experiments were performed to analyze an industrial scale three-tube series continuous pulping digester's hydrodynamic performance. An impulse of radiotracer ^{82}Br (γ energy source) was introduced at the inlet of the first tube. The radiotracer concentration in the liquid phase was traced at the outlet of each tube. The input behavior of the radiotracer converted to a non-ideal pulse tracer input for the second and third tubes of the digester. Numerical convolution is adopted to deal with the non-ideal pulse input of the radiotracer. A modeling procedure for determining the RTD from the outlet tracer concentration data is proposed. A plug flow component followed by axial dispersion model is considered, and is adjusted after its convolution with the inlet tracer concentration data to obtain the RTD of the individual tubes. The obtained RTD data are analyzed to explain the flow behavior, degree of dispersion, and flow abnormalities existing in the digester. The mean residence-time (MRT), and dispersion number are estimated for the model components for the three tubes. The vessel dispersion number is found to decrease from tube 1 to tube 3. Overall, the conversion of the highly dispersed flow regime into the plug-flow regime is observed in the whole digester.

Keywords: axial dispersion model, numerical convolution, pulp digester, radiotracer, residence-time distribution, vessel dispersion number

DOI: 10.1515/ijcre-2018-0192

Received: July 27, 2018; **Revised:** December 12, 2018; **Accepted:** January 10, 2019

1 Introduction

In pulping processes the pulp digester is used to produce the pulp and it is the heart of paper industry. A description of pulping process can be referred in literature (Sixta 2006; Smook 2001). The operating parameters of the pulp digester affect the operating cost, quality of the product, yield, and the amount of waste generation (Smook 2001). The optimization process may improve the performance of the pulping digester by the increased yield and quality of product, and the reduced amount of waste and operating cost. Numerous abnormalities can be encountered during the digestion process inside the digester, such as the presence of dead zone or stagnant volume, channeling, fouling, bypassing, recirculation, and back-mixing. These abnormalities and malfunctioning cause deleterious effect on the pulp digester operations and affect the digestion process, quality of the pulp, and energy consumption. These types of malfunctioning and abnormalities can be identified with the help of the hydrodynamic behavior of the pulp digester.

Residence-time distribution (RTD) analysis is a technique which describes the behavior of the flowing fluid and identifies the malfunctioning in the continuous process equipment (Danckwerts 1953). In chemical industries, the RTD analysis technique has been applied to investigate the influence of operating parameters on the flow behavior. In this technique, a small amount of tracing material is used to trace the process that provides the RTD information. This RTD information can be interpreted in terms of the hydrodynamic behavior of the process, liquid hold up, bypass, etc. The use of the radiotracer as a tracing material has numerous advantages of measuring the RTD without interfering with the flow and their use in opaque systems. Now a days, this technique is widely used over the conventional tracer technique due to the online sampling, high sensitivity to the detectors in very low concentration, wide variety of availability of radiotracers, limited effect on the system and use in hostile industrial environment (Pant and Yelgoankar 2002).

Avinash Chandra is the corresponding author.

Journal of Radioanalytical and Nuclear Chemistry (2020) 323:1373–1379
https://doi.org/10.1007/s10967-019-06730-3

Residence time distribution measurements in an industrial-scale pulp digester using technetium-99m as radiotracer

Sunil Goswami[1] · Harish Jagat Pant[1] · Meenakshi Sheoran[2] · Avinash Chandra[2] · Vijay Kumar Sharma[1] · Haripada Bhunia[2]

Received: 2 May 2019 / Published online: 29 August 2019

Abstract
This paper describes measurement of residence time distributions (RTD) of the liquid phase in an industrial-scale continuous pulp digester. The objective of the study was to quantify the degree of mixing of the liquid phase and optimization of operating conditions of digester. Technetium-99m (^{99m}Tc) was used as radiotracer to measure the RTD of liquid phase. A combined model was proposed for the simulation of experimental RTD curve. The quality parameter of pulping process was measured using chemical methods. From the comparison of pulping and mixing parameters the optimum operating condition of digester was identified.

Keywords Pulp digester · Wheat straw · Technitium-99m · Mean residence time · Kappa number · Residual alkali

Introduction

The consumption of paper and its products are continuously increasing with the development of civilization across the world. The widely used raw materials for the production of the paper worldwide are wood chips. At present, the supply of wood chips is not sufficient to meet the market demand of the paper. The low availability of wood chips as raw material is attributed to shrinkage of forests area and strict the environmental policies. Therefore, the paper industries are in constant search for non-wood fibrous raw material to produce paper [1]. The selection of the non-wood material for paper production is based on different factors such as content of cellulose in material, availability, cost, pre-cleaning process etc.[2]. Wheat straw is a cellulose rich raw material available at low cost in abundance for paper production in India. It is obtained as a residue or by-product after crop harvesting [3]. The conversion of raw materials (wood chip or wheat straw) to paper involves several chemical and physical processes. The key step in the production of the paper is pulping or delignification process [2]. In delignification process, the raw material having cellulose and basic binding material lignin are separated from each other. The different techniques applied for removal the lignin are divided in two categories i.e. mechanical and chemical. The mechanical pulping process always have high yield compared to the chemical pulping. However, the pulp fiber produced in mechanical pulping is severely damaged and contains high amount of lignin. Hence, the paper quality produced by the mechanical pulping has lower strength and quality [4]. Therefore, widely adopted pulping method for the production of high quality paper in the industries is the chemical pulping. The chemical pulping is carried out in digesters units of the paper industry. In this process the raw material is finely hacked, washed, cleaned and mixed

✉ Harish Jagat Pant
hjpant@barc.gov.in

Sunil Goswami
gsunil@barc.gov.in

Meenakshi Sheoran
meenakshi.shoren@tahpar.edu

Avinash Chandra
avinash.chandra@thapar.edu

Vijay Kumar Sharma
vksharma@barc.gov.in

Haripada Bhunia
hbhunia@thapar.edu

[1] Isotope and Radiation Application Division, Bhabha Atomic Research Centre, Trombay, Mumbai, Maharashtra 400085, India

[2] Department of Chemical Engineering, Thapar Institute of Engineering and Technology, Patiala, Punjab 147004, India

Industrial scale RTD measurement using gold radiotracer

Document Type: Research Article

Authors

Meenakshi Sheoran [1] ; Avinash Chandra [2] ; Haripada Bhunia [1] ; Pramod K Bajpai [1] ; Harish J Pant [3]

[1] Department of Chemical Engineering, Thapar Institute of Engineering & Technology, Patiala-147004, Punjab, India

[2] Department of Chemical Engineering, Thapar Institute of Engineering & Technology, Patiala-147004, Punjab

[3] Isotope Application Division, Bhabha Atomic Research Centre, Mumbai-400085, India

10.30492/IJCCE.2020.39047

Abstract

Residence time distribution (RTD) is a suitable method to find out the hydrodynamics of any industrial or lab-scale reactor. Radiotracer 198Au was used to trace the liquid phase of the industrial scale continuous pulp digester. The radiotracer was injected instantaneously as an impulse input in the liquid phase and concentration versus time data were collected at the inlet and outlet of each tube using a data acquisition system. The flow modeling of continuous pulp digester has been done in two ways. Firstly, the whole digester was considered a single reactor. Secondly, each tube of the digester was considered a single reactor separately. For the second case, the convolution procedure was opted to deal with a non-ideal input signal for the second and third tubes. Axial dispersion model and tank in series with a back-mixing model were used to simulate the experimental data. Mean residence time and Peclet numbers were calculated for each tube and the whole digester.

Keywords

Au-198 ; Axial dispersion model ; Convolution ; Pulp digester ; Radiotracer ; Tank in series with back-mixing model

Main Subjects

Catalysts, Kinetics, Reactor ; Process Design, Simulation & Control ; Pulp & Paper Industries

Articles in Press, Accepted Manuscript
Available Online from 19 April 2020